

NCKRI REPORT OF INVESTIGATION 7

**KARST GEOHAZARDS AND GEOPHYSICAL SURVEYS:
US 285, EDDY COUNTY, NEW MEXICO**



NATIONAL CAVE AND KARST RESEARCH INSTITUTE
REPORT OF INVESTIGATION 7

**KARST GEOHAZARDS AND GEOPHYSICAL SURVEYS:
US 285, EDDY COUNTY, NEW MEXICO**

Lewis Land
Colin Cikoski
David McCraw
George Veni

January 2018



Published and distributed by

National Cave and Karst Research Institute

Dr. George Veni, Executive Director

400-1 Cascades Avenue
Carlsbad, NM 88220 USA

www.nckri.org

The citation information:

Land L, Cikoski C, McCraw D, Veni G. 2018. Karst Geohazards and Geophysical Surveys: US 285, Eddy County, New Mexico. National Cave and Karst Research Institute Report of Investigation 7, Carlsbad, New Mexico.

Cover photo: Station 8.6 sinkhole, east shoulder of US 285 south of the village of Malaga, New Mexico, about 9.7 mi. (15.6 km) north of the Texas/New Mexico state line. Photo from Google Earth.

ISBN: 978-0-9910009-7-5

NCKRI Organization and Mission

NCKRI was created by the U.S. Congress in 1998 in partnership with the State of New Mexico and the City of Carlsbad. Initially an institute within the National Park Service, NCKRI is now a non-profit 501(c)(3) corporation that retains its federal, state, and city partnerships. Federal and state funding for NCKRI is administered by the New Mexico Institute of Mining and Technology (aka New Mexico Tech or NMT). Funds not produced by agreements through NMT are accepted directly by NCKRI.

NCKRI's enabling legislation, the National Cave and Karst Research Institute Act of 1998, 16 USC, §4310, identifies NCKRI's mission as to:

- 1) further the science of speleology;
- 2) centralize and standardize speleological information;
- 3) foster interdisciplinary cooperation in cave and karst research programs;
- 4) promote public education;
- 5) promote national and international cooperation in protecting the environment for the benefit of cave and karst landforms; and
- 6) promote and develop environmentally sound and sustainable resource management practices.

NCKRI Report of Investigation Series

NCKRI uses this report series to publish the findings of its research projects. The reports are produced on a schedule whose frequency is determined by the timing of the investigations. This series is not limited to any topic or field of research, except that they involve caves and/or karst. All reports in this series are open access and may be used with citation. To minimize environmental impact, few or no copies are printed. They may be downloaded at no cost from the NCKRI website at www.nckri.org.

TABLE OF CONTENTS

List of Figures	4
Abstract	9
Background	9
Methods	12
Surface reconnaissance	12
Geophysical surveys	12
Results	13
Sinkhole surveys	13
Bridge surveys.....	21
Reoccupation of seismic refraction survey areas.....	43
Summary	43
References	49
Appendix A: Karst Features and Electrical Resistivity Surveys in the Study Area.....	51
Appendix B: Detailed Geologic and Topographic Map of the Study Area, With Karst Features	66
Appendix C: Detailed Geologic, Aerial Photo, Karst Feature, and Electrical Resistivity Map of the Study Area	75

LIST OF FIGURES

Figure 1	
<i>Location of study area and sites with high estimated karst hazard potential.....</i>	<i>10</i>
Figure 2	
<i>Stratigraphy of US Highway 285 study area.....</i>	<i>10</i>
Figure 3	
<i>Geologic map of the survey area with the locations of sites identified as having high estimated hazard potential.....</i>	<i>11</i>
Figure 4	
<i>Short ER profile adjacent to sinkhole 0.75E</i>	<i>14</i>
Figure 5	
<i>Long ER profile adjacent to sinkhole 0.75E</i>	<i>14</i>
Figure 6	
<i>Short ER profile adjacent to sinkhole 0.75W.....</i>	<i>16</i>
Figure 7	
<i>Long ER profile adjacent to sinkhole 0.75W.....</i>	<i>16</i>
Figure 8	
<i>ER profile at station 7.75E</i>	<i>17</i>
Figure 9	
<i>ER profile at station 8.6W.....</i>	<i>18</i>
Figure 10	
<i>ER profile at station 8.6E</i>	<i>18</i>
Figure 11A	
<i>Short ER profile at station 9.7E.....</i>	<i>19</i>
Figure 11B	
<i>Long ER profile at station 9.7E.....</i>	<i>19</i>
Figure 12	
<i>ER profile at station 12.3W.....</i>	<i>20</i>
Figure 13	
<i>ER profile at station 12.3E.</i>	<i>20</i>
Figure 14	
<i>ER profile at station 14.1E</i>	<i>21</i>
Figure 15	
<i>Delaware River bridge.....</i>	<i>22</i>
Figure 16	
<i>ER survey of Delaware River bridge, south abutment.....</i>	<i>23</i>
Figure 17	
<i>ER survey of Delaware River bridge, first pier from the south.....</i>	<i>23</i>

Figure 18	
<i>ER survey of Delaware River bridge, second pier from the south</i>	24
Figure 19	
<i>ER survey of Delaware River bridge, third pier from the south</i>	24
Figure 20	
<i>ER survey of Delaware River bridge, fourth pier from the south</i>	25
Figure 21	
<i>ER survey of Delaware River bridge, fifth pier from the south</i>	25
Figure 22	<i>ER survey of Delaware River bridge, north abutment</i>
	26
Figure 23	
<i>ER survey of Delaware River Bridge, northeast abutment</i>	26
Figure 24	
<i>ER survey of Delaware River bridge, northwest abutment</i>	27
Figure 25	
<i>ER survey of Delaware River bridge, southeast abutment</i>	27
Figure 26	
<i>ER survey of Delaware River bridge, southwest abutment</i>	28
Figure 27	
<i>Deep profile, northeast side of Delaware River bridge</i>	28
Figure 28	
<i>Deep profile, southwest side of Delaware River bridge</i>	29
Figure 29	<i>ER survey of Red Bluff Draw bridge, south abutment</i>
	30
Figure 30	
<i>ER survey of Red Bluff Draw bridge, north abutment</i>	30
Figure 31	
<i>ER survey of Red Bluff Draw bridge, first pier from the south</i>	31
Figure 32	
<i>ER survey of Red Bluff Draw bridge, second pier from the south</i>	31
Figure 33	
<i>ER survey of Red Bluff Draw bridge, third pier from the south</i>	32
Figure 34	
<i>ER survey of Red Bluff Draw bridge, northeast abutment</i>	32
Figure 35	
<i>ER survey of Red Bluff Draw bridge, northwest abutment</i>	33
Figure 36	
<i>ER survey of Red Bluff Draw bridge, southeast abutment</i>	33
Figure 37	
<i>ER survey of Red Bluff Draw bridge, southwest abutment</i>	34

Figure 38	
<i>Deep profile, east side of Red Bluff Draw bridge.....</i>	<i>35</i>
Figure 39	
<i>Deep profile, west side of Red Bluff Draw bridge.</i>	<i>35</i>
Figure 40	
<i>ER survey between piers 1 and 2, counting from the south, Salt Draw bridge.....</i>	<i>36</i>
Figure 41	
<i>ER survey between piers 6 and 7, counting from the south, Salt Draw bridge.....</i>	<i>36</i>
Figure 42	
<i>ER survey between piers 2 and 3, counting from the south, Salt Draw bridge.....</i>	<i>37</i>
Figure 43	
<i>ER survey between piers 5 and 6, counting from the south, Salt Draw bridge.....</i>	<i>37</i>
Figure 44	
<i>ER survey between piers 7 and 8, counting from the south, Salt Draw bridge.....</i>	<i>38</i>
Figure 45	
<i>ER survey of Salt Draw bridge, northeast abutment.....</i>	<i>39</i>
Figure 46	
<i>ER survey of Salt Draw bridge, northwest abutment.</i>	<i>39</i>
Figure 47	
<i>ER survey of Salt Draw bridge, southeast abutment.....</i>	<i>40</i>
Figure 48	
<i>ER survey of Salt Draw bridge, southwest abutment.</i>	<i>40</i>
Figure 49	
<i>Deep profile, east side of Salt Draw bridge.</i>	<i>41</i>
Figure 50	
<i>Deep profile, west side of Salt Draw bridge.....</i>	<i>41</i>
Figure 51	
<i>ER survey of north abutment, Black River bridge.....</i>	<i>42</i>
Figure 52	
<i>ER survey of north pier, Black River bridge.....</i>	<i>42</i>
Figure 53	
<i>ER survey of south abutment, Black River bridge.....</i>	<i>44</i>
Figure 54	
<i>ER survey of south pier, Black River bridge.....</i>	<i>44</i>
Figure 55	
<i>ER survey of Black River bridge, northeast abutment.....</i>	<i>45</i>
Figure 56	
<i>ER survey of Black River bridge, southwest abutment.....</i>	<i>45</i>

Figure 57	
<i>ER survey of Black River bridge, northwest abutment</i>	46
Figure 58	
<i>ER survey of Black River bridge, southeast abutment.</i>	46
Figure 59	
<i>Deep profile, east side of Black River bridge</i>	47
Figure 60	
<i>Deep profile, west side of Black River bridge.</i>	47
Figure 61	
<i>ER survey of seismic refraction site SL02.</i>	48
Figure 62	
<i>ER survey of seismic refraction site SL04.</i>	48
Figure 63	
<i>ER survey of seismic refraction survey site SL05</i>	49
Figure A1	
<i>Station 0.1E profile</i>	52
Figure A2	
<i>Station 0.75E profile</i>	52
Figure A3	
<i>Station 0.75EE profile</i>	53
Figure A4	
<i>Station 0.75W profile.</i>	53
Figure A5	
<i>Station 0.75WW profile</i>	54
Figure A6	
<i>Station 7.75E profile</i>	55
Figure A7	
<i>Station 8.6W sinkhole and ER cable</i>	55
Figure A8	
<i>Station 8.6W profile.</i>	56
Figure A9	
<i>Station 8.6E profile</i>	57
Figure A10	
<i>Station 9.7 sinkhole in road base</i>	58
Figure A11	
<i>Station 9.7 possible cave entrance.</i>	58
Figure A12-A	
<i>Short ER profile Station 9.7</i>	59

Figure A12-B	
Long ER profile Station 9.7	59
Figure A13	
Station 9.82E profile.....	60
Figure A14	
Station 9.82W profile.....	60
Figure A15	
Station 12.0E sinkhole A	61
Figure A16	
Station 12.0E sinkhole B.....	61
Figure A17	
Station 12.0E sinkhole C.....	61
Figure A18	
Station 12.0E profile.....	62
Figure A19	
Station 12.1W profile.....	62
Figure A20	
Station 12.3W profile.....	63
Figure A21	
Station 12.3E profile.....	64
Figure A22	
Station 14.07E profile.....	64
Figure A23	
Station 14.1E profile.....	65

KARST GEOHAZARDS AND GEOPHYSICAL SURVEYS: US ROUTE 285, EDDY COUNTY, NEW MEXICO

Lewis Land
National Cave and Karst Research Institute

Colin Cikoski and David McCraw
New Mexico Bureau of Geology and Mineral Resources,
Socorro, New Mexico

George Veni
National Cave And Karst Research Institute

Abstract

Personnel with the National Cave and Karst Research Institute and the New Mexico Bureau of Geology and Mineral Resources conducted an assessment of karst geohazards southeast of Carlsbad, NM. The US Route 285 (US 285) corridor in this area is subject to high levels of oilfield traffic and is particularly prone to sinkholes, because of the presence of gypsum bedrock in the Rustler Formation at or near the surface throughout much of the study area. These features pose a geohazard for the transportation and pipeline network in this part of the state. The geotechnical properties of the Rustler Formation are influenced by soluble gypsum strata interbedded with mechanically weak mudstone and siltstone and more rigid dolomite beds. Surface reconnaissance mapping and near-surface electrical resistivity (ER) surveys indicate that most sinkholes formed in the Rustler are relatively shallow (<10 ft, or 3 m), without deep roots, probably due to the mixed lithology of soluble and insoluble bedrock. However, longer-array ER surveys have identified additional cavities at greater depths in some areas that do not breach the surface.

Background

On October 9, 2015, the New Mexico Department of Transportation (NMDOT) reported that a sinkhole had opened on the east shoulder of US Route 285 (US 285) south of the village of Malaga, New Mexico, about 9.7 mi.¹ (15.6 km) north of the Texas/New Mexico state line. This sinkhole is approximately six ft (1.8 m) in diameter and four ft (1.2 m) deep, and is less than 20 ft

(6 m) from the edge of the roadway, within the highway right-of-way. Because of nearby oil and gas activity, there is a substantial amount of traffic along this portion of US 285, including large trucks. The sinkhole thus poses a hazard to the traveling public. Surface geologic maps indicate that bedrock of the upper Permian Rustler Formation is present at or near the surface beneath US 285 from Malaga south to the state line, and crops out within ~20 ft (~6 m) of the new sinkhole. The Rustler is composed in part of highly soluble gypsum, thus making it prone to sinkhole formation. Because of the poor condition of the existing roadbed, NMDOT has proposed construction of a highway realignment 60 ft (18 m) west of the existing highway, extending from the state line to the community of Loving (22 mi., or 35.4 km) (Figure 1).

During the month of November 2016, personnel with the National Cave and Karst Research Institute (NCKRI) and the New Mexico Bureau of Geology and Mineral Resources (NMBGMR), under contract with Amec Foster Wheeler (AFW), conducted surface reconnaissance and geologic mapping of the US 285 right-of-way (NCKRI and NMBGMR, 2016). This phase of the investigation involved walking the entire route from the Texas state line to the outskirts of Loving, New Mexico (Figure 1). Sinkholes and other karst features were re-recorded and the geology mapped (Figures 2 and 3). While electrical resistivity (ER) methods are well established, two proof of concept ER surveys were conducted for NMDOT adjacent to the sinkhole at 9.7 mi. (15.6 km)

¹ Amec Foster Wheeler (AFW), the contractor for this project, requested that United States customary units be used in the reporting of results.

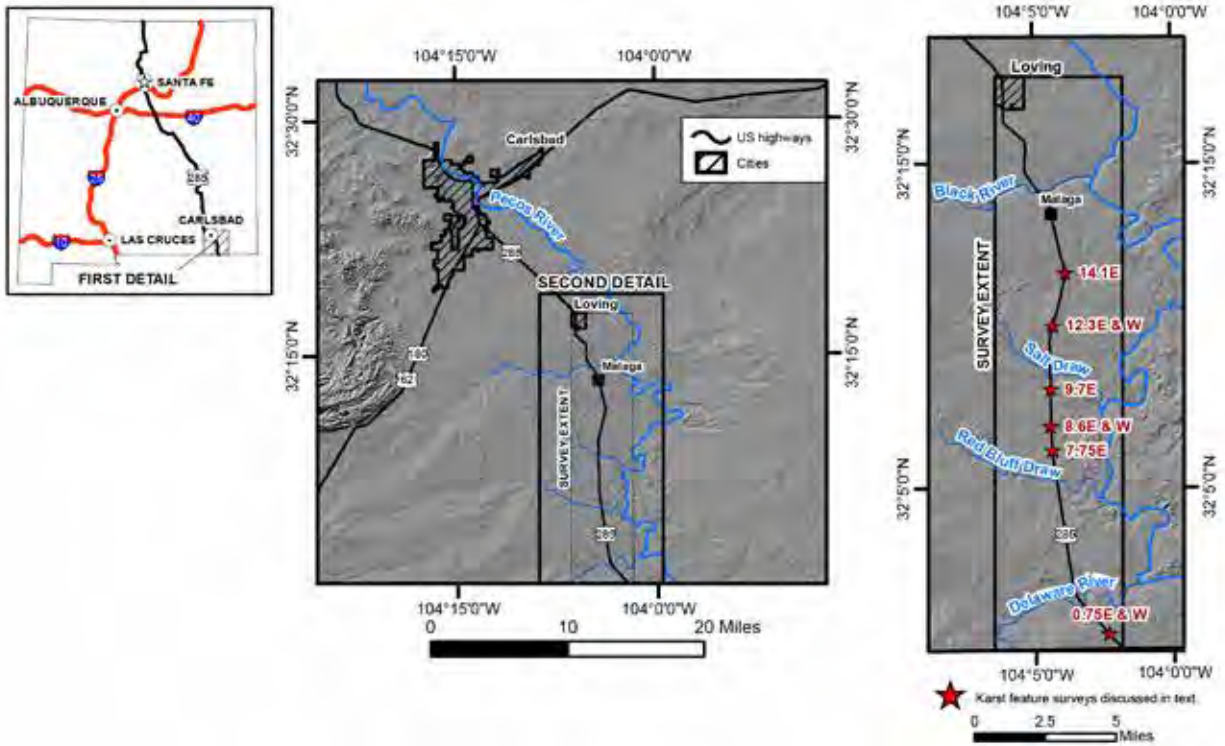


Figure 1. Location of study area and sites with high estimated karst hazard potential, as discussed in the text.

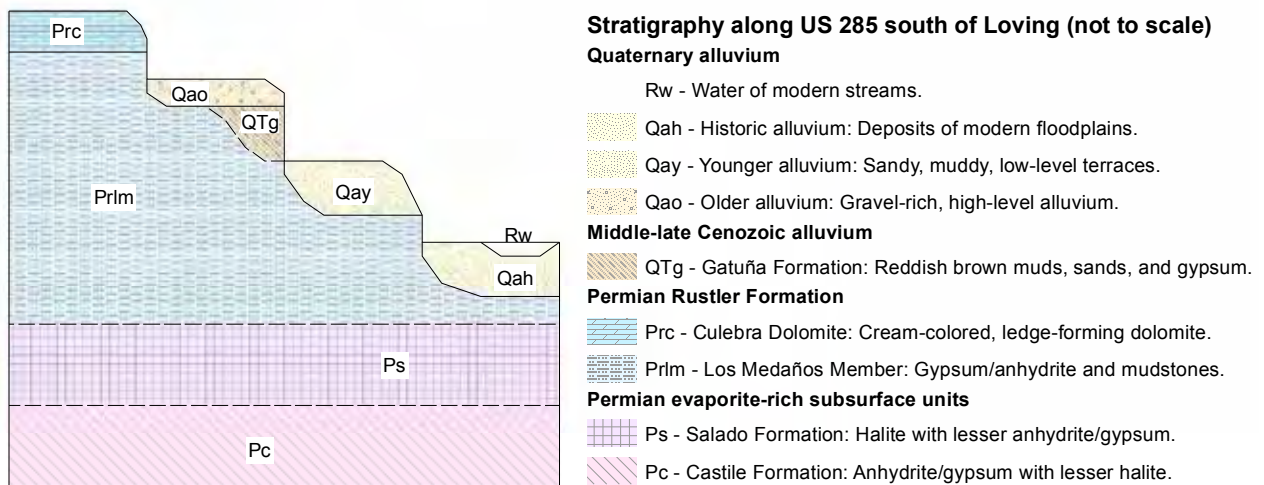


Figure 2. Stratigraphy of US Highway 285 study area.

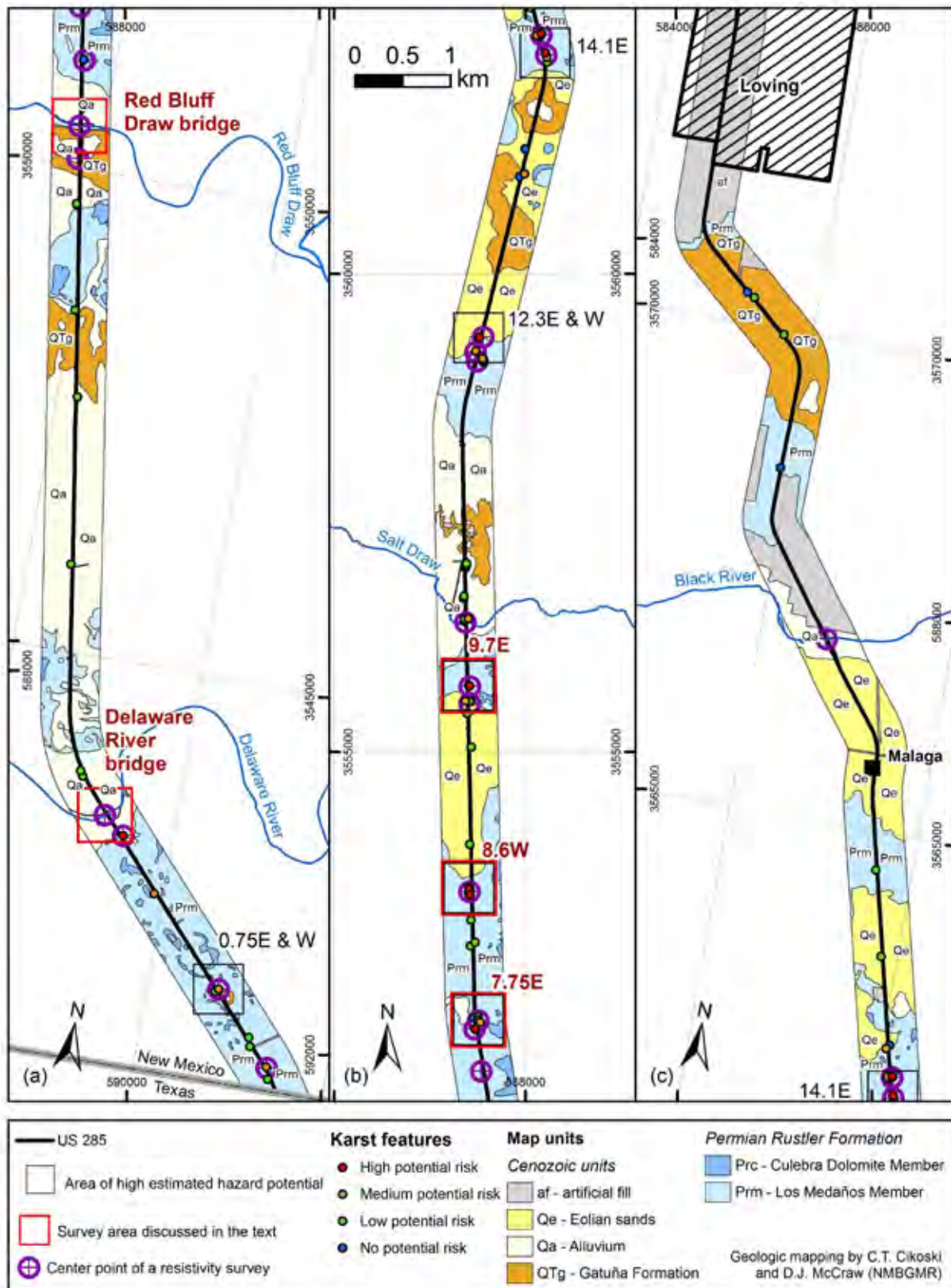


Figure 3. Geologic map of the survey area with the locations of sites identified as having high estimated hazard potential. Station numbers are based on highway distance in miles, roughly north from the state line. "E" and "W" refer to the relative position of a station east or west of the highway at the given mileage (details views in Appendix B and C).

that had generated the initial interest in this investigation. In March 2017, NCKRI and NMBGMR personnel conducted ER surveys of selected sinkholes and other potential karst geohazards that had been identified as high-risk features during the previous year's surface reconnaissance mapping. In April, May, and June, 2017, additional ER surveys were conducted at the abutments and piers of the four bridges in the study area.

Methods

Surface reconnaissance

Exploration for sinkholes, caves and other karst features was conducted with teams of two to four people walking no more than about 50 ft (15 m) apart and generally parallel to the highway. Most karst features within an area can be discovered with this spacing, although some small features with little surface expression may still be missed. Discovered features were marked with small, engraved aluminum tags and long strips of red and white survey tape, with their identification numbers marked on the tape in waterproof ink. The locations of newly discovered karst features were measured with Universal Transverse Mercator (UTM) coordinates captured with hand-held global positioning system (GPS) receivers. The GPS units were allowed to gather and process data as a feature was evaluated in order to get low estimated position errors (EPE), typically within 6–10 ft (2–3 m). Geologic contacts and outcrops were also similarly discovered and located during this survey, with all of the data later processed by geographic information system (GIS) software for display and spatial analysis.

By request of AFW, caves were not entered and karst features were not excavated when discovered, although some loose materials were removed to allow for better geohazard assessment. These evaluations included identification of lithology, measurement of fractures, and observations of flow features, sediment, water flow, and air flow. This information was recorded on forms designed for such surveys, and with a sketch to scale of each feature, including a profile and/or cross section.

Data from the forms were placed in an Excel spreadsheet designed to quantitatively predict which karst features posed the greatest risk of collapse or subsidence. The general method was discussed and successfully applied by Veni (1999). Per that method, the spreadsheet was adjusted to the local geology after weighing factors such as limestone vs. gypsum bedrock, predominant mode of cave development and morphology, preferential fracture orientations along which large and potentially unstable caves are more likely to develop, and related factors that may further suggest structural stability or instability of karstic cavities. The characteristics of each karst feature

were tallied with point values commensurate with the significance of each characteristic in demonstrating its potential for collapse or subsidence. All non-karst features were classified as artificial. The sum of the assigned point values was multiplied by a point value assigned to the feature type. Based on experience and comparison with related karst features in this and other areas, the significance of a feature was ranked as no potential risk for 0 points, low potential risk for 1–150 points, moderate potential risk for 151–250 points, and high potential risk for >250 points. These ranks were color coded and the features plotted on the geologic map created from the field survey, allowing prioritized selection of areas for geophysical investigation.

Geophysical surveys

Electrical resistivity surveys are a common and effective geophysical method for detection of subsurface voids (e.g., Land and Veni, 2012; Land, 2013; Land and Asanidze, 2015). The basic operating principle for an ER survey involves generating a direct current between two metal electrodes implanted in the ground, while measuring the ground voltage between two other implanted electrodes. Given the current flow and voltage drop between the electrodes, differences in subsurface electrical resistivity can be determined and mapped. Modern resistivity surveys employ an array of multiple electrodes connected with electrical cable. Over the course of a survey, pairs of electrodes are activated by means of a switchbox and resistivity meter. The depth of investigation for a typical ER survey is approximately one-fifth the length of the array of electrodes.

Resistivity profiles illustrate vertical and lateral variations in subsurface resistivity. The presence of water or water-saturated soil or bedrock will strongly affect the results of a resistivity survey. Air-filled caves or air-filled pore space in the vadose zone are easy to detect using the ER method, since air has near-infinite resistivity, in contrast to surrounding bedrock, which has 10 to 15 orders of magnitude greater conductivity.

A SuperSting R8/IP electrical resistivity system provided by Advanced Geosciences, Inc. (AGI) was used to collect resistivity data, employing a dipole-dipole array configuration. All of the ER surveys conducted in March, April, and May used a 42-electrode array at 3.3-ft (1-m) electrode spacing, for a target depth of investigation of ~35 ft (11 m). Rollalong methods were used at some sites to extend the length of the survey lines. The ER surveys of bridges conducted in June employed 56-electrode arrays at 10-ft (3-m) electrode spacing for a target exploration depth of ~100 ft (~30 m). These surveys extended across the entire stream valleys and

included all bridge abutments and piers.

While resistivity data were collected, a Topcon GR3 GPS instrument package was used to collect survey-grade GPS coordinates for each electrode in the arrays. Elevation data collected during these surveys were used to correct the resistivity data for variations in topography at each survey site. ER data were processed using EarthImager-2D™ software. The EarthImager software chooses a resistivity scale designed to highlight natural conditions in the subsurface; resistivity profiles shown in this report may thus not have the same resistivity scale. AGI technical staff report that, in general, it is not advisable to force the software to adhere to a specific scale, and attempts to do so may yield misleading results.

The ends of ER profiles are areas where fewer data points are available for interpretation; resistivity anomalies that occur in those parts of the profile are thus more ambiguous and may represent data processing artifacts. ER profiles usually display clipped ends to eliminate those areas of a survey that are based on a smaller number of ER measurements. The rollalong surveys overlapped enough to eliminate sections of lower quality data, except for the very ends of the surveys, where they were unavoidable.

High resistivity anomalies may represent either void space in the subsurface (caves or potential sinkholes), or brecciated/leached zones in gypsum bedrock with air-filled pore space. Laterally continuous layers of high or low resistivity may reflect near-surface stratigraphy, such as gypsum or dolomite beds (generally higher resistivity), or mudstone/shale layers (lower resistivity) in the Los Medaños; or interbedded finer- and coarser-grained sediments in alluvial deposits. Very near-surface high resistivity layers often result from air-filled porosity in soil or weathered bedrock. Areas of medium resistivity may reflect sediment-filled voids.

Results

Sinkhole surveys

Processed data for all the resistivity surveys of karst features identified during surface reconnaissance are provided in Appendix A. Maps showing locations of the surveys with respect to surface geology are provided in Figures 2 and 3, and in more detail in Appendix B and C.

This section of the report addresses the six specific areas with a high estimated hazard potential based on surface geologic mapping, quantitative evaluation of the features, and ER surveys. The southernmost area (stations 0.75E/0.75W) is located about three-fourths of a mile

(1.2 km) from the Texas state line (as indicated, “E” and “W” refer to the relative position of a station east or west of the highway at the given mileage). The remaining five potential hazard areas are located between 7.5 and 14.5 mi. (12-23 km) north of the Texas state line (stations 7.75E, 8.6E/8.6W, 9.7E, 12.3E/12.3W, and 14.1E). All of these sites are located in areas where the gypsiferous Los Medaños member of the Rustler Formation crops out or is present within 2 ft (0.6 m) of the surface.

Where surface karst features are present within 15 ft (4.6 m) of the survey line, their positions are projected onto the resistivity profiles and indicated by black rectangles. Individual resistivity surveys discussed below are labelled according to their proximity to specific karst features identified during the surface reconnaissance. Numbers along the top of each profile represent the distance, in feet, from the beginning of the resistivity survey. Because of the United States customary unit notation of the resistivity profiles, references to specific positions on the profiles are given in feet without metric equivalents in the figures.

Station 0.75E

The southernmost site is on the east shoulder right-of-way at mile 0.75, where a 3 x 8 ft (0.9 x 2.4 m) collapse sinkhole ~3 ft (~0.9 m) deep was identified, formed in an outcrop of gypsum bedrock. The sinkhole appears to be fracture-controlled and displays possible slight airflow.

An ER survey conducted on 31 March 2017 identified a high resistivity anomaly between 80 to 100 ft (24.4-30.5 m) on the profile, ~20 ft (6 m) below ground level (bgl) (Figure 4). This anomaly does not closely correspond to any surface features. The surface sinkhole is underlain by a shallow, laterally extensive layer of moderately high resistivity ~6 ft (~1.8 m) bgl.

Because of the position of the deeper high-resistivity anomaly near the end of the profile, station 0.75E was reoccupied and additional resistivity data were collected on 20 April 2017; the reoccupied section of station 0.75E extended north of the March 2017 survey line. This second survey passes directly over the sinkhole, shown on the profile by a black bar and a depression in the topographic profile. An extensive zone of high resistivity is present beneath that feature (Figure 5), underlain by smaller pods of higher resistivity material, which may be cavities or brecciated zones in gypsum bedrock. A more laterally extensive high resistivity layer ~25 ft (~8 m) bgl probably represents stratigraphic layering of gypsum and/or mudstone within the Rustler Formation.

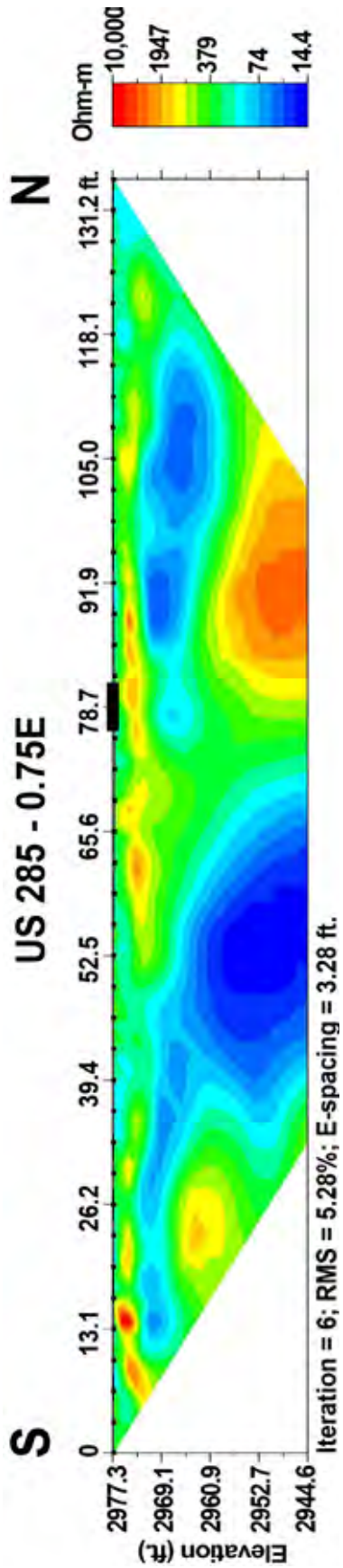


Figure 4. Short ER profile adjacent to sinkhole 0.75E. Sinkhole location shown by black bar.

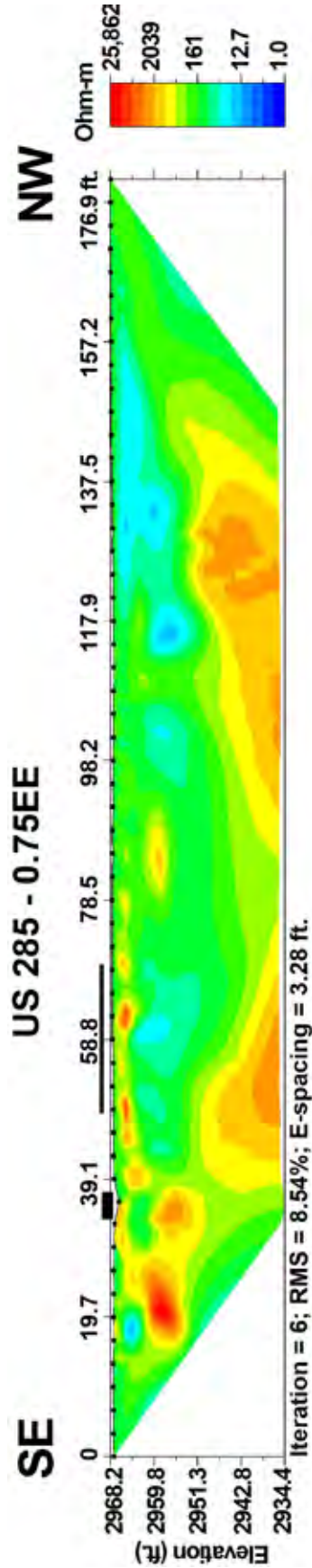


Figure 5. Long ER profile adjacent to sinkhole 0.75E. Sinkhole location shown by black bar. The position of the high resistivity anomaly originally identified at the north end of line 0.75E is shown by a black line centered on 58.8 feet.

The high resistivity anomaly originally identified at the north end of the profile is not visible in this record, suggesting that it was a data-processing artifact.

Station 0.75W

The southernmost site on the west shoulder, directly across from station 0.75E, includes a 4 x 5 ft (1.2-1.5 m) sinkhole ~1 ft (~0.3 m) deep, plus three smaller holes <1 ft in diameter. An ER survey conducted on 31 March 2017 shows a high resistivity anomaly between 95-110 ft (29-33.5 m) on the profile, ~15 ft (~5 m) bgl (Figure 6). The anomaly does not correspond to any surface features. The surface sinkholes are underlain by a laterally extensive zone of moderately high resistivity.

Because of the position of the deeper high resistivity anomaly near the end of the profile, station 0.75W was reoccupied and additional resistivity data were collected on 20 April 2017 that was extended north of the March 2017 survey line. The original high resistivity anomaly, shown by a black line in Figure 7, is underlain by a laterally extensive zone of moderately high resistivity ~6 ft (~1.8 m) bgl, which may represent a leached zone in gypsum bedrock. A pod of very high resistivity not present in Figure 5 is present at the extreme southern end of this profile, which suggests that it may be a data processing artifact.

Station 7.75E

Three large sinkholes (>10 ft or 3 m diameter and 5 ft or 1.5 m deep) were identified at this site, formed in Quaternary sediment underlain by gypsum bedrock, which is exposed at the bottom of the sinkholes. These features occur in a broad swale on both sides of the right-of-way fence. An ER survey was conducted on 30 March 2017 immediately west of two of the sinkholes on the east side of the fence and skirted one large sinkhole on its west side. The latter feature shows up clearly as a high resistivity anomaly between ~170 to 180 ft (~51.8-54.9 m) on the profile (Figure 8). An elongate depression on the east side of the fence with a deep sinkhole at the south end roughly coincides with a zone of moderate to high resistivity between 80-115 ft (24.4-35.1 m) on the ER profile. AFW borehole 9 encountered a possible cavity at 7.5 ft (2.3 m) bgl, projected onto the survey line at 98 ft (29.9 m). Given the size of the sinkholes at this site, it is interesting to note that none of the high resistivity anomalies extend more than 15 ft (4.6 m) bgl.

Station 8.6W

This site has a very high concentration of sinkholes, some of which may be cave entrances, over a distance of about 250 ft (76 m), formed in soil and gypsum bedrock on the eastern edge of a broad, shallow (<2

ft/0.6 m deep) subsidence depression. An ER survey was conducted on 29 March 2017, with the array of cable deployed between and immediately adjacent to most of the sinkholes. The ER profile shows some high resistivity anomalies that coincide with the surface features (Figure 9). However, none of the anomalies extend more than 10 ft (3 m) beneath the surface, possibly due to a layer of insoluble mudstone underlying the gypsum beds, which is indicated by a layer of more conductive material on the profile (blue shading). The north end of the survey line actually passes directly over two sinkholes, as can be seen on the topographic profile, yet those features do not manifest at all in the ER survey data. Thus, in spite of the abundance of surface features, these sinkholes do not appear to have deep roots.

Station 8.6E

An ER survey was conducted at this site on 21 April 2017. No surface karst features are present at this station; motivation for this survey was proximity to the extensive cluster of sinkholes directly across the highway at station 8.6W (Figure 9). The ER profile (Figure 10) shows a large high resistivity zone between 105-130 ft (32-39.6 m) on the profile, ~15 ft (~4.6 m) bgl, along with several smaller anomalies beneath the western half of the survey line. Maximum resistivity is only 7000 ohm-m, so these features may represent highly brecciated or leached intervals in gypsum bedrock rather than open cavities. Alternatively, the deeper anomaly may simply be the result of irregular paleotopography, i.e., a karst pinnacle, developed on top of the Los Medaños gypsum (e.g., Land and Asanidze, 2015). Nevertheless, the presence of abundant surface karst features on the west shoulder and high resistivity anomalies beneath the east shoulder suggests a high karst hazard potential at mile 8.6.

Station 9.7E

This station includes the sinkhole originally identified by NMDOT in 2015, plus two additional sinkholes formed in gypsum bedrock that crops out within 20 ft (6 m) of the original sinkhole. One of the sinkholes may be the entrance to a cave, but it is not enterable by humans. Additional sinkholes are present on the east side of the right-of-way fence.

Two resistivity surveys were conducted at this site as a proof of concept of the ER survey method to NMDOT. The survey conducted on 11 November 2016 used 70 electrodes at 3.3 ft (1 m) spacing for a target exploration depth of 35 ft (11 m; Figure 11A). The ER survey line passes 6 ft (1.8 m) east of the possible cave entrance formed in gypsum bedrock at ~112 ft (34.1 m) on the profile. That feature is represented by a shallow (3-8 ft

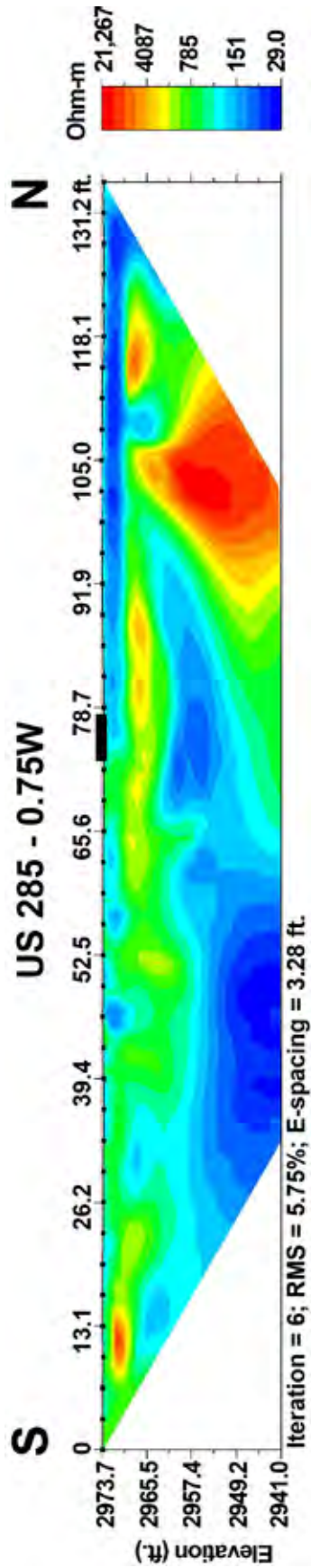


Figure 6. Short ER profile adjacent to sinkhole 0.75W. Sinkhole location shown by black bar.

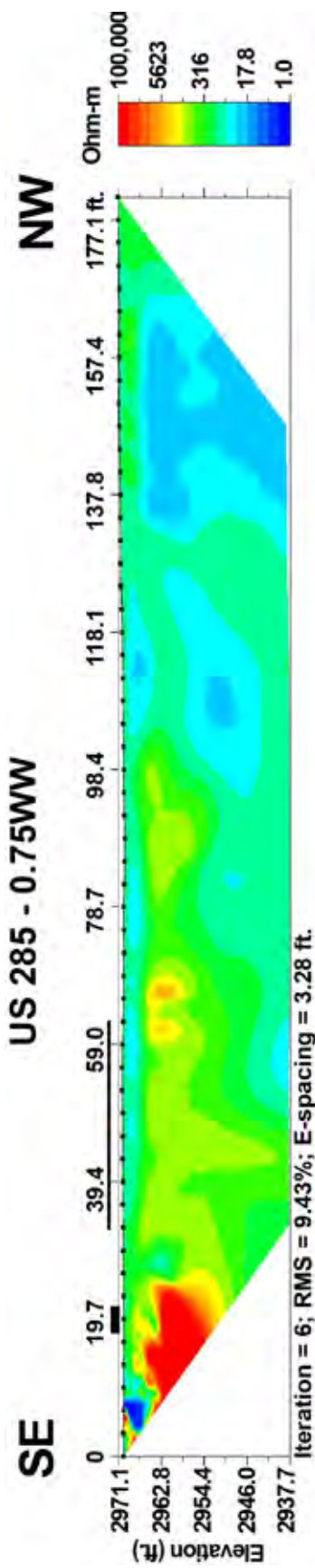


Figure 7. Long ER profile adjacent to sinkhole 0.75W. Sinkhole location shown by black bar. The position of the high resistivity anomaly originally identified at the north end of line 0.75W is shown by a black line centered on 50 feet.

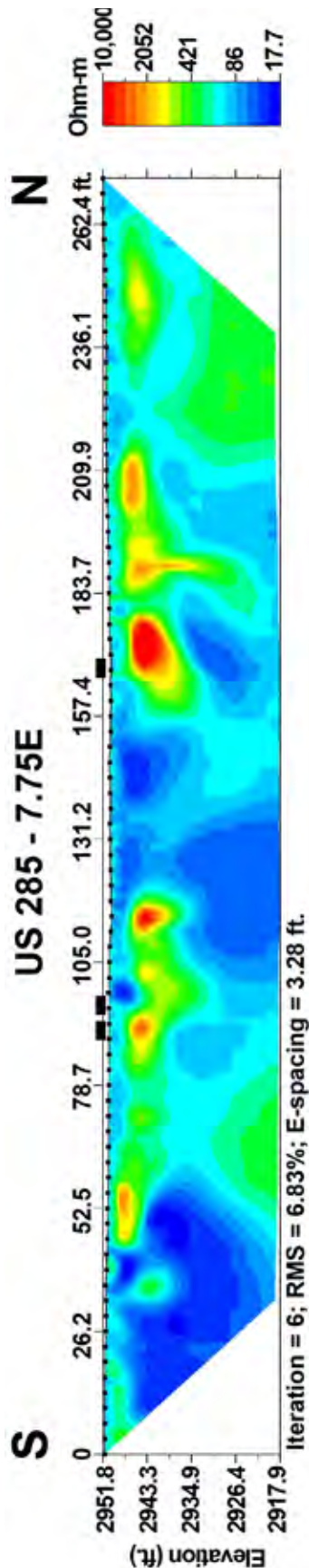


Figure 8. ER profile at station 7.75E. Sinkhole locations are projected onto the survey line and shown by black bars.

deep) zone of high resistivity that extends laterally from ~65-125 ft (~19.8-38.1 m). That high ER anomaly connects to a deeper zone of high resistivity at the south end of the profile, ~20 ft (~6 m) bgl, indicating the presence of either a subsurface cavity or brecciated zone within Rustler gypsum. In contrast to most of the other sites surveyed, the surface karst features identified at station 9.7E appear to extend deeper into the subsurface.

The survey conducted on 8 November 2016 used 112 electrodes at 19.7-ft (6-m) spacings, and achieved an exploration depth of 410 ft (125 m; Figure 11B). This survey is centered on the shorter array, which is shown in Figure 11B by a red bar. The shallow karst features imaged on the 70-electrode survey are still visible as near-surface high resistivity anomalies. This survey also shows a pod of moderately high resistivity (~2000-5000 ohm-m) near the center of the profile ~130 ft (~40 m) bgl, which may indicate the presence of a filled cavity or brecciated zone.

Station 12.3W

An ER survey was conducted at this site on 28 March 2017 adjacent to two large sinkholes ~5 ft (1.5 m) in diameter and 4 ft (1.2 m) deep, with cave openings at the bottom in gypsum bedrock. Two near-surface (<5 ft or 1.5 m bgl) high resistivity anomalies coincide with locations of the two sinkholes mapped at the surface, which are ~15 ft (~4.6 m) west and 3 ft (0.9 m) east of the survey line (Figure 12). A resistivity anomaly of similar depth at the south end of the profile does not correspond with any observed surface features. These anomalies do not appear to extend more than 6 ft (1.8 m) bgl. A deeper discontinuous layer of somewhat higher resistivity (<500 ohm-m) probably reflects subsurface stratigraphy (gypsum beds).

Station 12.3E

An ER survey was conducted at this station on 20 April 2017. No surface karst features were observed at this station; motivation for this survey was the presence of large sinkholes directly across US 285 on the west shoulder. A distinct pod of high resistivity is present ~10 ft (3 m) bgl at the south end of the survey line (Figure 13). Abundant oil field infrastructure is present in this area; it is thus possible that this anomaly may represent a buried pipeline. However, the relatively high resistivity values (>10,000 ohm-m), combined with the presence of large sinkholes directly across the highway, support the possibility that this feature may be a subsurface void.

Station 14.1E

An ER survey was conducted at this site on 27 March 2017. This station is so designated because it begins

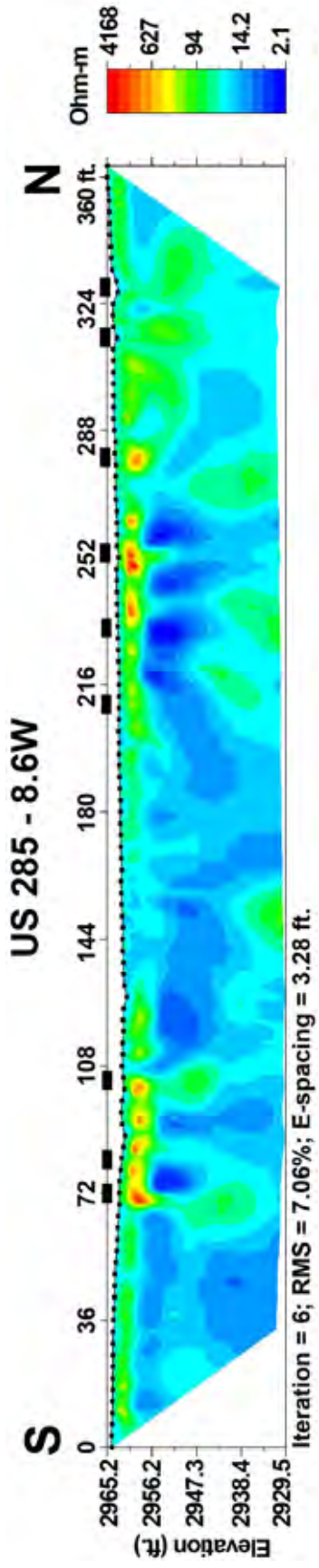


Figure 9. ER profile at station 8.6W. Sinkhole locations are projected onto the survey line and shown by black bars.

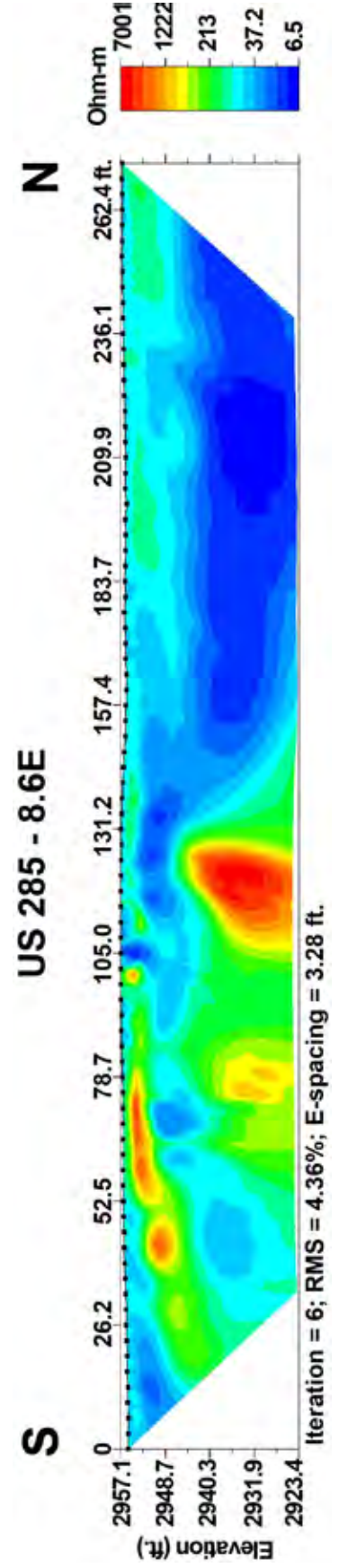
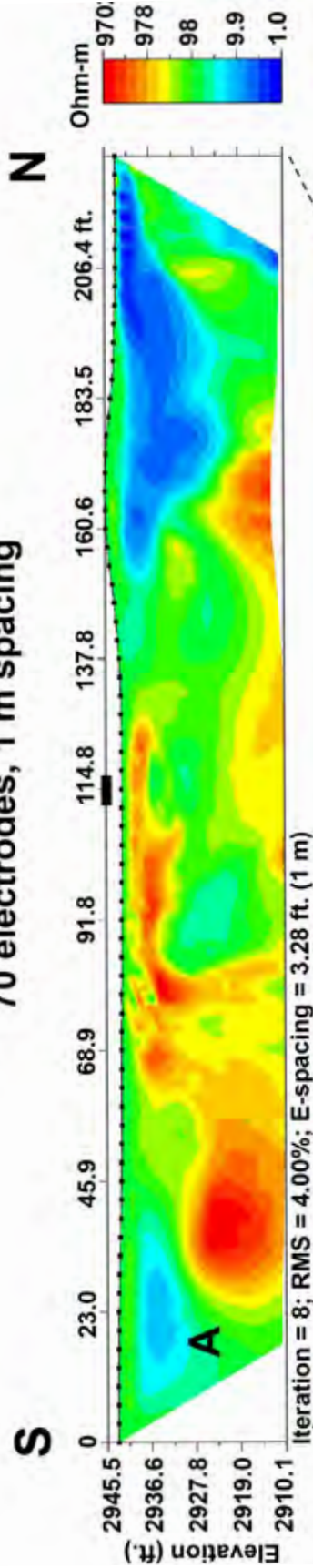


Figure 10. ER profile at station 8.6E.

**US 285, east shoulder, 9.7 miles:
70 electrodes, 1 m spacing**



**US 285, east shoulder, 9.7 miles:
112 electrodes, 6 m spacing**

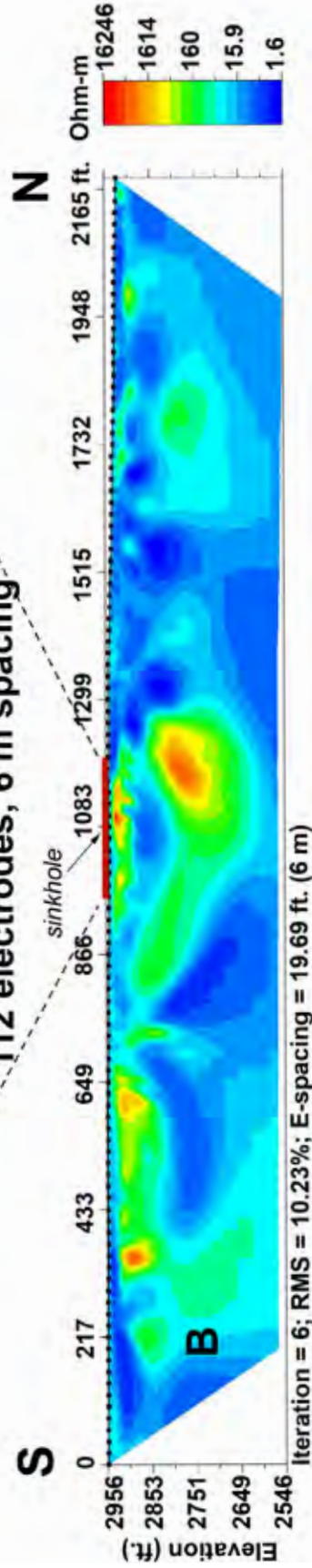


Figure 11A. Short ER profile at station 9.7E, 70 electrodes; electrode spacing = 3.3 feet (1 m). Sinkhole location projected onto survey line and shown by black bar.

Figure 11B. Long ER profile at station 9.7E, 112 electrodes, electrode spacing = 19.7 feet (6 m). Position of the sinkhole with the possible cave entrance is projected onto the profile in 10A and indicated in 10B by an arrow. Position of the 70-electrode profile with respect to the 112-electrode profile is shown by a red bar in Figure 10B.

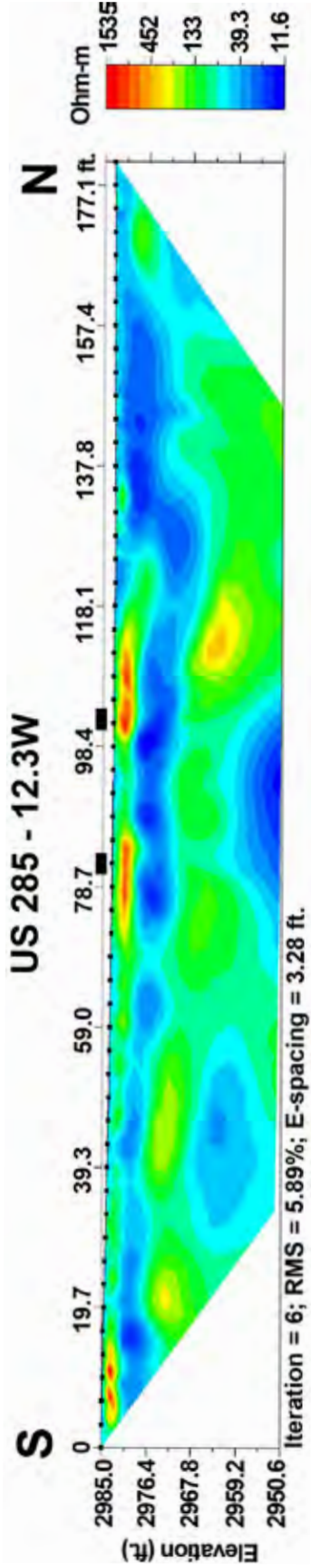


Figure 12. ER profile at station 12.3W. Sinkhole locations are projected on the survey line and shown by black bars.

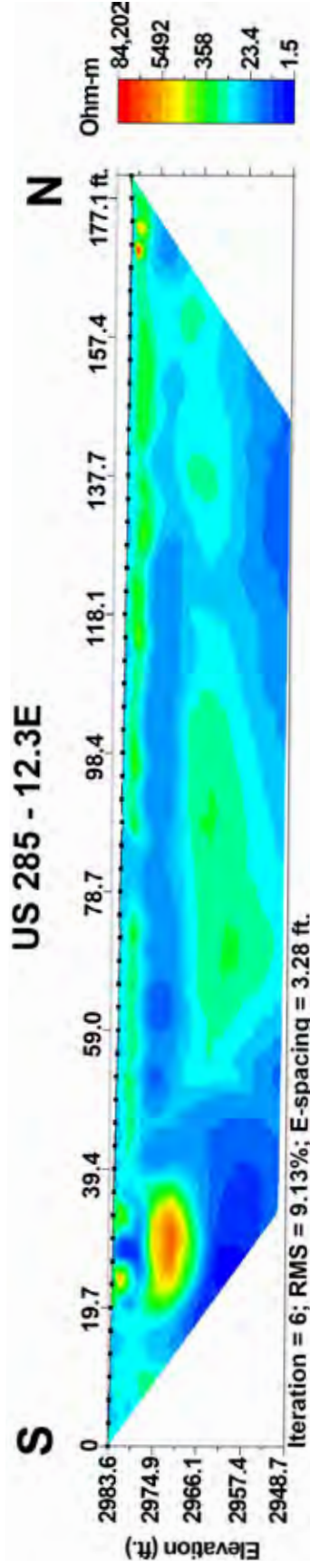


Figure 13. ER profile at station 12.3E.

near karst feature 285E-14.1. The ER survey line is directly adjacent to karst feature 285E-14.2a, a sinkhole 4 ft (1.2 m) in diameter and 7 ft (2.1 m) deep, formed in gypsum bedrock with a small cave entrance, and displaying slight airflow. A high resistivity anomaly is clearly visible ~5 ft (1.5 m) bgl between ~177 and 203 ft on the profile (Figure 14). The specific location of the sinkhole is at 203 ft; the resistivity data thus suggest that the cavity may extend laterally 25 ft (7.6 m) to the south in the shallow subsurface. Two additional pods of high resistivity occur near the north end of the profile that do not correspond to any observed surface karst features. In spite of the presence of a cave entrance with airflow at the bottom of the sinkhole, the ER data do not indicate any deeper-seated voids.

Bridge surveys

NCKRI and NMBGMR personnel conducted ER surveys of the four bridges in the study area in three phases during the months of April, May, and June 2017. The April surveys focused on the bridge abutments and piers and were conducted perpendicular to the roadway, along the slopes beneath the bridges. Surveys of the bridge abutments parallel to the roadway and at road level were conducted in May. The April and May expeditions used 42-electrode arrays with a 3.3-ft (1-m) electrode spacing for a target exploration depth of ~35 ft (~11 m). Surveys conducted in June were configured to achieve 100-ft (30-m) depths of investigation, and employed 56-electrode arrays at 10-ft (3-m) spacing. These surveys paralleled the highway and extended across the entire stream valleys.

Delaware River bridge surveys

ER surveys were conducted beneath the Delaware River bridge (Figure 15) on 17–18 April 2017 at the base of the north and south bridge abutments and the five piers supporting the bridge span. No surface karst features were observed at this site, and surface material consisted of alluvial sediment of the Delaware River floodplain. The profiles in general display low to moderate resistivity values, typical of finer-grained silt and mud (Figures 16–22). Small, shallow (<10 ft or 3 m bgl) pods of higher resistivity probably represent air-filled porosity in coarser-grained sand and gravel bars.

Two exceptions to the above characterization of the Delaware River bridge surveys were observed. The Delaware River flows between the fourth and fifth bridge piers (counting from the south). The resistivity survey conducted adjacent to the fourth pier from the south shows several high resistivity pods beneath the northeast end of the survey line and under the northeast edge of the bridge (Figure 20). A USGS stream gage

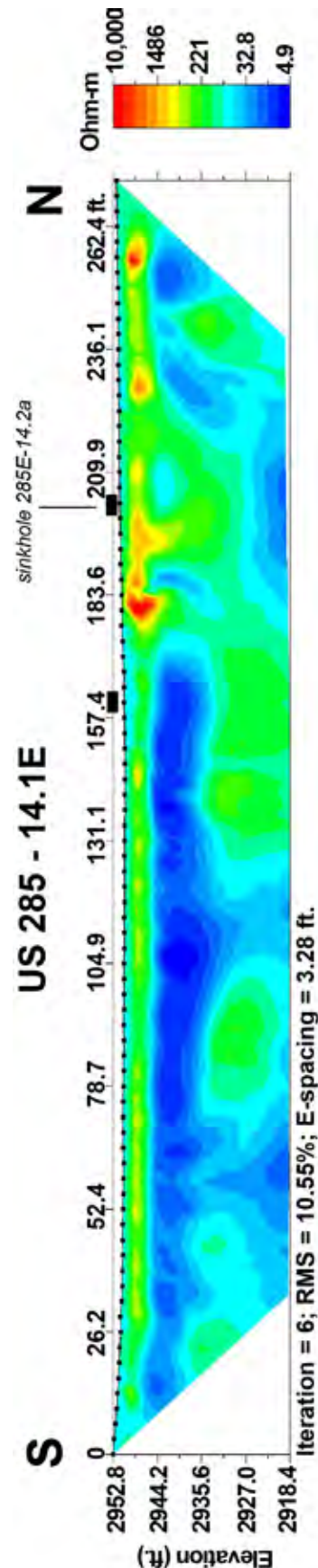


Figure 14. ER profile at station 14.1E. Sinkhole locations are projected onto the survey line and shown by black bars.



Figure 15. Delaware River bridge

is attached to the bridge at this location, with a stilling well constructed of corrugated metal. The gaging station is telemetered, and discussion with USGS personnel confirmed that the stilling well is being used to ground their instruments. The high resistivity anomalies are probably the result of noisy data caused by the grounded electronics.

A second anomalous feature is present on the ER survey conducted at the base of the northern bridge abutment, where a broad zone of very conductive material (<5 ohm-m) occurs beneath the bridge ~15 ft (~4.6 m) bgl (Figure 22). Discussion with AFW engineers revealed that broad concrete aprons and other buried anthropogenic material are present beneath the Red Bluff Draw and Salt Draw bridge abutments (discussed below). It thus seems probable that the very low resistivity observed on the profile of the north abutment reflects the presence of a buried concrete apron containing electrically conductive iron reinforcing rods.

Road-level ER surveys of the Delaware River bridge abutments were conducted on 3–4 May 2017, parallel to US 285. The ER survey of the northeast abutment shows a shallow high resistivity anomaly centered at ~13 ft (~4 m) from the north end of the profile and another centered at ~26 ft (~8 m; Figure 23). This section of the resistivity array was located on an old roadbed immediately adjacent to a concrete pad ~25 ft (~7.6 m) long. The high ER anomaly is thus probably indicative of concrete and other roadbed material (but apparently no rebar) at the surface and in the shallow subsurface. A broad zone of higher resistivity 20-25 ft (6-7.6 m) bgl

probably reflects gypsum bedrock, which crops out on both sides of the river valley.

The three remaining bridge abutment surveys (Figures 24–26) show a discontinuous layer of higher resistivity (green shading) extending across the profiles at 15–20 ft (4.6–6 m) bgl. This layer probably also represents gypsum bedrock. A small pod of higher resistivity material ~15 ft (~4.6 m) bgl is present on the southwest abutment survey between 65-78 ft (19.8-23.8 m) that may represent a filled cavity or brecciated zone. Otherwise, there is no significant evidence of karst geohazards on these surveys.

Long-array ER surveys were conducted on both sides of the Delaware River bridge, perpendicular to the stream valley, on 5–6 June 2017, achieving a depth of investigation of ~130 ft (40 m) (Figures 27 and 28). The survey of the northeast side of the bridge was shortened by 108 ft (33 m) because of a dense stand of mesquite blocking the survey line. The ER profiles for the most part show moderate to low resistivity material (<3000 ohm-m), with no evidence of deeper-seated cavities or other karst geohazards.

An interesting feature of both profiles is an indication of more generally resistive material on the northwest side of the river valley. This phenomenon may reflect differences in the bedrock weathering profile of the Los Medaños gypsum. Surface geologic mapping indicates that a more extensive alluvial cover as well as older alluvial deposits are present northeast of the Delaware River than are observed to the southwest. This distribu-

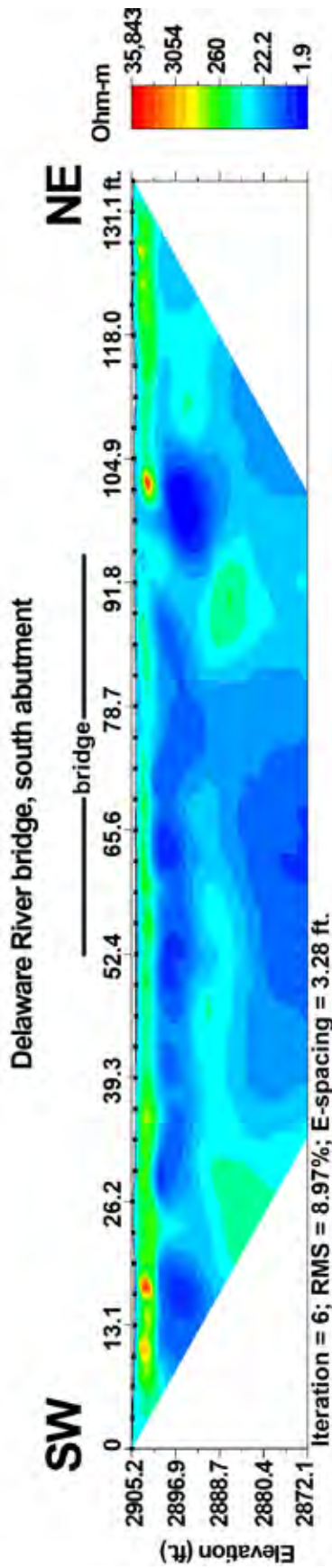


Figure 16. ER survey of Delaware River bridge, south abutment. Position of bridge shown by black bar.

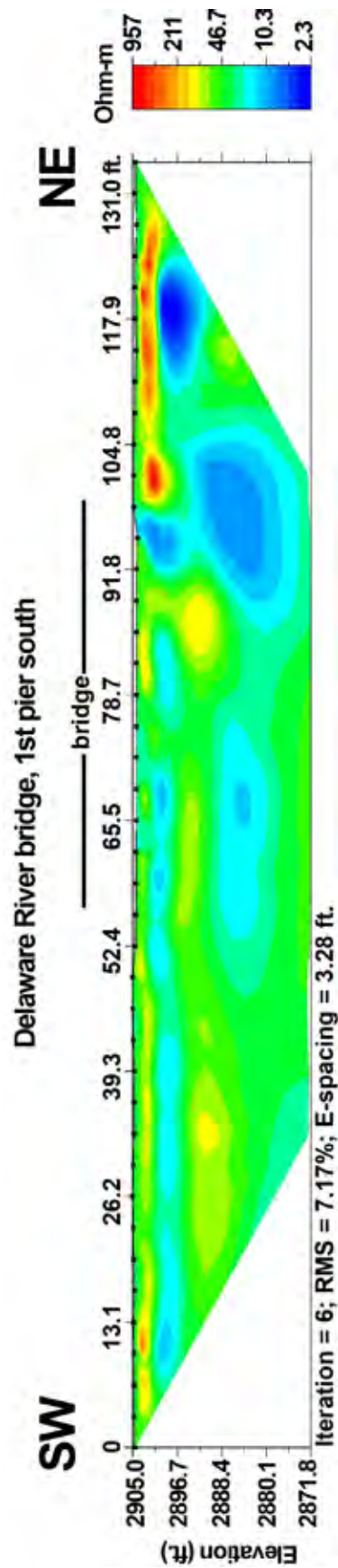


Figure 17. ER survey of Delaware River bridge, first pier from the south. Position of bridge shown by black bar.

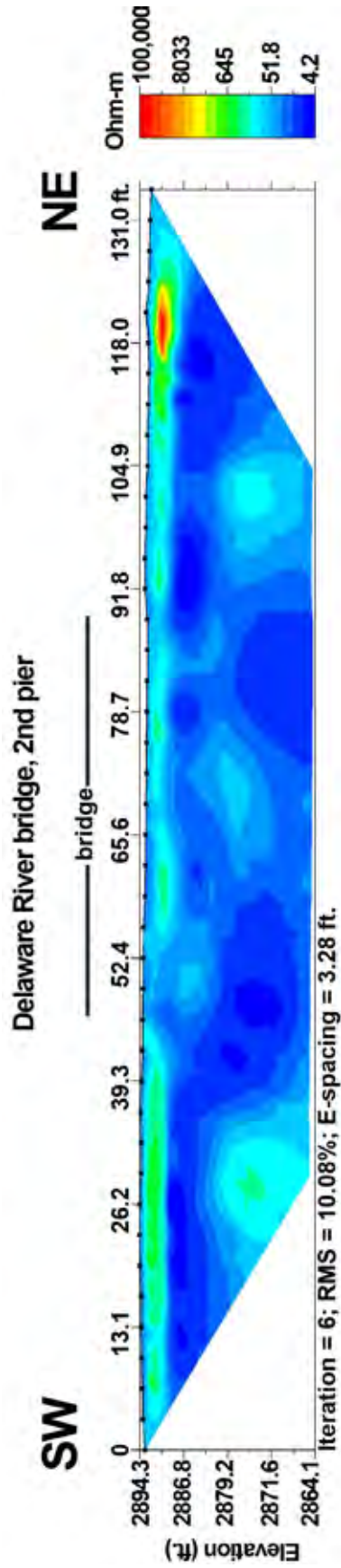


Figure 18. ER survey of Delaware River bridge, second pier from the south. Position of bridge shown by black bar.

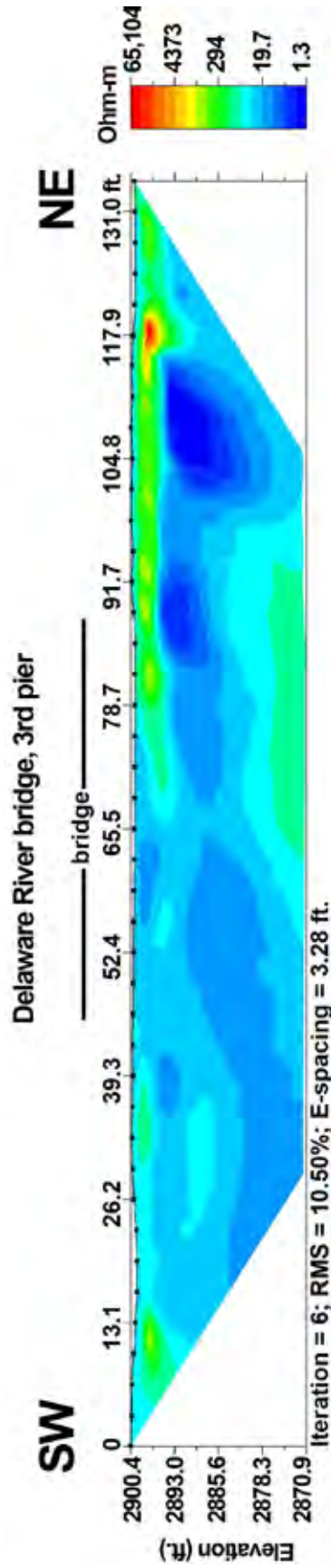


Figure 19. ER survey of Delaware River bridge, third pier from the south. Position of bridge shown by black bar.

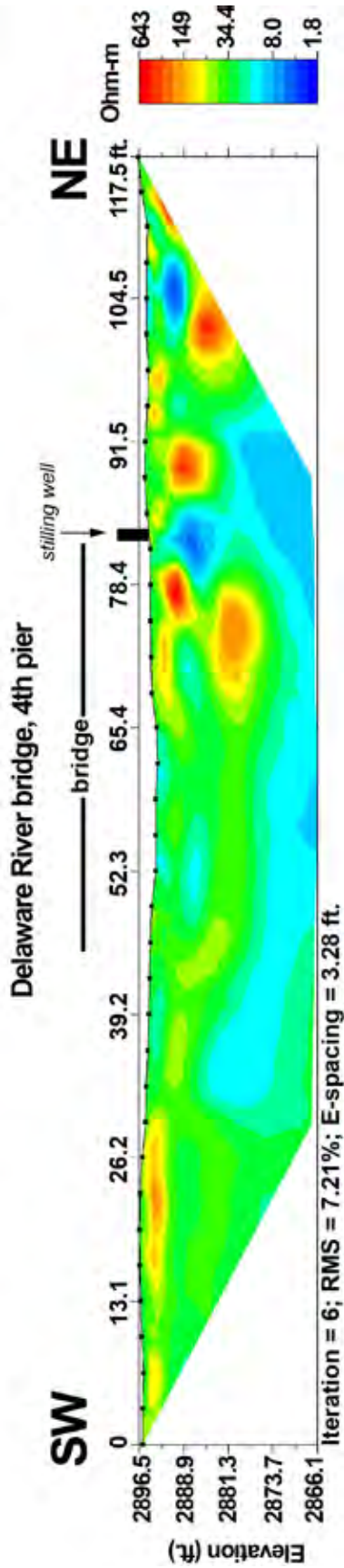


Figure 20. ER survey of Delaware River bridge, fourth pier from the south. Position of bridge shown by black bar.

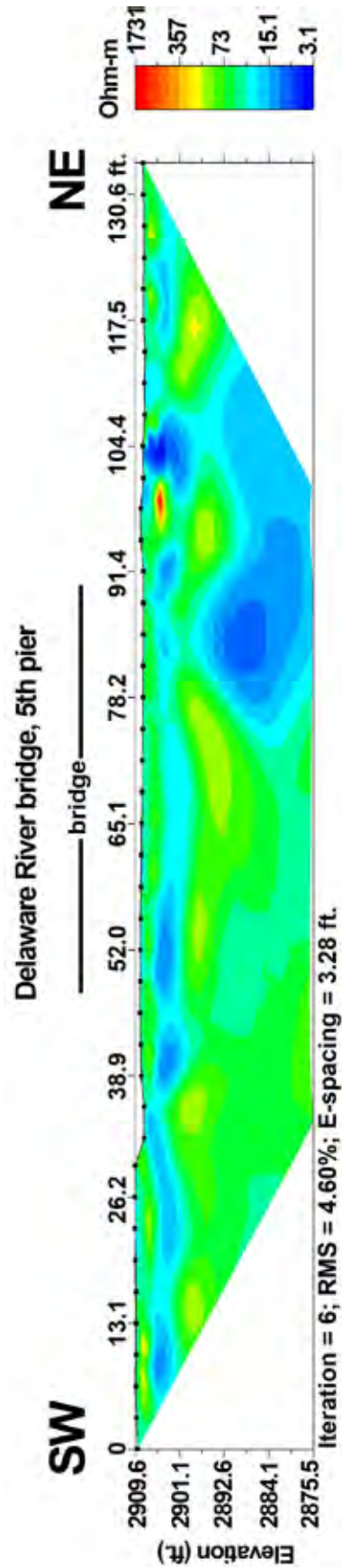


Figure 21. ER survey of Delaware River bridge, fifth pier from the south. Position of bridge shown by black bar.

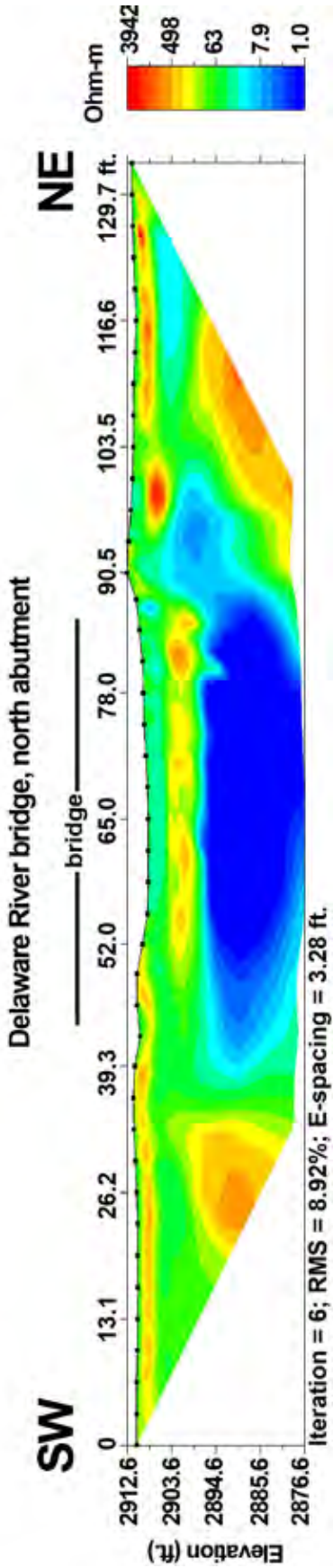


Figure 22. ER survey of Delaware River bridge, north abutment. Position of bridge shown by black bar.

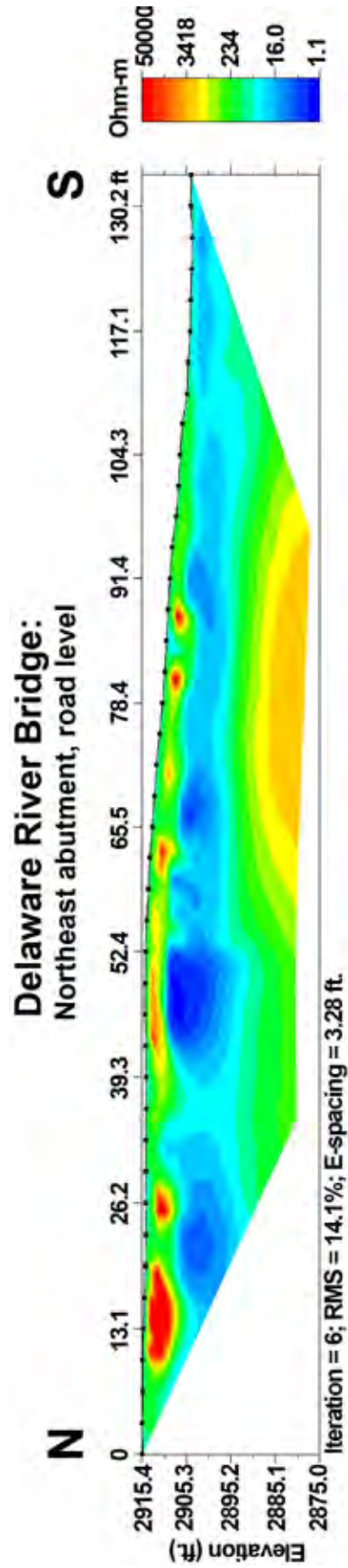


Figure 23. ER survey of Delaware River Bridge, northeast abutment.

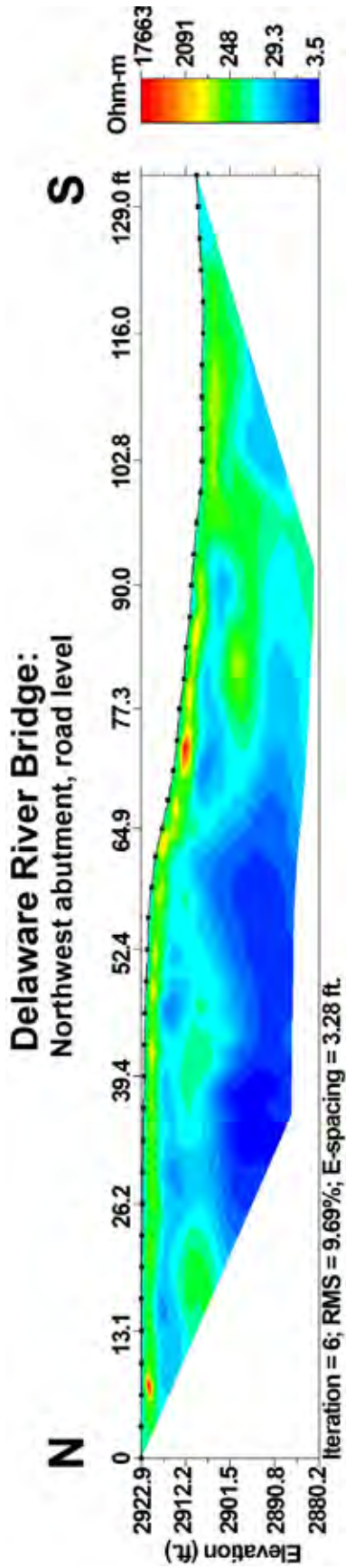


Figure 24. ER survey of Delaware River bridge, northwest abutment.

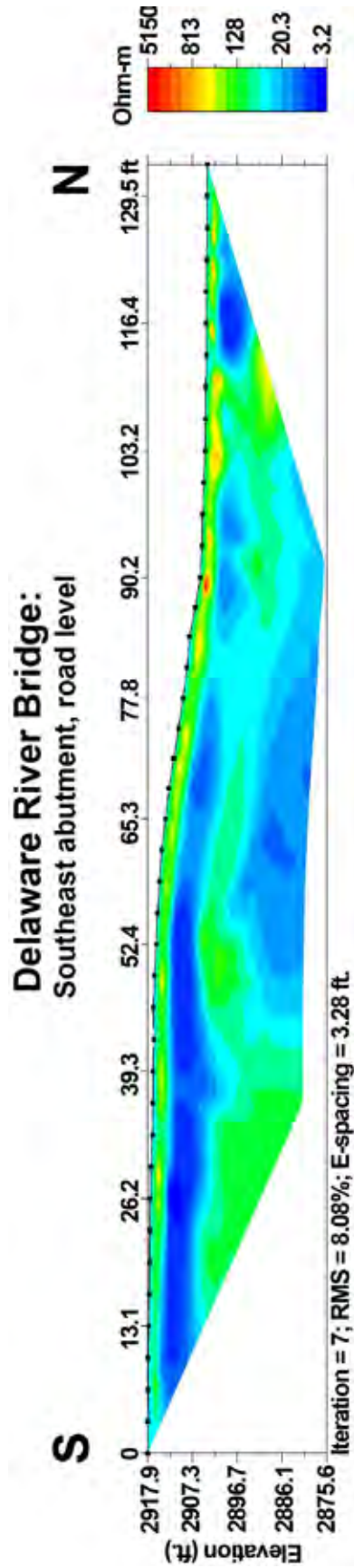


Figure 25. ER survey of Delaware River bridge, southeast abutment.

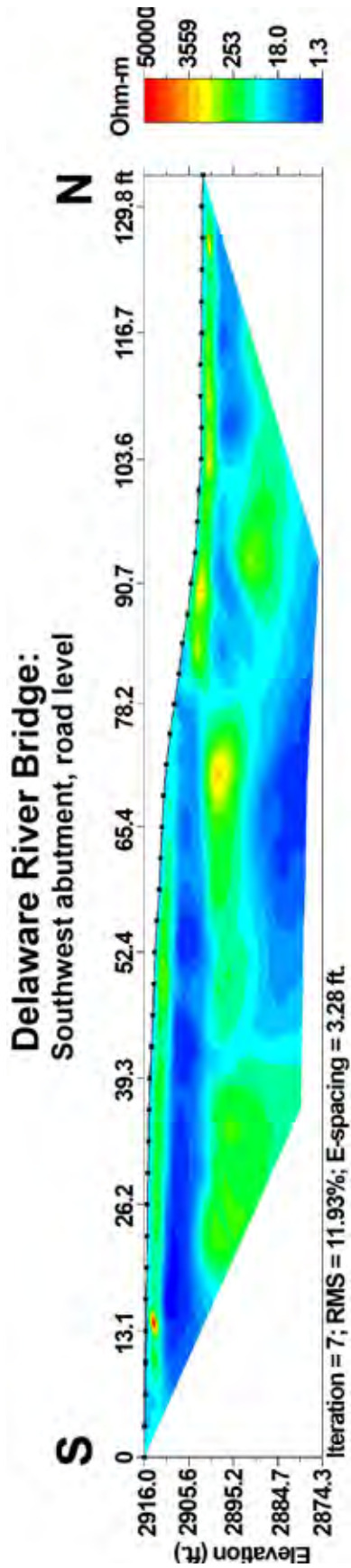


Figure 26. ER survey of Delaware River bridge, southwest abutment.

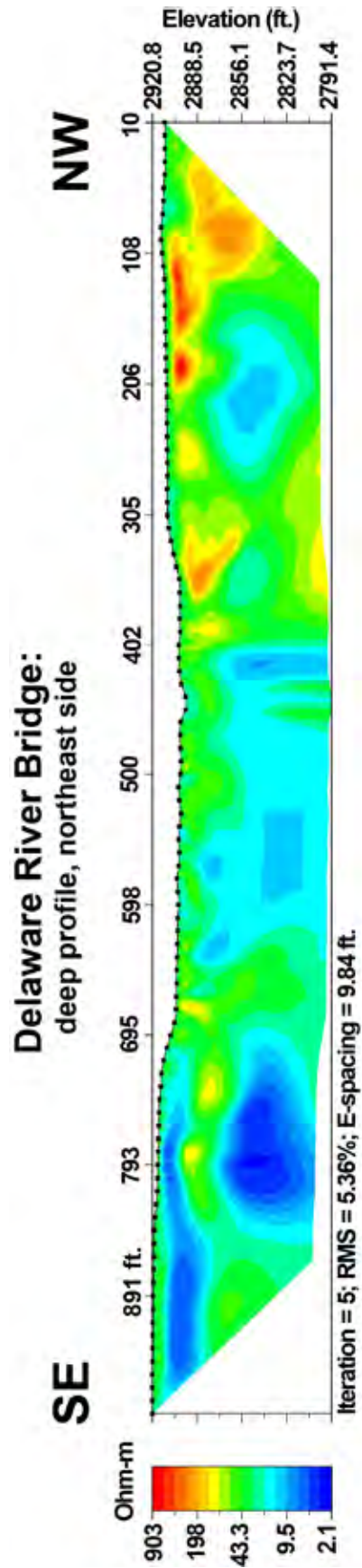


Figure 27. Deep profile, northeast side of Delaware River bridge.

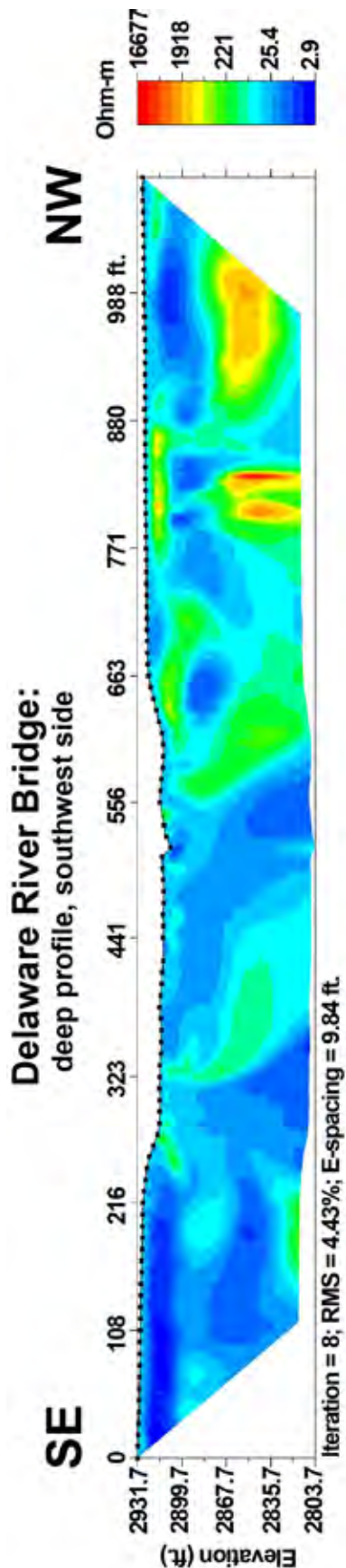


Figure 28. Deep profile, southwest side of Delaware River bridge.

tion of alluvial material suggests that the Delaware River may have previously flowed along a trend further to the northwest of its current location. At that time, leakage from the river could have preferentially weathered the gypsum bedrock, resulting in a lower density lithology and thus higher electrical resistivity. Although speculative, this model would explain some of the variations in bedrock resistivity observed during this investigation. A similar observation would apply to seismic velocities.

Red Bluff Draw bridge surveys

ER surveys were conducted beneath the Red Bluff Draw bridge on 18-19 April 2017 at the base of the north and south bridge abutments and the three piers supporting the bridge span. No surface karst features were observed in the survey area, and surface material consisted of alluvial sediment of the Red Bluff Draw floodplain. The surveys conducted at the base of the north and south bridge abutments show broad zones of very conductive material (<5 ohm-m) beneath the bridge ~15 ft (~4.6 m) bgl (Figures 29 and 30). AFW engineers were able to locate the original drawings for the bridge, which was constructed in 1932. The drawings indicate that both abutments have buried concrete aprons containing metal reinforcing rods, which are probably the cause of the low resistivity values.

The surveys conducted at the base of the three bridge piers (Figures 31–33) all indicate low resistivity material (<100 ohm-m) typical of fine-grained alluvium of the Red Bluff Draw floodplain. Laterally extensive layers of higher and lower resistivity are probably the result of stratification within the floodplain sediment. No evidence of surface or subsurface karst features was observed.

Road-level resistivity surveys of the Red Bluff Draw bridge abutments were conducted on 3 May 2017, parallel to US 285. All four profiles (Figures 34–37) show generally conductive material typical of floodplain sediment. Broad zones of very conductive material (<5 ohm-m) directly beneath all abutments probably result from buried concrete aprons containing rebar, discussed above. The ER data indicate no apparent karst geohazards.

Long-array ER surveys were conducted on both sides of Red Bluff Draw bridge, perpendicular to the stream valley, on 6 June 2017, achieving a depth of investigation of ~125 ft (~38 m). These surveys extended parallel to each side of the bridge across the entire valley of Red Bluff Draw.

The east side profile of Red Bluff Draw bridge shows a

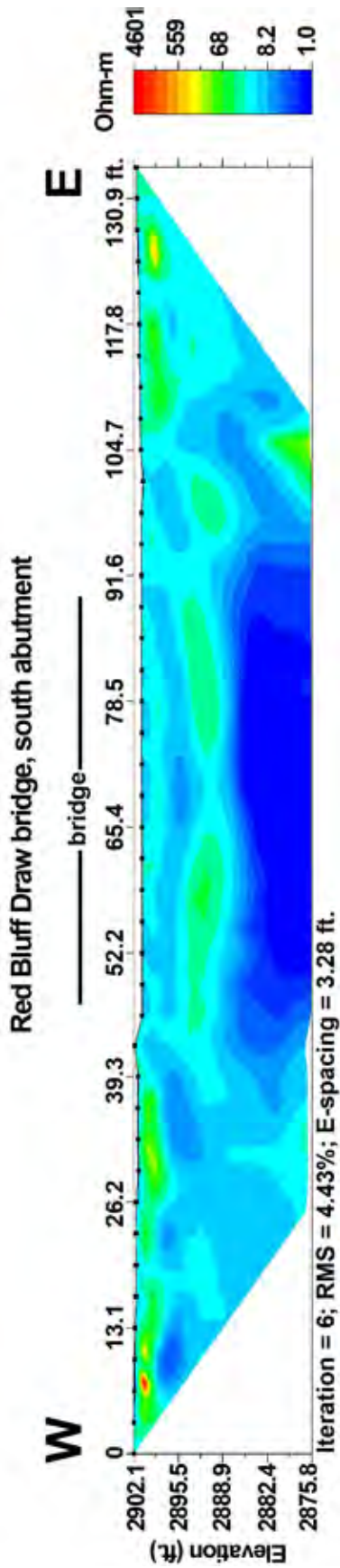


Figure 29. ER survey of Red Bluff Draw bridge, south abutment. Position of bridge shown by black bar.

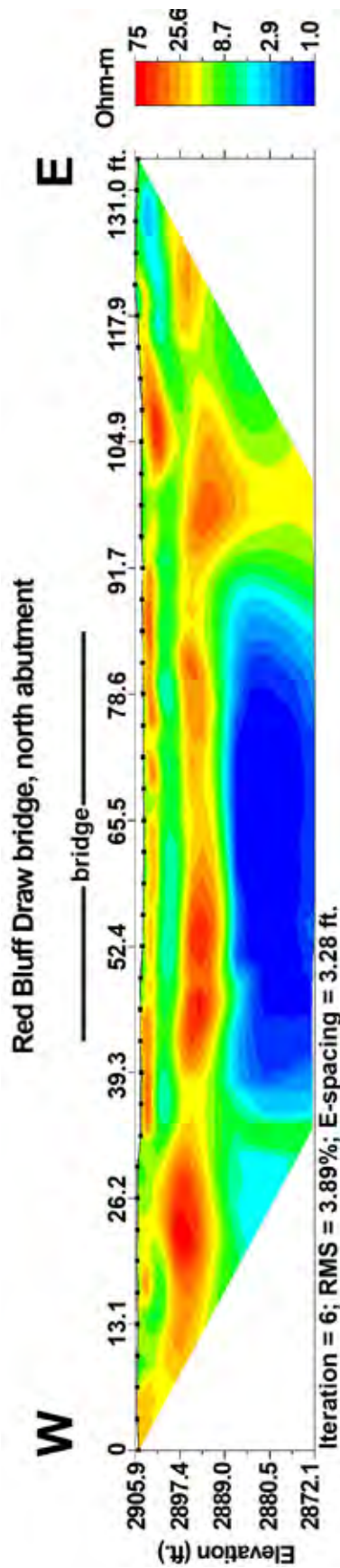


Figure 30. ER survey of Red Bluff Draw bridge, north abutment. Position of bridge shown by black bar.

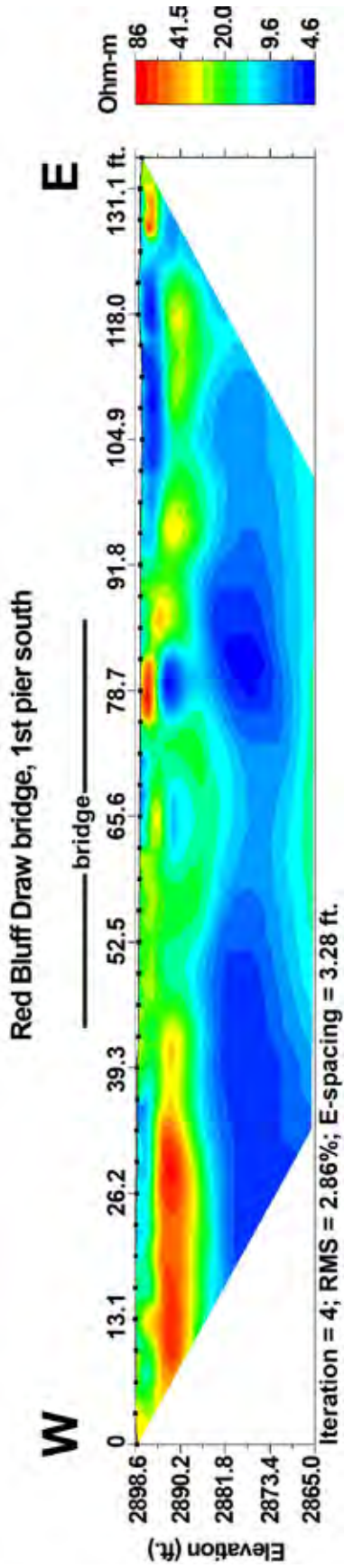


Figure 31. ER survey of Red Bluff Draw bridge, first pier from the south. Position of bridge shown by black bar.

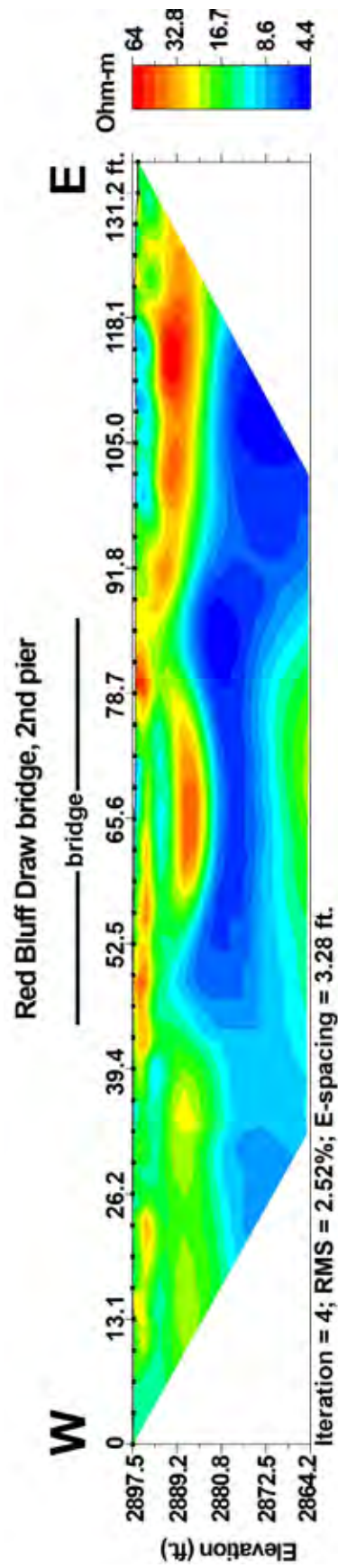


Figure 32. ER survey of Red Bluff Draw bridge, second pier from the south. Position of bridge shown by black bar.

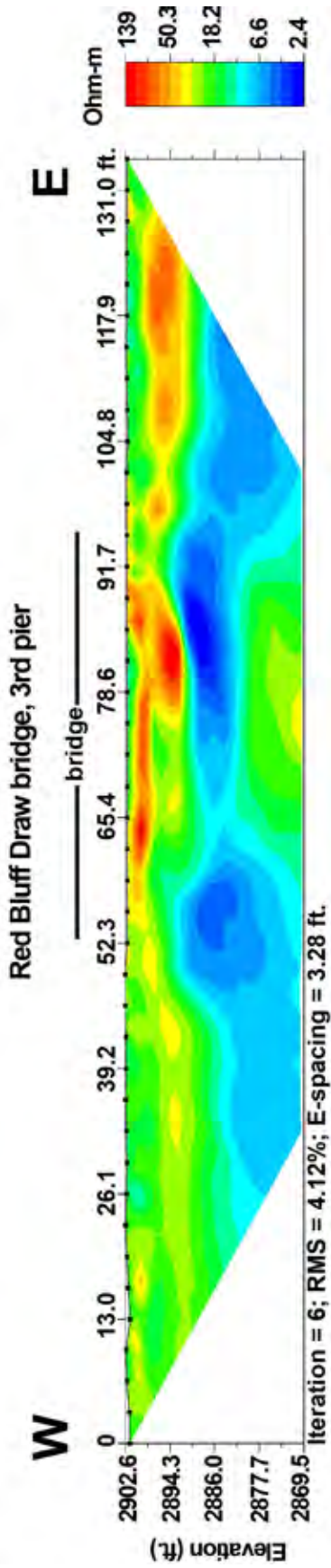


Figure 33. ER survey of Red Bluff Draw bridge, third pier from the south. Position of bridge shown by black bar.

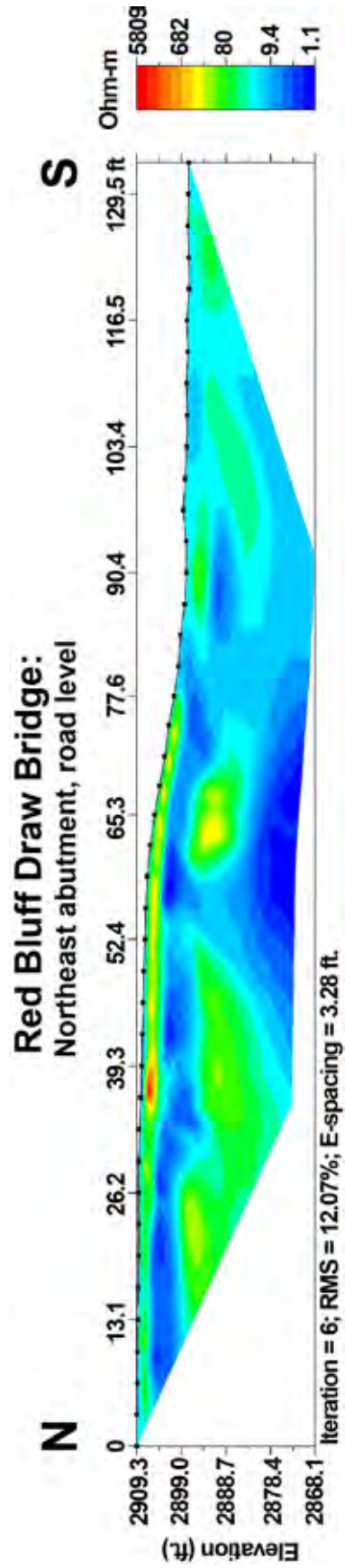


Figure 34. ER survey of Red Bluff Draw bridge, northeast abutment.

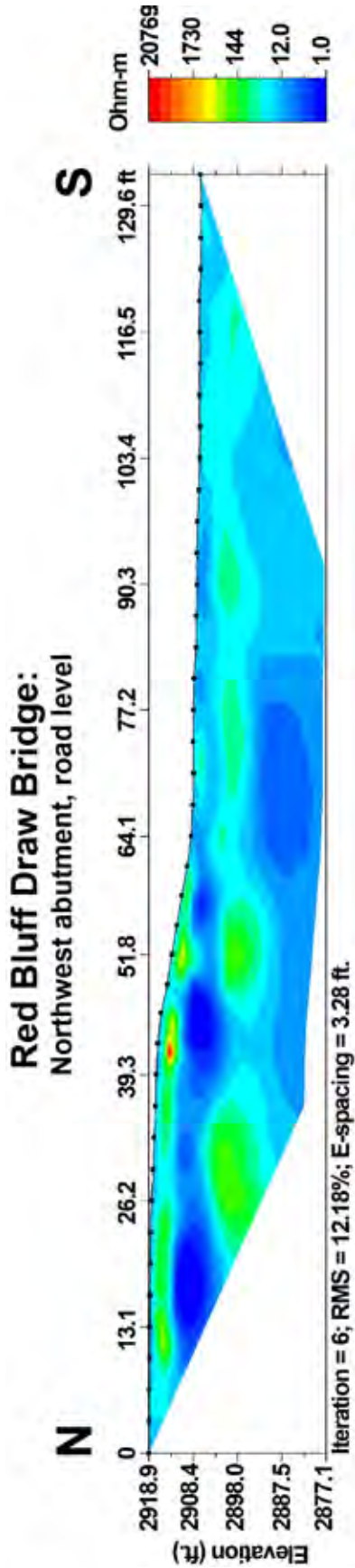


Figure 35. ER survey of Red Bluff Draw bridge, northwest abutment.

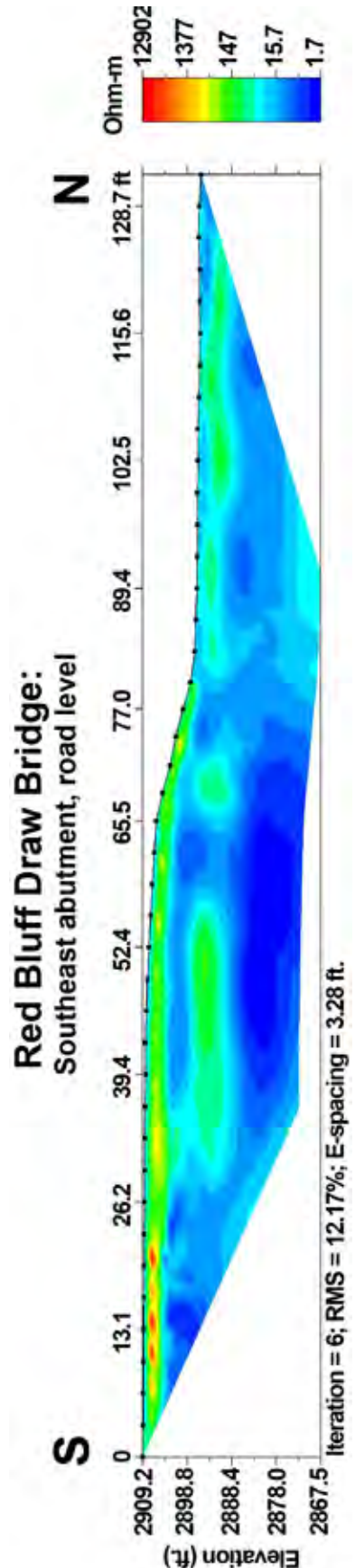


Figure 36. ER survey of Red Bluff Draw bridge, southeast abutment.

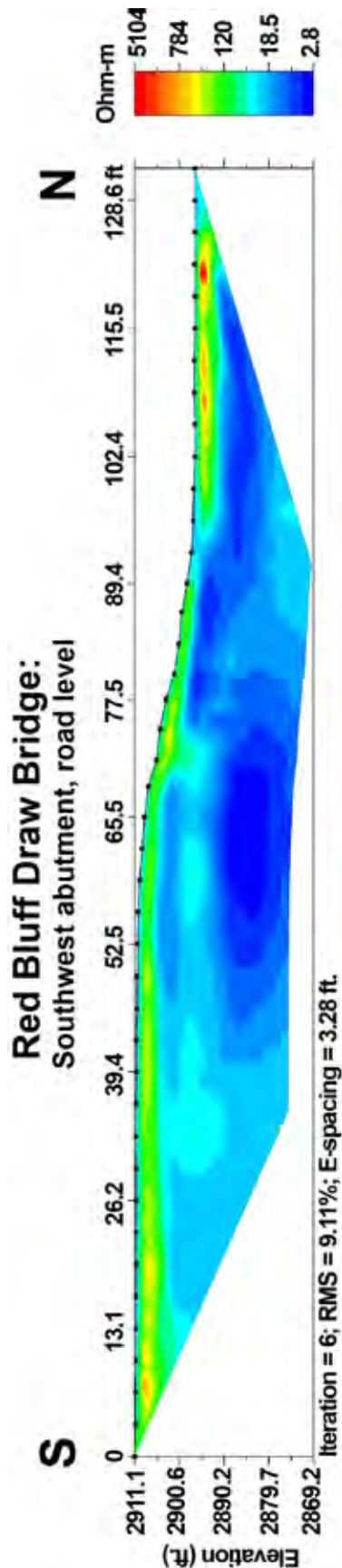


Figure 37. ER survey of Red Bluff Draw bridge, southwest abutment.

distinct zone of higher resistivity ($>70,000$ ohm-m) beneath the south abutment, ~ 75 ft (~ 23 m) bgl (Figure 38). The west side profile shows a resistivity anomaly of similar size beneath the south abutment at about the same depth (Figure 39). A second ER anomaly is present on the west side profile at ~ 60 ft (~ 18 m) bgl beneath the stream bed, centered at ~ 312 ft (~ 95 m). These features probably indicate subsurface cavities in gypsum bedrock,

Salt Draw bridge surveys

ER surveys were conducted beneath Salt Draw bridge on 19–20 April 2017. The Salt Draw bridge surveys presented several challenges because of (1) the presence of anthropogenic material in the subsurface and (2) pier construction, which consisted of steel rather than concrete columns. An additional challenge was that (3) the bases of the north and south abutments were protected by rip-rap with angle iron embedded in the rocks, and the space between the rip-rap/angle iron material and the adjacent steel piers was too narrow to conduct valid ER surveys. Two attempts at the base of the south abutment yielded root-mean-square (RMS) error values $>85\%$. AFW engineers were able to locate the drawings and reports for the Salt Draw bridge, which revealed that the bridge was replaced in 1969, but much of the older bridge foundation material was left behind in the subsurface. Drawings indicated that substantial concrete and metal are buried in the bays between piers 1 and 2; piers 3 and 4; and piers 6 and 7, counting from south to north.

Because the steel columns were sources of electrical noise, it was not possible to conduct ER surveys immediately adjacent to the piers; instead, survey lines were centered on the bays between the piers. The surveys conducted in the bays between piers 1 and 2 (Figure 40), and between piers 6 and 7 (Figure 41), show broad zones of very low resistivity (<5 ohm-m) 10 to 15 ft (3–4.6 m) bgl, confirming evidence provided by AFW personnel of the presence of conductive anthropogenic material in the subsurface (these surveys were conducted prior to discussion with AFW engineers).

The surveys conducted in the bays between piers 2 and 3 (Figure 42); 5 and 6 (Figure 43); and 7 and 8 (Figure 44) all show layers of relatively low resistivity material (<50 ohm-m) that probably represent alluvial floodplain sediments. Thin, shallow layers of higher resistivity material reflect the presence of coarser lenses of sand and gravel within the floodplain material. No evidence of karst geohazards was observed on the ER profiles.

Road-level resistivity surveys of the Salt Draw bridge

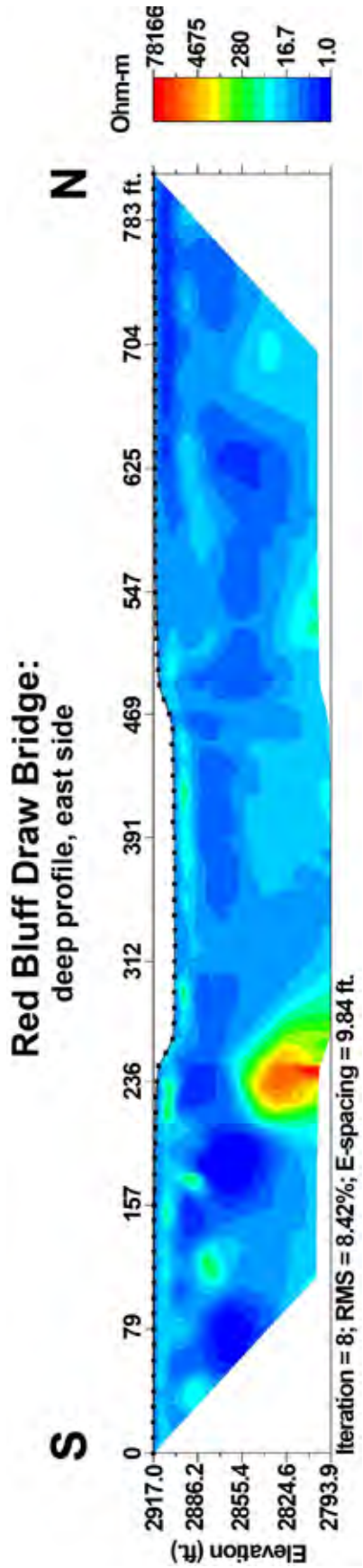


Figure 38. Deep profile, east side of Red Bluff Draw bridge.

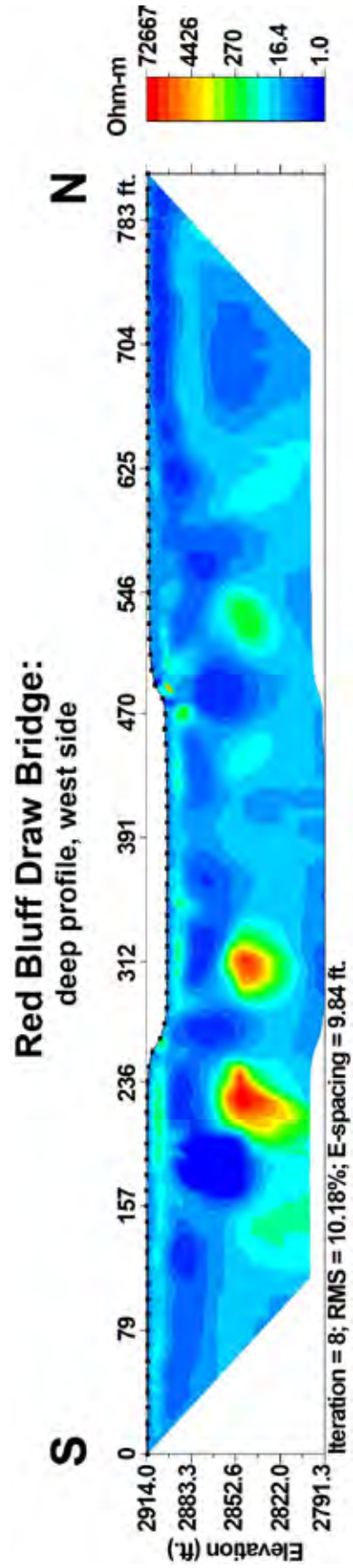


Figure 39. Deep profile, west side of Red Bluff Draw bridge.

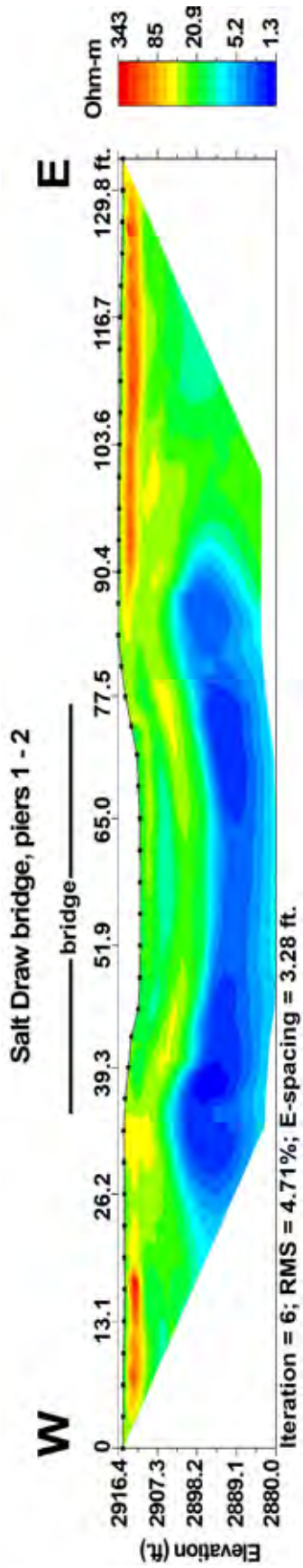


Figure 40. ER survey between piers 1 and 2, counting from the south, Salt Draw bridge. Position of bridge shown by black bar.

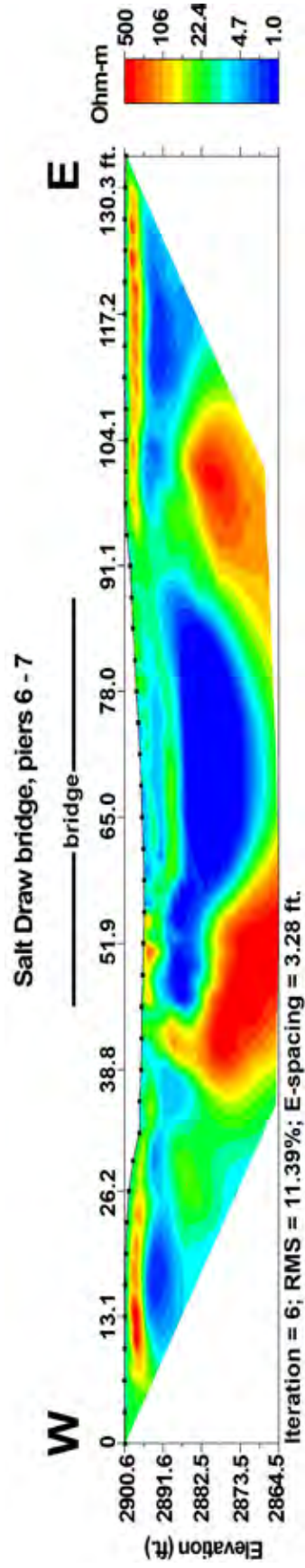


Figure 41. ER survey between piers 6 and 7, counting from the south, Salt Draw bridge. Position of bridge shown by black bar.

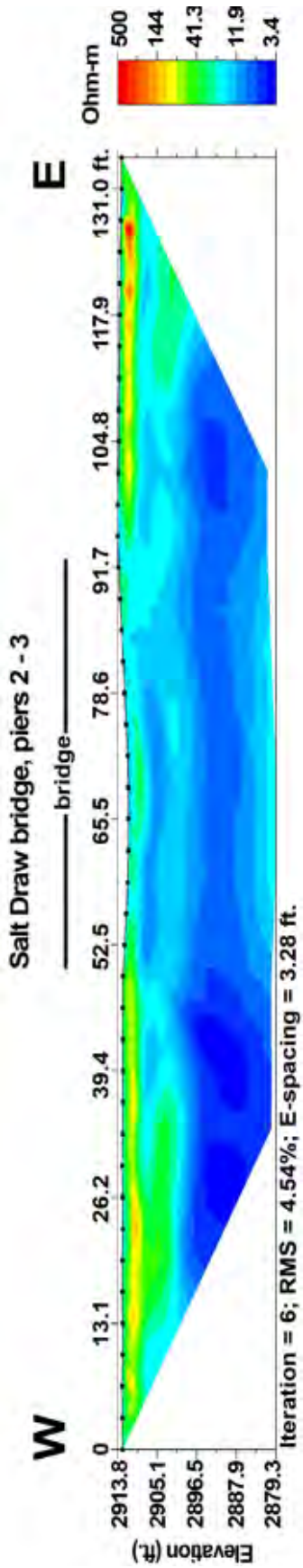


Figure 42. ER survey between piers 2 and 3, counting from the south, Salt Draw bridge. Position of bridge shown by black bar.

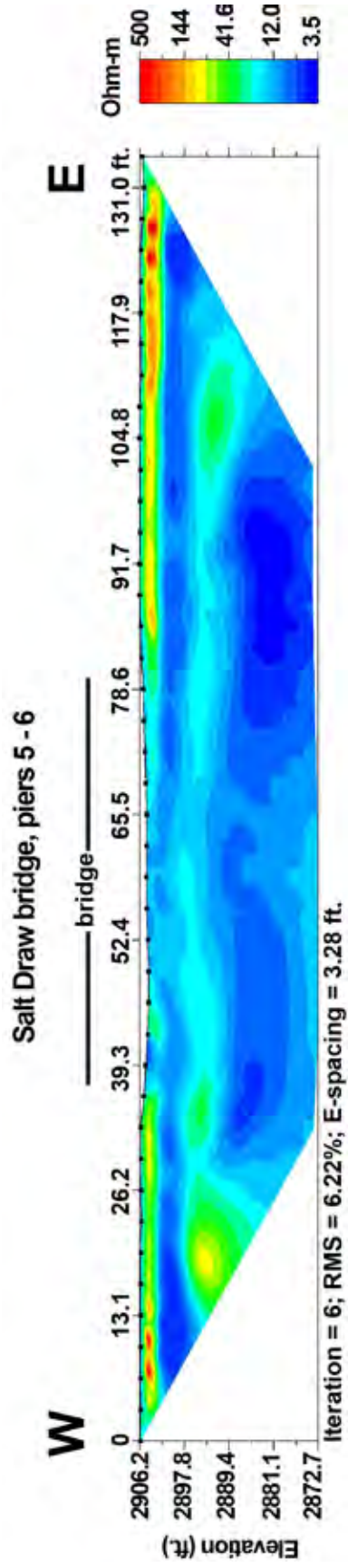


Figure 43. ER survey between piers 5 and 6, counting from the south, Salt Draw bridge. Position of bridge shown by black bar.

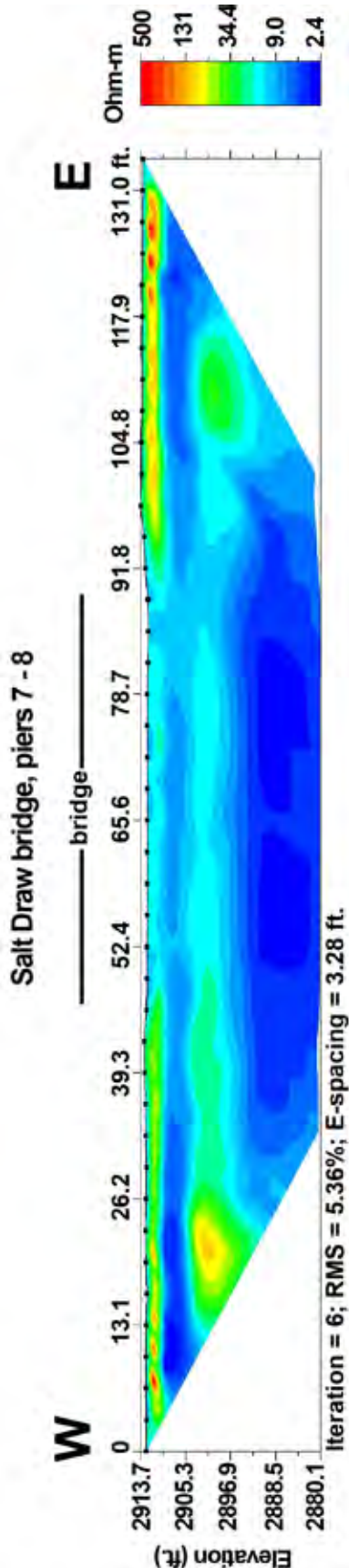


Figure 44. ER survey between piers 7 and 8, counting from the south, Salt Draw bridge. Position of bridge shown by black bar.

abutments were conducted on 2 May 2017, parallel to US 285. All four surveys show zones of very low resistivity beneath the north and south abutments 10 to 15 ft (3–4.6 m) bgl (Figures 45–46). These features probably represent old bridge foundation material (concrete aprons filled with iron reinforcing rods) similar to the buried concrete aprons at Red Bluff Draw bridge. The northeast and northwest profiles also show distinct high resistivity anomalies about 15 ft (4.6 m) bgl beneath the abutments. However, one should note that the resistivity values displayed by these anomalies are not that high (≤ 1300 ohm-m), and may be artifacts produced by the EarthImager inversion process in response to the adjacent very conductive material beneath the abutments.

The southeast and southwest abutment surveys both show a small, shallow pod of high resistivity 5 to 10 ft (1.5–3 m) bgl beneath the stream bed adjacent to the south abutment (Figures 47 and 48). These features may be caused by a shallow cavity, but could also be modeling artifacts associated with adjacent conductive material. Assuming this interpretation is correct, the ER bridge abutment surveys show no real evidence of subsurface cavities or other karst geohazards.

Long-array resistivity surveys were conducted on both sides of the Salt Draw River bridge, perpendicular to the stream valley, on 7 June 2017, achieving a depth of investigation of ~120 ft (~37 m). These surveys extended parallel to each side of the bridge across the entire valley of Salt Draw.

A small pod of high resistivity is present beneath the south abutment on the east side profile, ~15 ft (~4.6 m) bgl (Figure 49). Because this feature coincides with similar ER anomalies on the southeast and southwest bridge abutment surveys discussed above, it may simply be a modeling artifact. Resistivity values displayed on the west side profile (Figure 50) are < 400 ohm-m. Apart from the ambiguous resistivity anomaly observed on the east side profile, the deep ER surveys at Salt Draw bridge do not show any evidence of karst geohazards.

Electrical resistivity surveys were conducted beneath the Black River bridge adjacent to the north and south piers and abutments on 1–2 May 2017. ER profiles of the north abutment and north pier show mostly electrically conductive material associated with fluvial sediment (Figures 51 and 52). A small high resistivity pod at the east end of the north pier survey is probably the result of a shallow buried culvert crossed by the survey line.

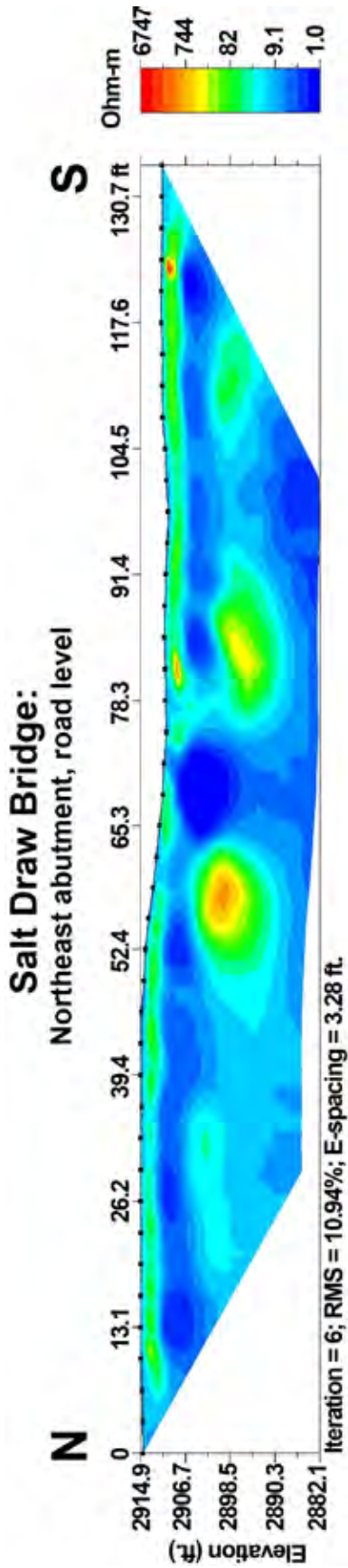


Figure 45. ER survey of Salt Draw bridge, northeast abutment.

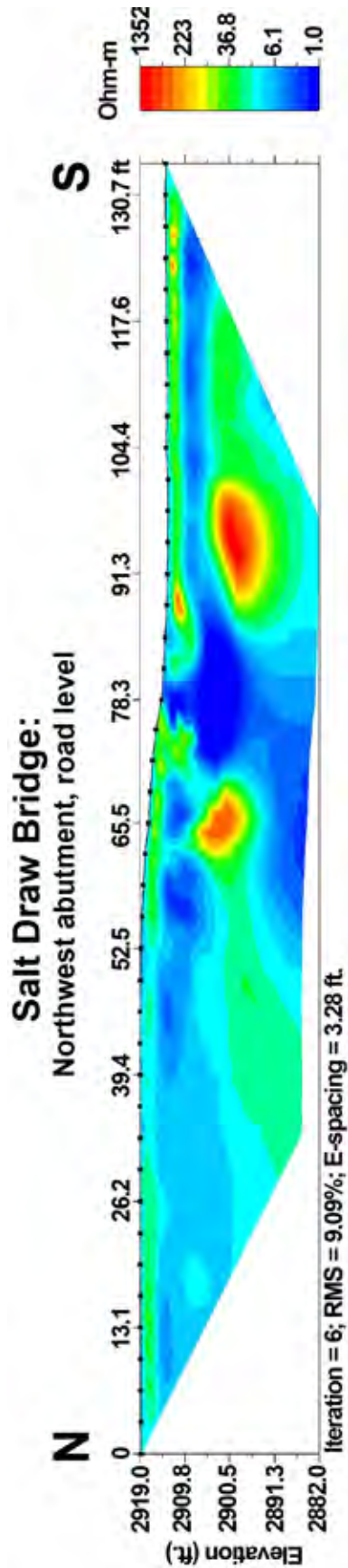


Figure 46. ER survey of Salt Draw bridge, northwest abutment.

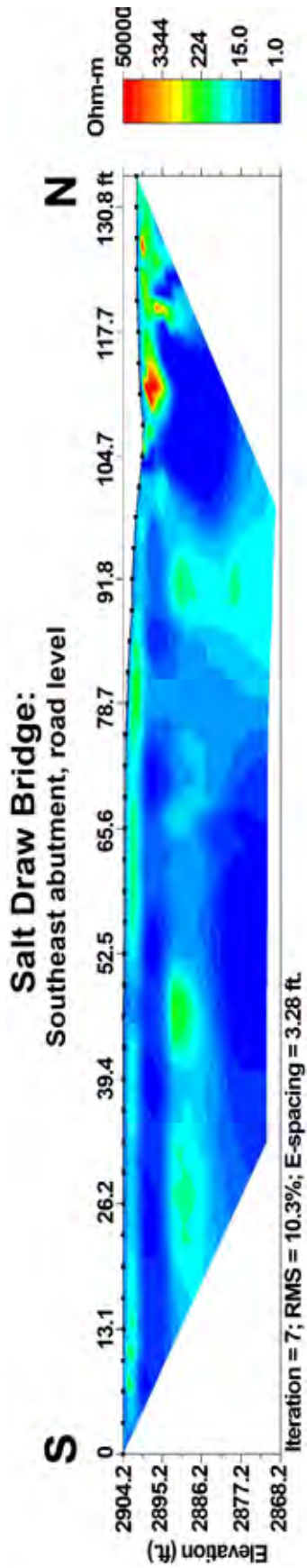


Figure 47. ER survey of Salt Draw bridge, southeast abutment.

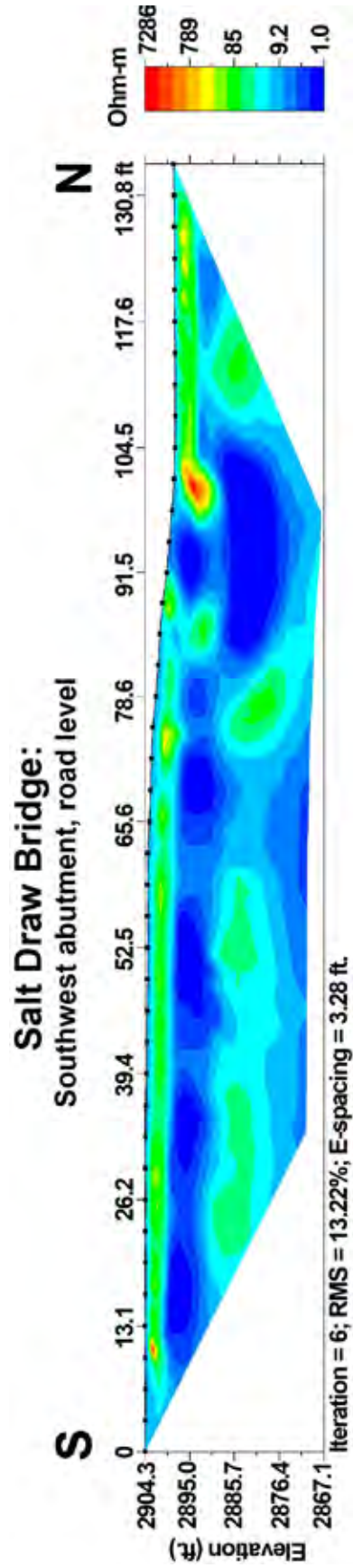


Figure 48. ER survey of Salt Draw bridge, southwest abutment.

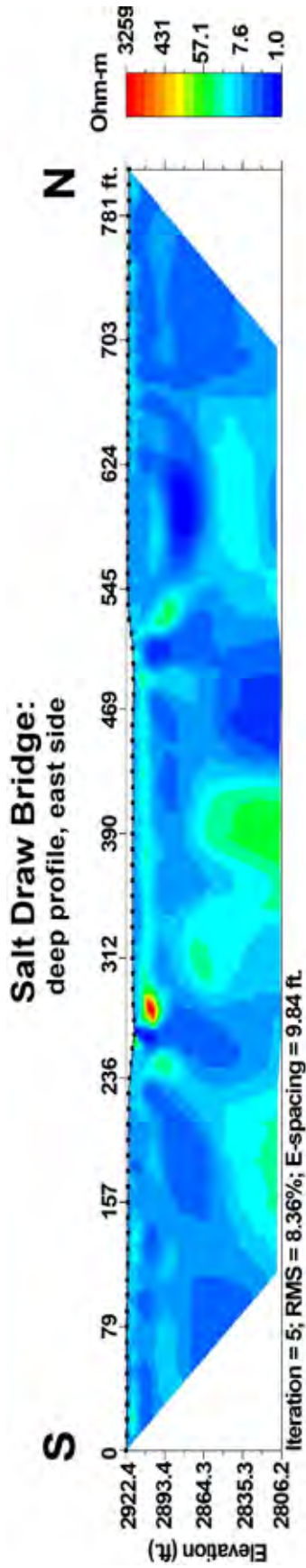


Figure 49. Deep profile, east side of Salt Draw bridge.

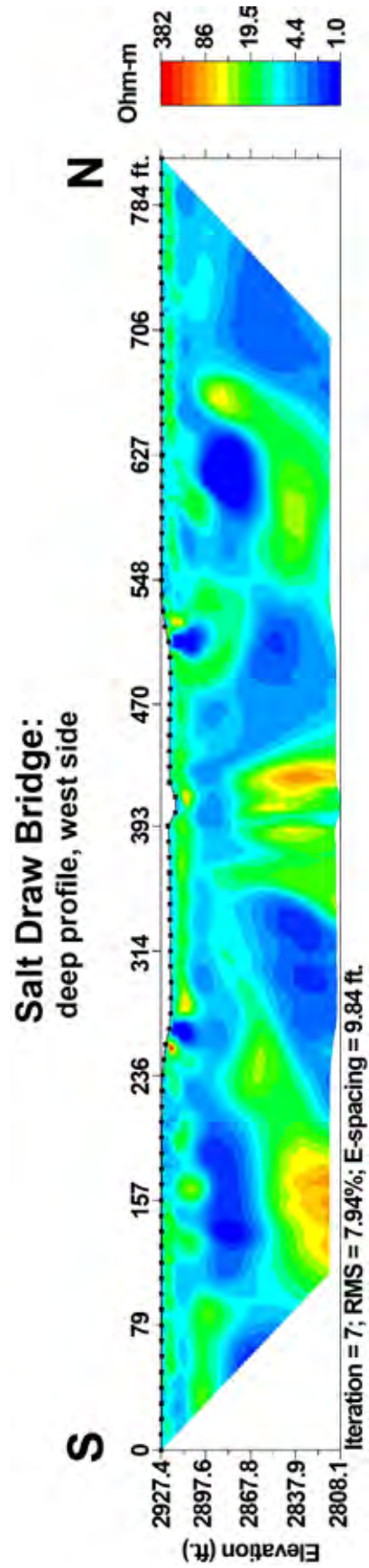


Figure 50. Deep profile, west side of Salt Draw bridge.

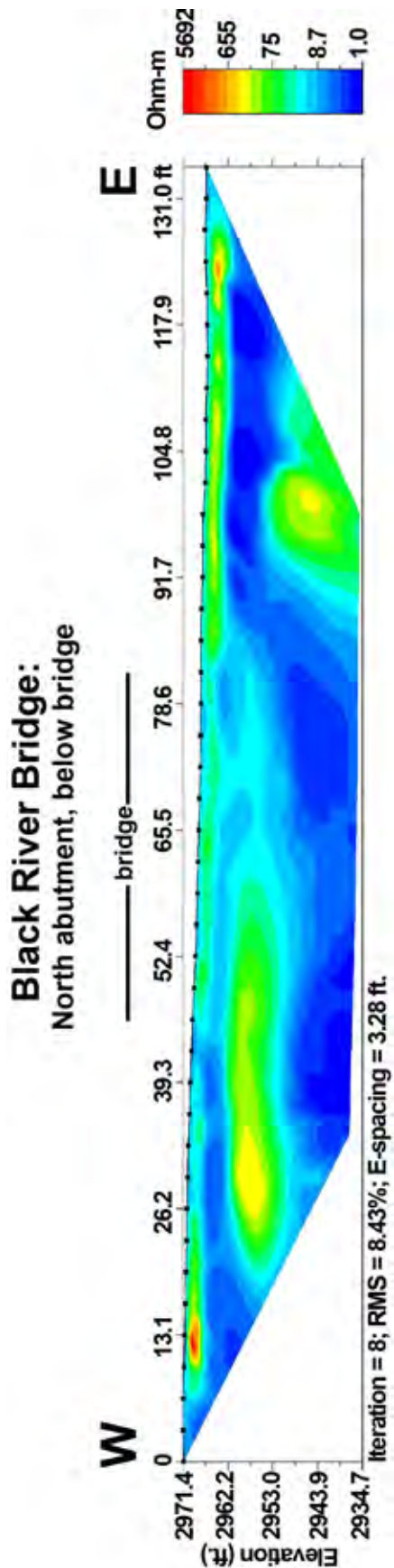


Figure 51. ER survey of north abutment, Black River bridge. Position of bridge shown by black bar.

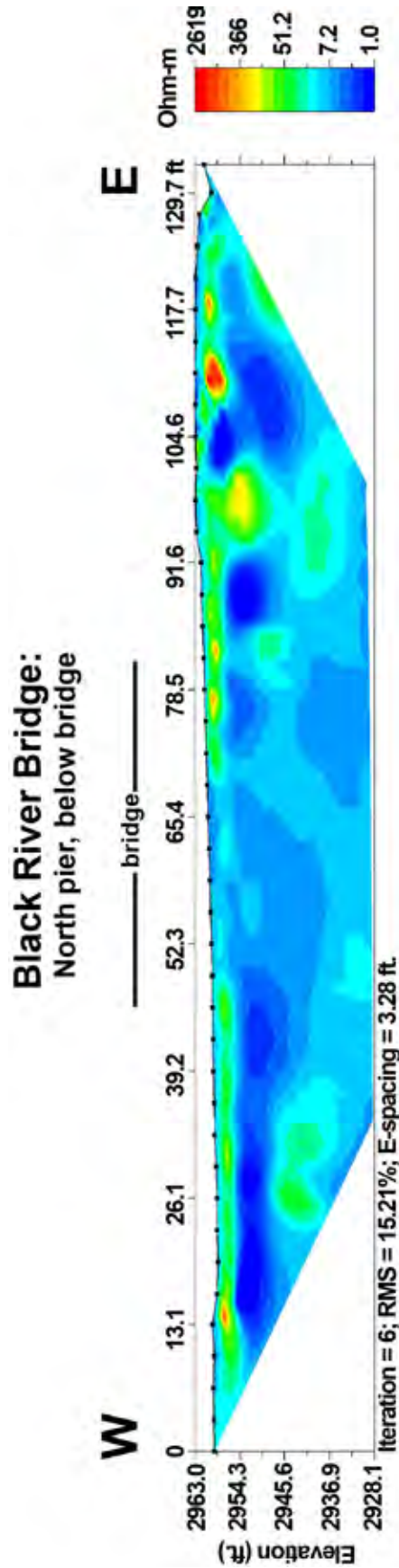


Figure 52. ER survey of north pier, Black River bridge. Position of bridge shown by black bar.

The ER survey conducted adjacent to the south abutment shows a large, relatively high resistivity anomaly (~3000 ohm-m) centered at 26 ft (7.9 m), 15–20 ft (4.6–6 m) bgl (Figure 53). This feature may represent a brecciated zone or filled cavity. However, it should be noted that portions of the foundation of an older bridge are visible at the surface on this side of the river; it is thus possible that this anomaly may be caused by electrically resistive remnants of that earlier bridge. A very small high resistivity pod is present at the west end of the south pier survey, ~5 ft (1.5 m) bgl (Figure 54). This feature may also result from anthropogenic material—specifically chunks of concrete—in the shallow subsurface.

Road-level resistivity surveys of the Black River bridge abutments were conducted on 1–2 May 2017, parallel to US 285. The road level survey of the northeast abutment shows a laterally extensive zone of relatively high resistivity 15–20 ft (4.6–6 m) bgl between 78–95 feet (23.8–29 m) (Figure 55). This feature may represent either a brecciated zone or filled cavity, or stratigraphic layering within Quaternary alluvium. No apparent karst geohazard features were observed on the southwest, northwest, and southeast bridge abutment surveys (Figures 56 to 58). The southwest abutment survey shows a small, shallow (~5 ft or ~1.5 m bgl) pocket of very high resistivity directly beneath the abutment at 105 ft (32 m) (Figure 56). This feature is probably the result of air-filled porosity in a layer of rip-rap distributed across the southwest abutment into which two of the electrodes were driven.

Long-array resistivity surveys were conducted on both sides of the Black River bridge, perpendicular to the stream valley, on 8 June 2017, achieving a depth of investigation of ~120 ft (~37 m). These surveys extended parallel to each side of the bridge across the entire valley of the Black River. On each profile, four electrodes in the river were skipped from the data collection process because it was not possible to accurately determine their spacing, given the water depth and current flow.

The most distinctive features of the east side survey are two high resistivity anomalies present beneath and north of the northeast abutment, ~20 ft (6 m) bgl (Figure 59). The east-side survey was a particularly noisy data set that required removal of a number of data outliers, so these features may simply be data processing artifacts. However, the anomalies persisted through several iterations and refinements of the inverse modeling procedure. The anomaly beneath the abutment, centered at 660 feet, also approximately coincides

with an anomaly identified on the shallow survey of the northeast abutment, discussed above. These two features suggest the presence of possible cavities or brecciated zones in the shallow subsurface beneath the northeast abutment.

A high resistivity anomaly is also present on the west side survey beneath the south abutment 25–30 ft (7.6–9 m) bgl (Figure 60). This feature approximately coincides with the anomaly identified on a shallow survey of the south abutment of the Black River bridge. As discussed above, this high resistivity anomaly may indicate the presence of a filled cavity or brecciated zone, or it may result from the presence of electrically resistive remnants of an older bridge foundation.

Reoccupation of seismic refraction survey areas

Resistivity surveys were conducted at three seismic refraction survey sites in May and June 2017, using 42-electrode arrays at 3.3-ft (1-m) electrode spacing. Surveys conducted at sites of the SL02 and SL04 seismic refraction surveys show no evidence of significant karst geohazards (Figures 61 and 62). Shallow high resistivity pockets on these two surveys probably represent air-filled porosity in soil or weathered bedrock. The ER survey of the SL05 site (Figure 63) shows a prominent layer of moderately high resistivity extending across the entire profile at depths ranging from 5–20 ft (1.5–6 m) bgl, dipping down to the south. Given that the maximum resistivity of this survey is only 365 ohm-m, it is unlikely that this feature is a cave. This phenomenon probably reflects near-surface stratigraphy, possibly gypsum bedrock in the shallow subsurface dipping up to the north. AFW borehole 8 is located next to electrode 13 at 39.4 ft (12 m). Gypsum fragments were observed in borehole cuttings still present on the ground while this survey was conducted.

Summary

Six specific areas have been identified with a high estimated sinkhole hazard potential based on surface geologic mapping and electrical resistivity surveys. The southernmost area is located approximately three-fourths of a mile (1.2 km) from the Texas state line on both sides of US 285. The remaining five karst geohazard areas are located between 7.5 and 14.5 mi. (12–23 km) north of the state line. All of these sites are located in areas where the gypsiferous Los Medaños Member of the Rustler Formation crops out or is present within 2 ft (0.6 m) of the surface. Most of the sinkholes in the study area are relatively shallow (<10 ft or 3 m). Resistivity surveys conducted adjacent to the sinkholes indicate that in most

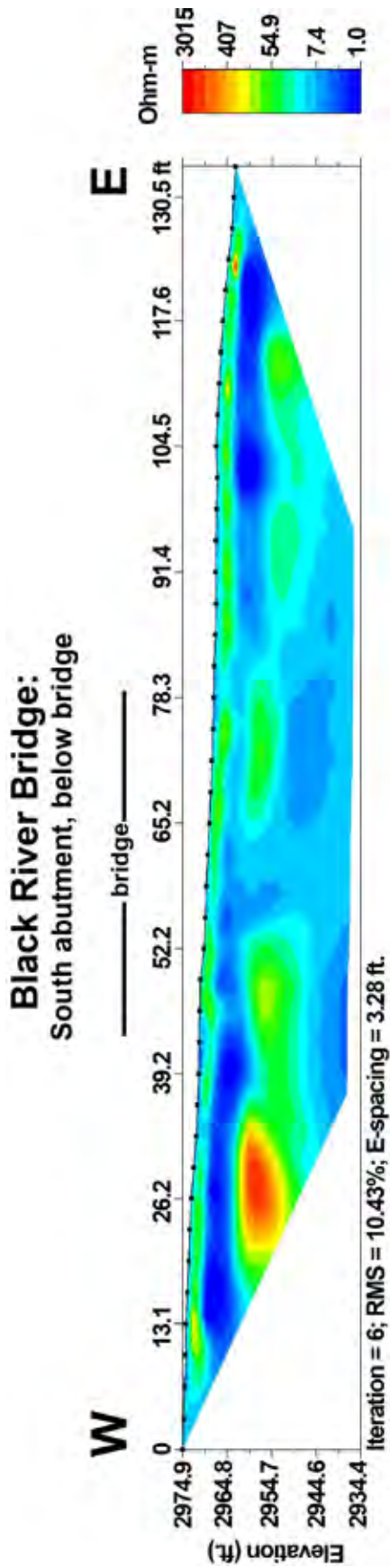


Figure 53. ER survey of south abutment, Black River bridge. Position of bridge shown by black bar.

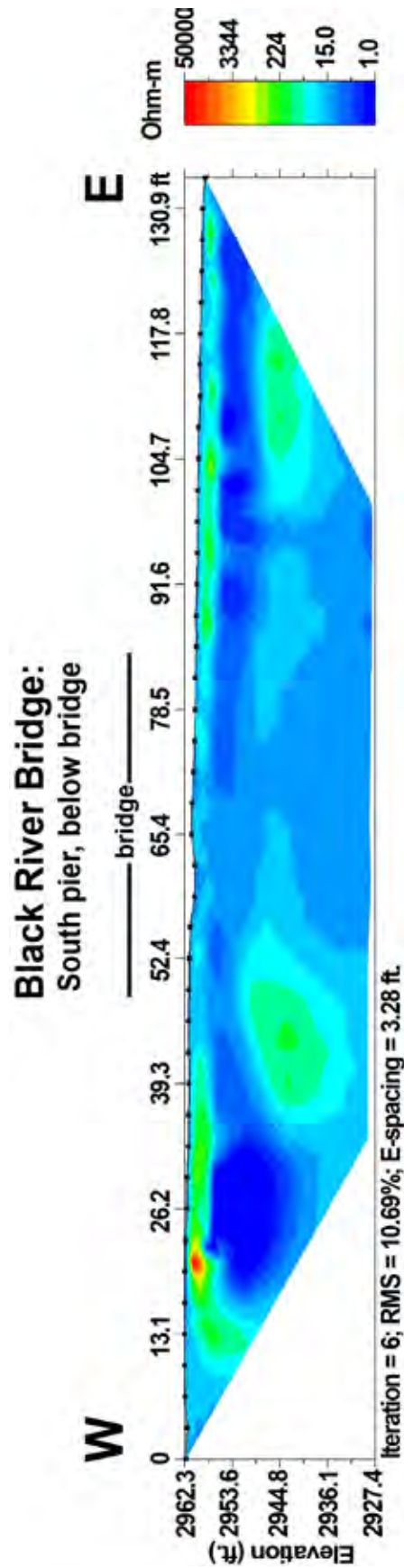


Figure 54. ER survey of south pier, Black River bridge. Position of bridge shown by black bar.

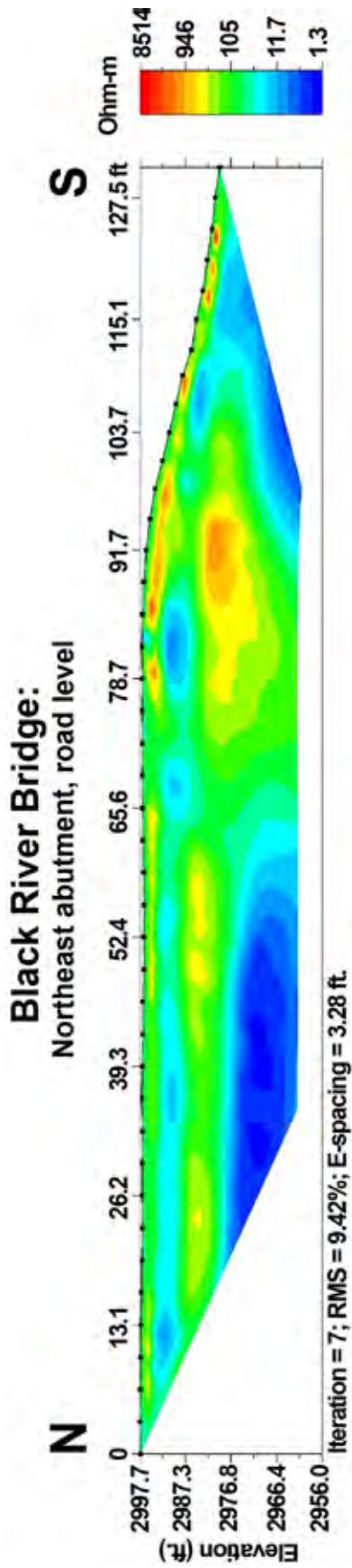


Figure 55. ER survey of Black River bridge, northeast abutment.

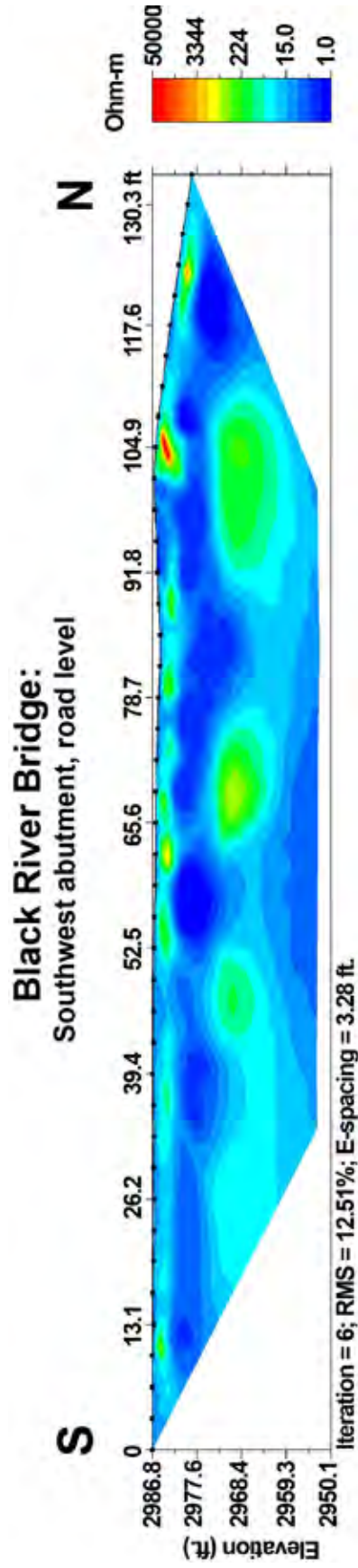


Figure 56. ER survey of Black River bridge, southwest abutment.

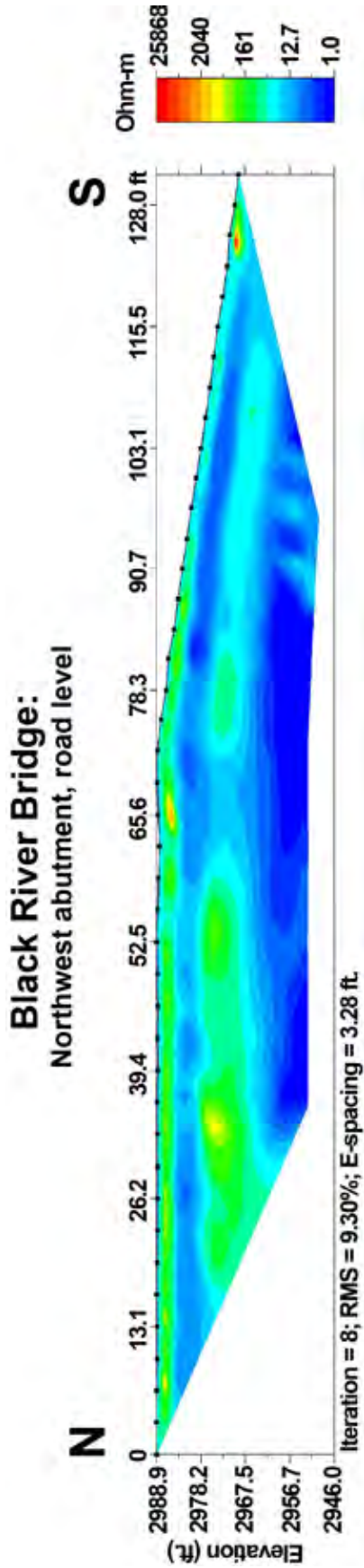


Figure 57. ER survey of Black River bridge, northwest abutment

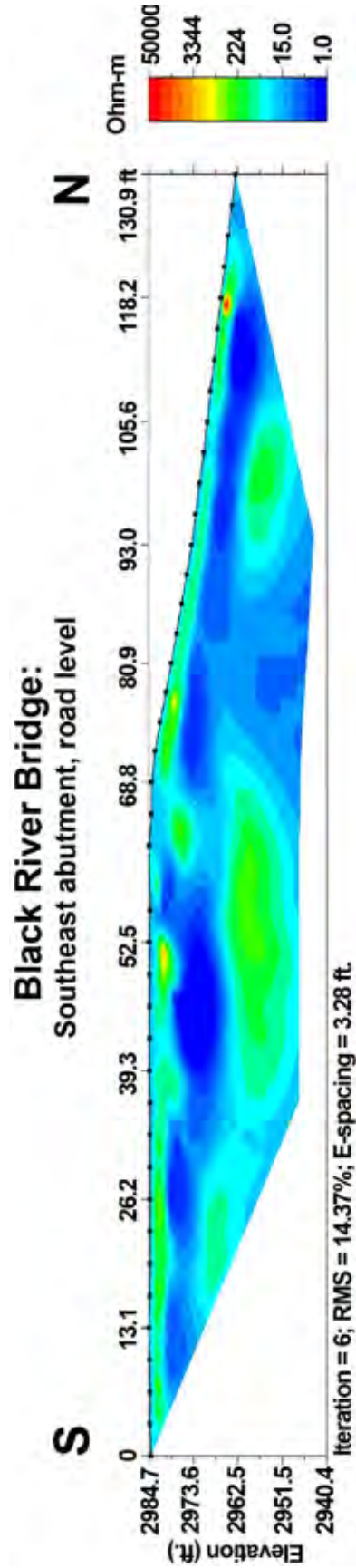


Figure 58. ER survey of Black River bridge, southeast abutment.

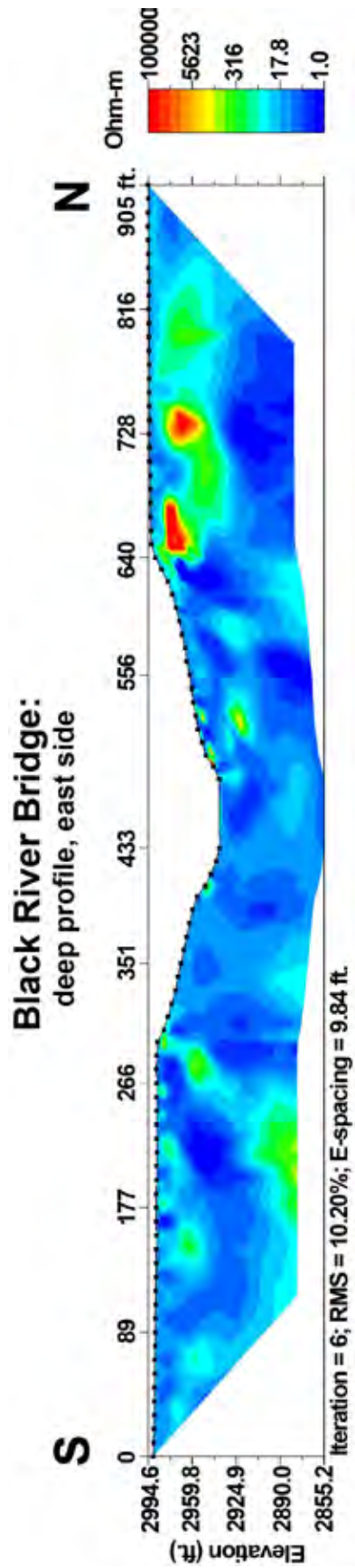


Figure 59. Deep profile, east side of Black River bridge.

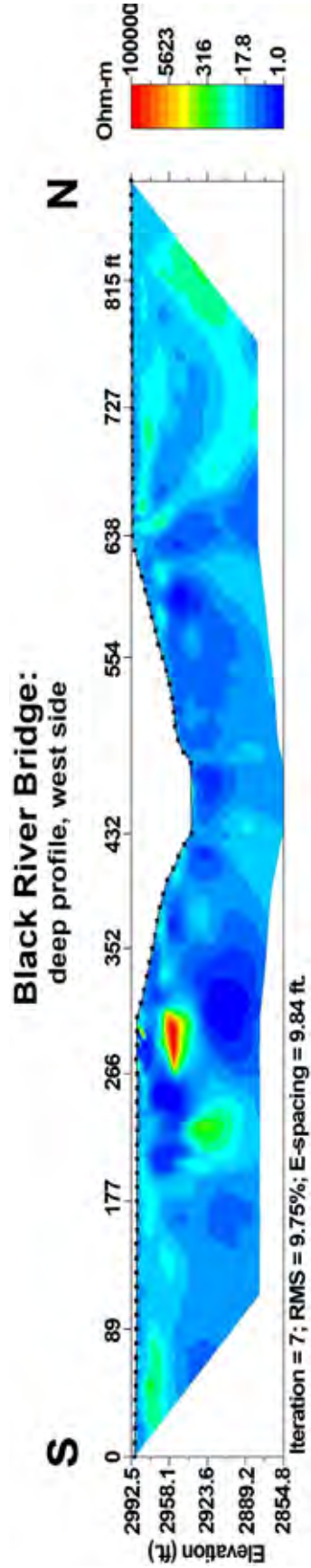


Figure 60. Deep profile, west side of Black River bridge.

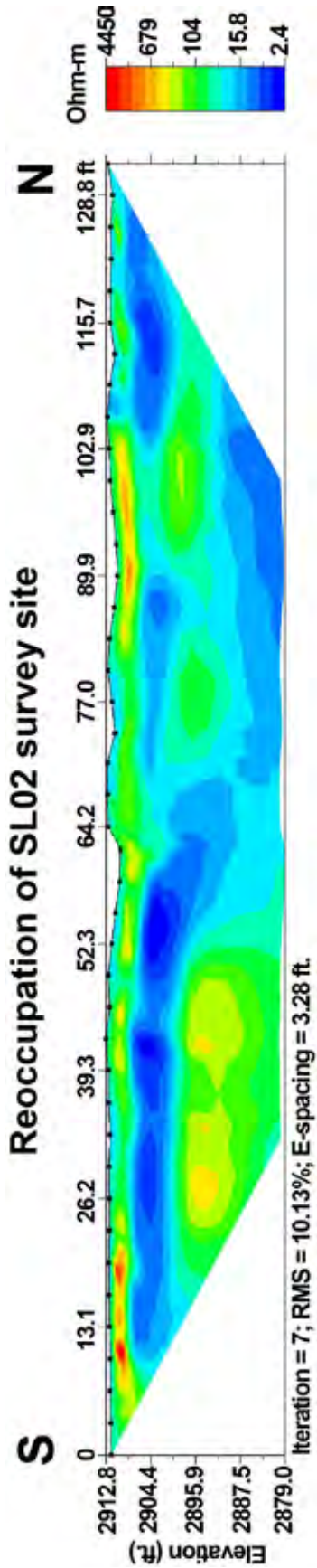


Figure 61. ER survey of seismic refraction site SL02.

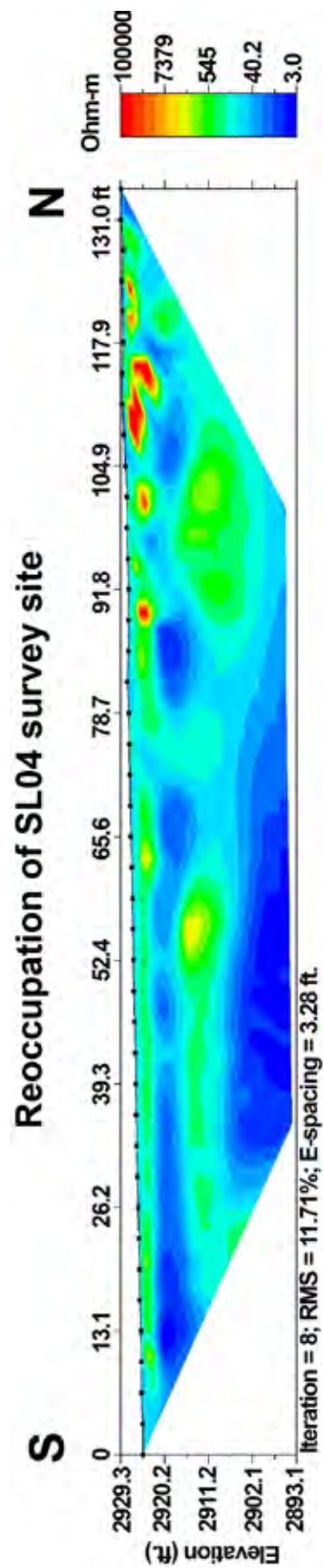


Figure 62. ER survey of seismic refraction site SL04.

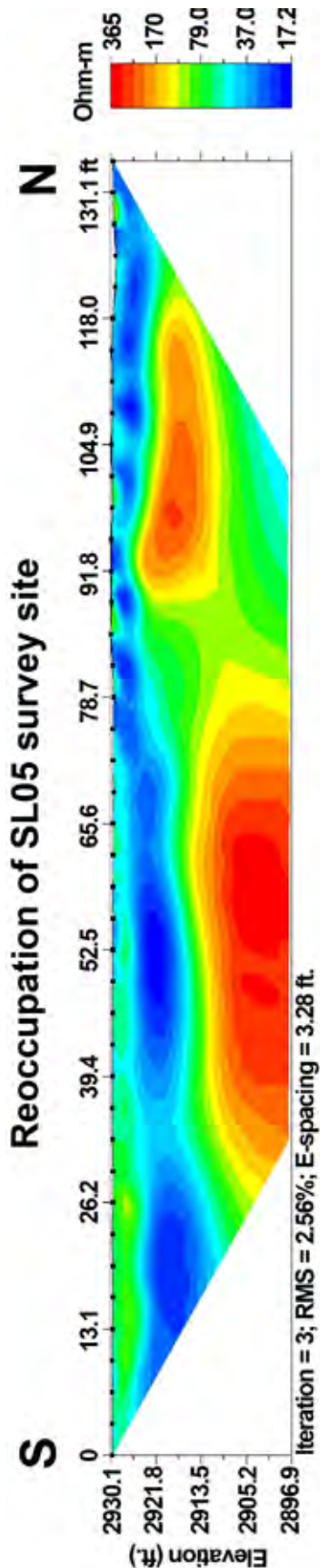


Figure 63. ER survey of seismic refraction survey site SL05.

cases they do not have deep roots, rarely extending more than 15 ft (4.6 m) below ground level (station 9.7E may be the one exception). The shallow extent of sinkholes in the study area probably results from the mixed lithology of soluble and insoluble bedrock (interbedded gypsum, mudstone, and dolomite) in the Rustler Formation. However, longer-array electrical resistivity surveys have identified additional cavities at greater depths in some areas that do not breach the surface.

Electrical resistivity surveys of the four bridges on the US 285 corridor show strong evidence that a subsurface void is present beneath the south abutment of the Red Bluff Draw bridge about 60 ft (18 m) bgl. Resistivity surveys of Black River bridge indicate that cavities may be present beneath the northeast and southwest bridge abutments, 20–30 ft (6–9 m) below ground level, although the evidence is less conclusive, given the presence of old bridge foundation material at that site. No evidence of karst geohazards was found during surveys of the Delaware River and Salt Draw bridges.

Variations in specific values of bedrock electrical resistivity were observed over the course of this investigation, particularly on the long array surveys with greater exploration depth (e.g., the Delaware River bridge surveys). This phenomenon may reflect lateral variations in bedrock weathering properties of the Los Medaños gypsum, resulting in variations in bedrock resistivity. It is worth noting that seismic refraction velocities would also be influenced by such variations in bedrock weathering properties.

References

- Land L. 2013. Geophysical records of anthropogenic sinkhole formation in the Delaware Basin region, southeast New Mexico and west Texas, USA. *Carbonates and Evaporites* 28 (1–2): 183–190.
- Land L, Veni G. 2012. Electrical resistivity surveys of anthropogenic karst phenomena, southeastern New Mexico. *New Mexico Geology* 34 (4): 117–125.
- Land L, Asanidze L. 2015. Rollalong resistivity surveys reveal karstic paleotopography developed on near-surface gypsum bedrock. In: Doctor DH, Land L, Stephenson JB (eds.), *Proceedings of the Fourteenth Multidisciplinary Conference on Sinkholes and the Engineering and Environmental Impact of Karst*, Rochester, Minnesota. National Cave and Karst Research Institute Symposium 5. Carlsbad (NM): National Cave and Karst Research Institute, pp. 365–370.

NCKRI and NMBGMR. 2016. US Highway 285 Road-

way Improvements 2016–17, Geotechnical Scoping Report, Geology and Karst Evaluation. Unpublished report to Amec Foster Wheeler, 14 December, five pages.

Veni, G. 1999. A geomorphological strategy for conducting environmental impact assessments in karst areas. *Geomorphology* 31: 151–180. Reprinted in: 2000. Proceedings of the 28th Binghamton Symposium: Changing the Face of the Earth – Engineering Geomorphology, J. Rick Giardino, Richard A. Marston, and Marie Morisawa (eds.), Elsevier Publishers, pp. 151–180.

Appendix A:

Karst Features and Electrical Resistivity Surveys in the Study Area

All karst features or potential karst features discovered during this project are described in this appendix. Any ER surveys associated with those features are included and evaluated (all ER surveys along the bridges are discussed in the main part of the report). The estimated hazard potential of the features is given on a 1–10 scale, where 10 is the highest potential. Hazard risk is primarily related to collapse by failure of a cavity's bedrock roof or by cover collapse, where the soil or overlying sediments are piped downward into bedrock caves to create soil cavities that are prone to collapse.

Station 0.1E

Collapse sinkhole 5 x 7 ft, ~2 ft deep (1.5 x 2 m, ~0.6 m deep) formed in gypsum bedrock, in a broad swale between two knolls of Culebra dolomite. Beds on the south margin of the swale are possibly rotated beds that may suggest collapse or subsidence.

The ER survey was conducted on 30 March 2017. The depth of investigation was ~30 ft (~9 m), total survey length was 138 ft (42 m), and the root-mean-square (RMS) error was 9.37% (Figure A1). A pod of moderately high resistivity occurs between 30-35 ft (9-10.7 m) on the profile, ~8 ft (~2.4 m) bgl is a possible brecciated zone. It does not correspond to any surface features. The observed sinkhole does not manifest on the ER profile.

Estimated hazard potential 3.

Station 0.75E

Collapse sinkhole 3 x 8 ft, 3 ft deep (1 x 2.4 m, 1 m deep) formed in gypsum bedrock, fracture-controlled, with possible slight airflow.

The ER survey was conducted on 31 March 2017. Depth of investigation was ~33 ft (~10 m), total survey length 138 ft (42 m), the RMS error was 5.28% (Figure A2). A high resistivity zone occurs between 80-100 ft (24–30 m) on profile, ~20 ft (~6 m) bgl. This possible brecciated zone does not correspond to any surface features. The observed sinkhole does not manifest on the ER profile.

Estimated hazard potential 8, mainly because of size of the resistivity anomaly.

Station 0.75EE

The ER survey was conducted on 20 April 2017. Depth of investigation was ~34 ft (~10.4 m), total survey

length 184 ft (56 m), and the RMS error was 8.54% (Figure A3). It is the northward extension of ER line 0.75E.

The survey line passes directly over three small sinkholes, shown on the profile by a black rectangle. An extensive zone of high resistivity is present beneath those features. The position of the high resistivity anomaly originally identified at the north end of line 0.75E is shown by a black bar centered on 58.8 ft (17.9 m), underlain by small pods of higher-resistivity material, probably brecciated or leached zones in gypsum bedrock. A more laterally extensive high resistivity layer ~25 ft (~7.6 m) bgl probably represents stratigraphic layering (gypsum and mudstone) within the Rustler Formation. **Estimated hazard potential 8, because of presence of the sinkhole and ER anomaly.**

Station 0.75W

Collapse sinkhole 4 x 5 ft, 1 ft deep (1.2 x 1.5 m, 0.3 m deep).

The ER survey was conducted on 31 March 2017. Depth of investigation was ~33 ft (~10 m), total survey length 138 ft (42 m), and the RMS error was 5.75% (Figure A4). A high resistivity anomaly occurs between 95-110 ft (29-33.5 m) on the profile, ~15 ft (~4.6 m) bgl is a possible brecciated zone or cavity. It does not correspond to any surface features. The observed surface sinkhole does not manifest on the ER profile. **Estimated hazard potential 8, mainly because of the size of the resistivity anomaly.**

Station 0.75WW

The ER survey was conducted on 20 April 2017. Depth of investigation was ~33 ft (~10 m), total survey length 184 ft (56 m), and the RMS error was 5.75% (Figure A5). It is the northward extension of ER line 0.75W.

A cluster of three small sinkholes (<1 ft or 0.6 m diameter) and one larger sinkhole (~5 ft or 1.5 m diameter and 2 ft or 0.6 m deep) is present on either side of the survey line at 19.7 ft (6 m), indicated by a black rectangle on the profile. These features are underlain by a high resistivity anomaly in the shallow subsurface. The position of the high resistivity anomaly originally identified at the north end of line 0.75W is shown by a black bar

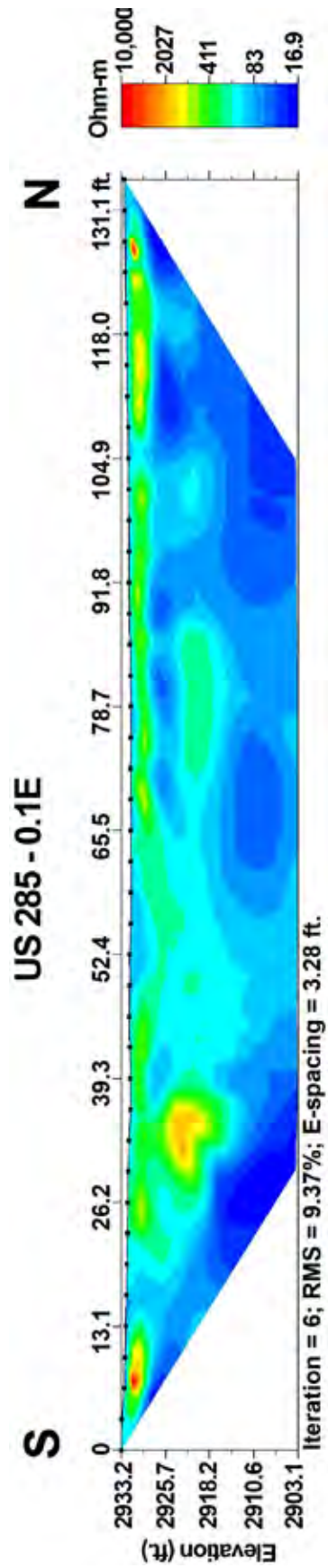


Figure A1. Station 0.1E profile.

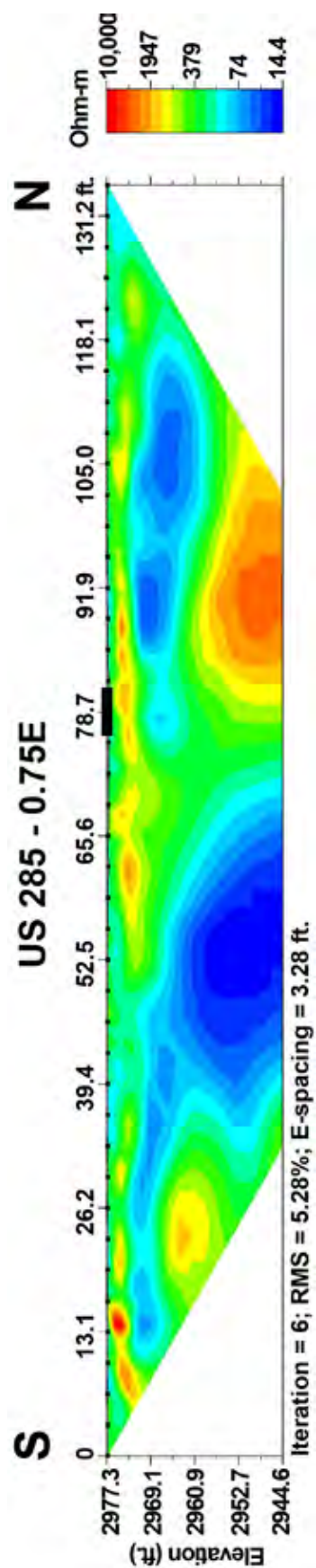


Figure A2. Station 0.75E profile.

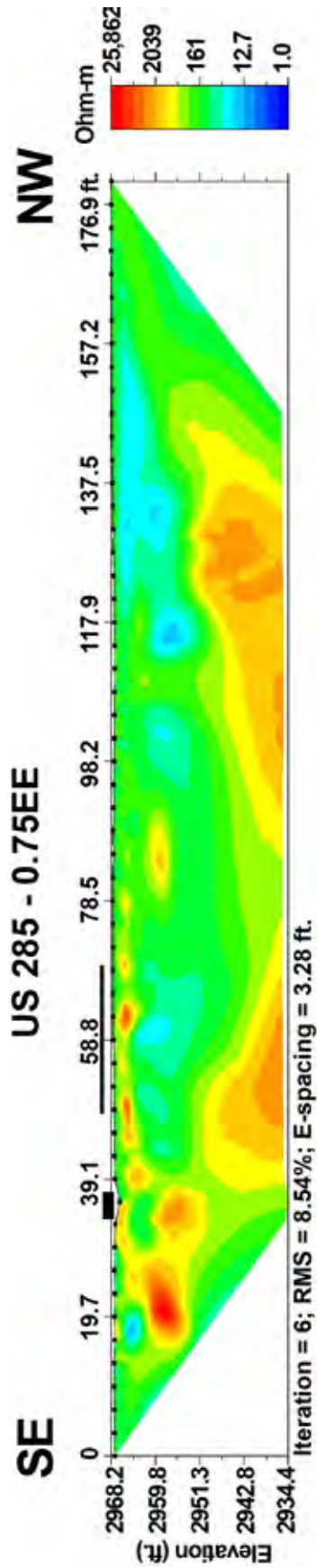


Figure A3. Station 0.75EE profile.

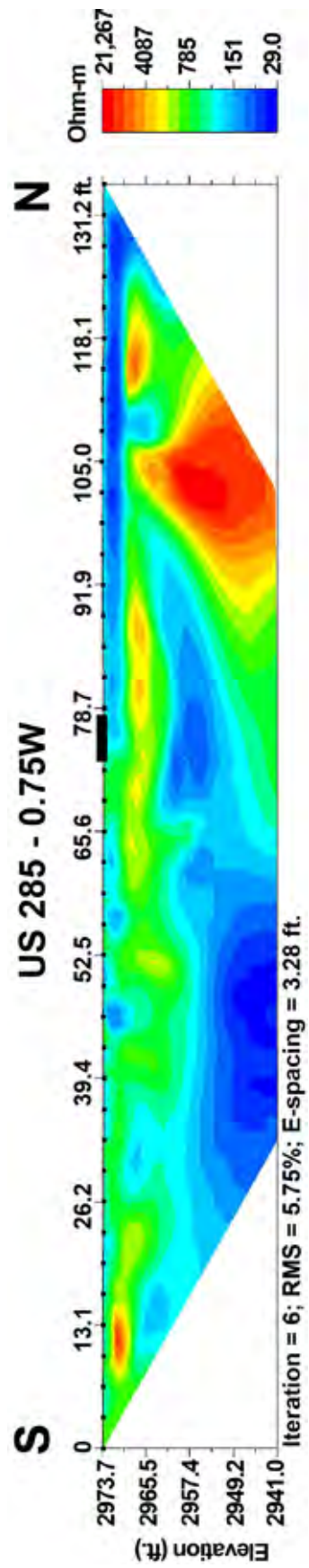


Figure A4. Station 0.75W profile.

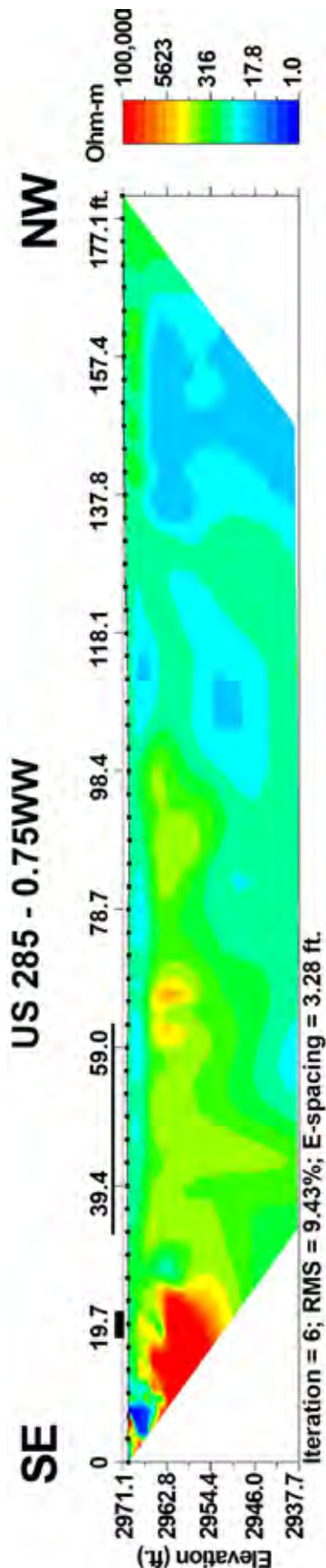


Figure A5. Station 0.75WW profile.

centered at 50 ft (15.2 m), underlain by a layer of higher resistivity material, probably brecciated or leached zones in gypsum bedrock. **Estimated hazard potential 6.**

Station 2.0E

Two small (<1 ft or 0.3 m diameter) sinkholes in exposed gypsum bedrock, just south of the Delaware River.

An ER survey was conducted on 30 March 2017. It had a total survey length of 138 ft (42 m), the data were very noisy with an RMS error of 54.19%, possibly due to buried infrastructure. **The estimated hazard potential is 3 based on the sinkholes' morphology; the ER survey could not be interpreted reliably.**

Station 7.69W

Collapse sinkhole 2 x 8 ft (0.6 x 2.4 m) in gypsum bedrock. The ER survey was conducted on 30 March 2017. The total survey length was 138 ft (42 m) but the data were very noisy with an RMS error of 42.31%, probably due to buried pipeline ~35 ft (~10.7 m) west and parallel to ER survey line. **The estimated hazard potential is 4 based on the sinkholes' morphology; the ER survey could not be interpreted reliably.**

Station 7.75E

Three large sinkholes (>10 ft or 3 m diameter and 5 ft or 1.5 m deep) with gypsum bedrock at the bottom, in a broad swale on both sides of the right-of-way fence.

The ER survey was conducted on 30 March 2017. Depth of investigation was ~34 ft (~10.4 m), total survey length 276 ft (84 m), and the RMS error was 6.83% (Figure A6). This survey was conducted just west of the three large sinkholes. The ER survey line skirted the large sinkhole on the west side of the fence. An elongate depression on the east side of the fence with a deep sinkhole at the south end roughly coincides with a zone of moderate to high resistivity between 80-115 ft (24.4-35.1 m) on the profile. **Estimated hazard potential 9, based on the size and number of surface features and the subsurface high resistivity anomalies.**

Station 8.6W

Multiple sinkholes, some of which are possible cave entrances if excavated (Figure A7), formed in soil and gypsum bedrock on the east margin of a broad, shallow subsidence depression on the west shoulder of the highway.

The ER survey was conducted on 29 March 2017. Depth of investigation was ~35 ft (11 m), total survey length 367 ft (112 m), and the RMS error was 7.06% (Figure A8).

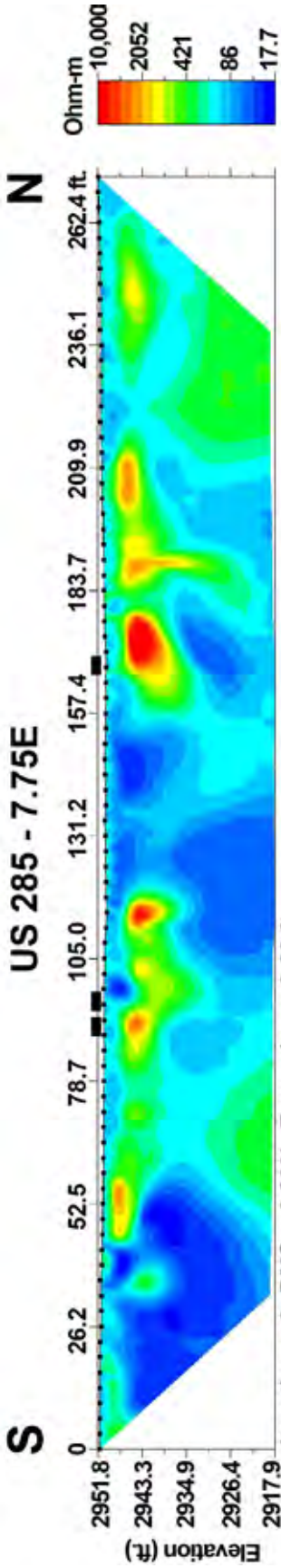


Figure A6. Station 7.75E profile.



Figure A7. Station 8.6W sinkhole and ER cable.

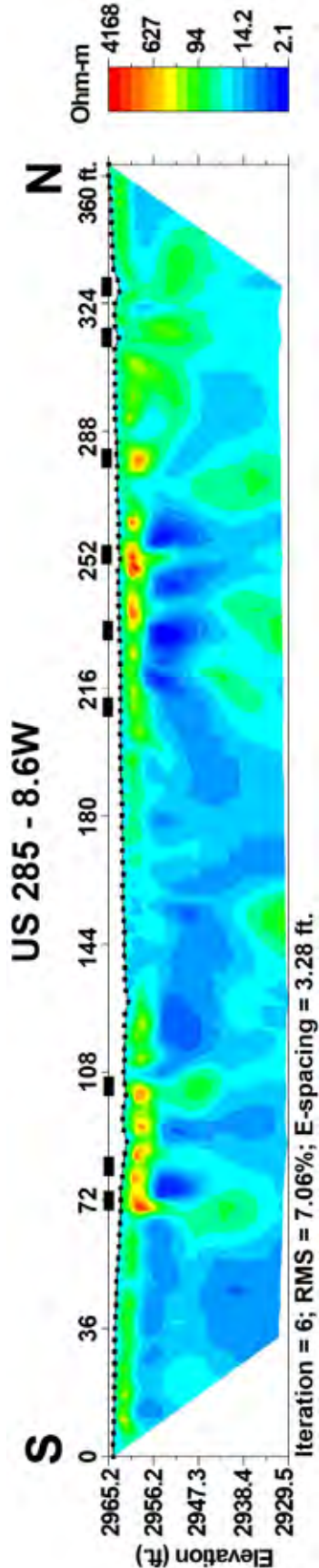


Figure A8. Station 8.6W profile.

This site has a very high concentration of sinkholes over a distance of about 250 ft (76 m). The ER profile shows some high resistivity anomalies that coincide with the surface features. Surprisingly, none of these features extend more than 10 ft (3 m) beneath the surface. **Estimated hazard potential 9, based on the size and number of surface features and ER anomalies.**

Station 8.6E

The ER survey was conducted on 21 April 2017. Depth of investigation was ~33 ft (~10 m), total survey length 276 ft (84 m), and the RMS error was 4.36% (Figure A9). This survey was conducted directly across from the extensive cluster of sinkholes originally identified on the west shoulder of US 285.

No surface karst features were identified at this site during the field survey. However, a large high resistivity zone is present between 105-130 ft (32-39.6 m) on the profile, ~15 ft (~4.6 m) bgl, along with several smaller anomalies beneath the western half of the survey line. Following the field work, a broad, shallow, seasonally ponded sinkhole was found in that location, apparent only by aerial imagery (cover photo). **Estimated hazard potential 7, based on the size and number of surface features and ER anomalies.**

Station 9.7E

Three sinkholes formed in gypsum bedrock or roadbed material; additional larger features occur on the east side of the fence. The sinkhole formed in roadbed material is the one that first attracted NMDOT's attention to this area's karst hazards (Figure A10). The larger sinkhole in gypsum is a small entrance to a possible cave (Figure A11). The smaller gypsum sinkhole leads into an impassibly small conduit. Note that in spite of the station designation, these features are actually located at 9.9 mile.

The ER survey was conducted on 8 November 2016. Depth of investigation was ~410 ft (125 m), total survey length 2185 ft (666 m), and the RMS error was 10.23% (Figure A1-A). This survey is centered on the shorter array, which is shown by a red bar and described in the next paragraph. The shallow karst features imaged on the 70-electrode survey are still visible as near-surface high resistivity anomalies. This survey also shows a pod of moderately high resistivity (~2000–5000 ohm-m) near the center of the profile ~130 ft (~40 m) bgl, which may indicate the presence of a filled cavity or brecciated zone.

The shorter ER survey was conducted on 11 November 2016. Depth of investigation was ~35 ft (11 m), total survey length 230 ft (70 m), and the RMS error was

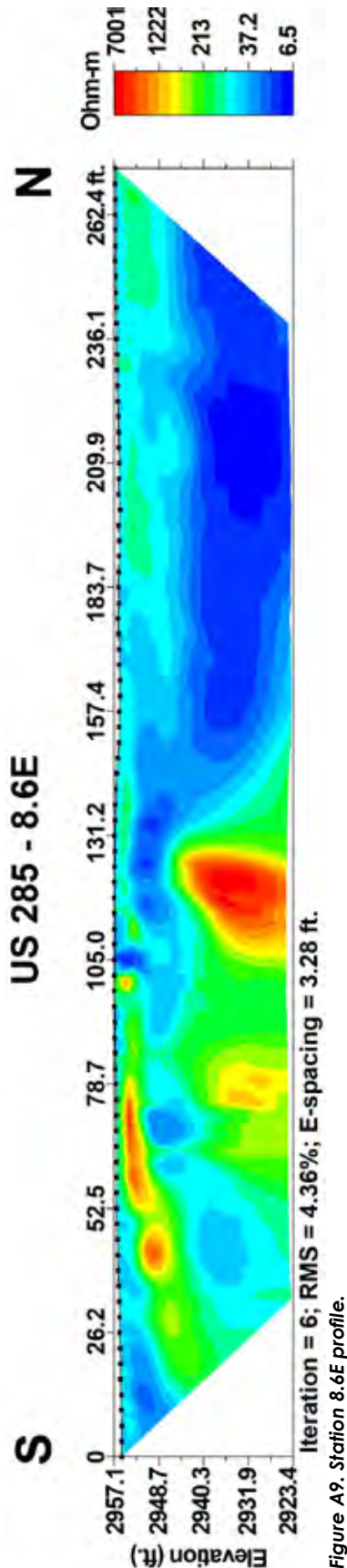


Figure A9. Station 8.6E profile.

4.83% (Figure A12-B). The ER survey line passes 6 ft (1.8 m) east of a sinkhole with a small possible cave entrance formed in gypsum bedrock (Figure A12) at ~102 ft (31.1 m) on the profile.

That feature is represented by a shallow (3–8 ft or 1–2.4 m deep) zone of high resistivity that extends from ~65–125 ft (~19.8–38.1 m) on the profile. **Estimated hazard potential 9, based on the size and number of surface features and subsurface high resistivity anomalies.**

Station 9.82E

Elongate shallow swale with many small divots and depressions, including one small closed depression about 1 ft (0.3 m) in diameter.

The ER survey was conducted on 29 March 2017. Depth of investigation was ~35 ft (11 m), total survey length 184 ft (56 m), and the RMS error was 4.34% (Figure A13). The ER survey yields a rather colorful profile, but the resistivity scale ranges from 9.3 to just 150 ohm-m; in other words, the color variations are simply showing subtle variations in stratigraphy and moisture content in the vadose zone. The near surface blue layer overlying a slightly higher resistivity layer probably represents clay-rich soil and weathered bedrock overlying gypsum strata. The small surface features probably represent soil disturbed by cattle. **Estimated hazard potential 0.**

Station 9.82W

Large deep sinkhole (8 ft or 2.4 m diameter and 5 ft or 1.5 m deep) next to a fence, cutting into a coppice dune, diagonally across the highway from the original sinkholes that initiated interest in this project.

The ER survey was conducted on 29 March 2017. Depth of investigation was ~33 ft (~10 m), total survey length 138 ft (42 m), and the RMS error was 2.83% (Figure A14). This profile is similar to the one from survey 9.82E. Horizontal color variations probably represent subtle variations in subsurface stratigraphy, not cavities, since the maximum resistivity is just 303 ohm-m. **Estimated hazard potential 3, due to presence of surface karst.**

Station 12.0E

Three large sinkholes (>15 ft or 4.6 m diameter and 10 ft or 3 m deep), located east of a fence, thus not on the US 285 right-of-way; their size and proximity to the road nevertheless indicate the necessity of surveying the right-of-way in this area. Note: Those sinkholes were designated 11.35A, B, and C (Figures A15, A16, and A17) on the surface mapping survey, although they are located very near the 12-mile marker.



Figure A10. Station 9.7 sinkhole in road base.



Figure A11. Station 9.7 possible cave entrance.

The ER survey was conducted on 28 March 2017. Depth of investigation was ~36 ft (11 m), total survey length 367 ft (112 m), and the RMS error was 11.95% (Figure A18). In spite of its proximity to large sinkholes 150–200 ft (46–61 m) east of the right-of-way, the ER profile shows nothing significant. A shallow layer of higher resistivity at the south end of the profile is probably air-filled pore space in soil and weathered bedrock. **Estimated hazard potential 3, primarily due to proximity to surface features farther east.**

Station 12.1W

Several small (<1 ft or 0.3 m diameter) sinkholes in gypsum bedrock.

The ER survey was conducted on 28 March 2017. Depth of investigation was ~34 ft (~10.4 m), total survey length 184 ft (56 m), and the RMS error was 7.30% (Figure A19). The ER profile shows nothing significant, with the exception of one small pod of high resistivity at ~165 ft (50.3 m) on the profile, 3–5 feet (1–1.5 m) bgl, which is a possible brecciated zone or air-filled pore space. The observed sinkholes do not manifest on the

profile. **Estimated hazard potential 1.**

Station 12.3W

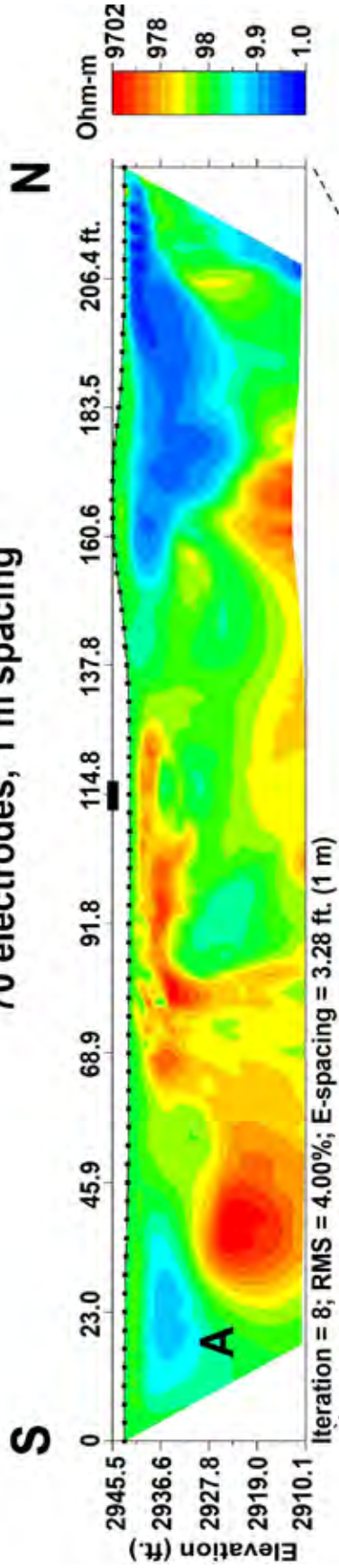
Two large sinkholes ~5 ft (1.5 m) diameter, 4 ft (1.2 m) deep, with possible cave entrances at the bottom in gypsum bedrock.

The ER survey was conducted on 28 March 2017. Depth of investigation ~34 ft (10.4 m), total survey length 184 ft (56 m), and the RMS error was 5.89% (Figure A20). The two near-surface (<5 ft or 1.5 m bgl) high resistivity anomalies coincide with the locations of the two sinkholes mapped at the surface, which are ~15 ft (~4.6 m) west and 3 ft (1 m) east of the survey line. A resistivity anomaly of similar depth at the south end of the profile does not correspond to any observed surface features. These anomalies do not appear to extend more than 6 ft (1.8 m) bgl. **Estimated hazard potential 7, based on presence of surface karst and near-surface resistivity anomalies.**

Station 12.3E

The ER survey was conducted on 20 April 2017. Depth

**US 285, east shoulder, 9.7 miles:
70 electrodes, 1 m spacing**



**US 285, east shoulder, 9.7 miles:
112 electrodes, 6 m spacing**

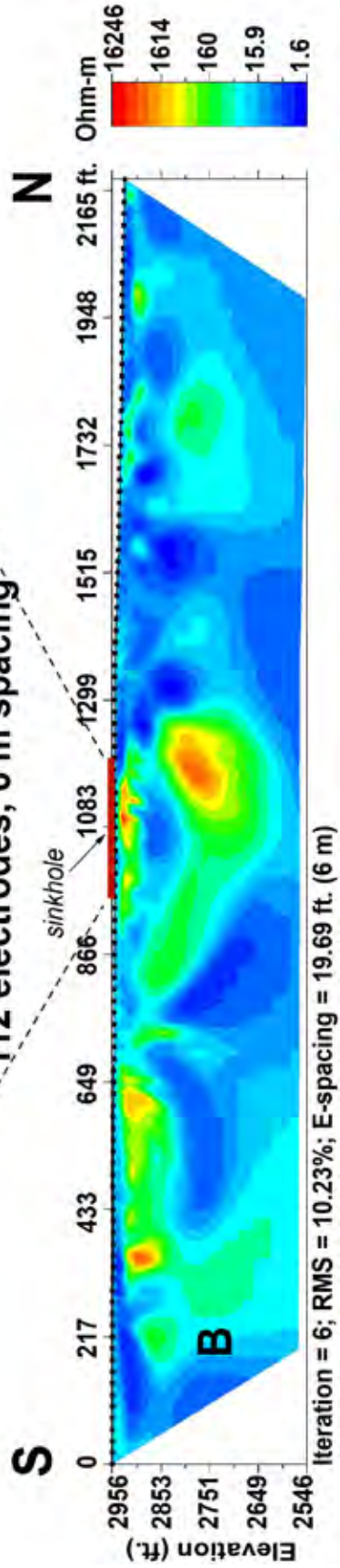


Figure A12-A. Short ER profile Station 9.7: 70 electrodes; electrode spacing = 3.3 ft. A12-B: Long ER profile Station 9.7: 112 electrodes, electrode spacing = 19.7 ft.

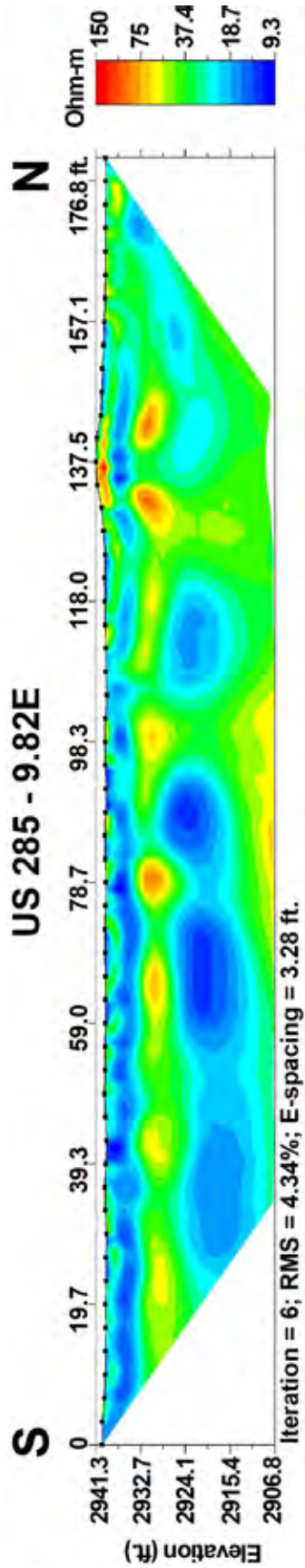


Figure A13. Station 9.82E profile.

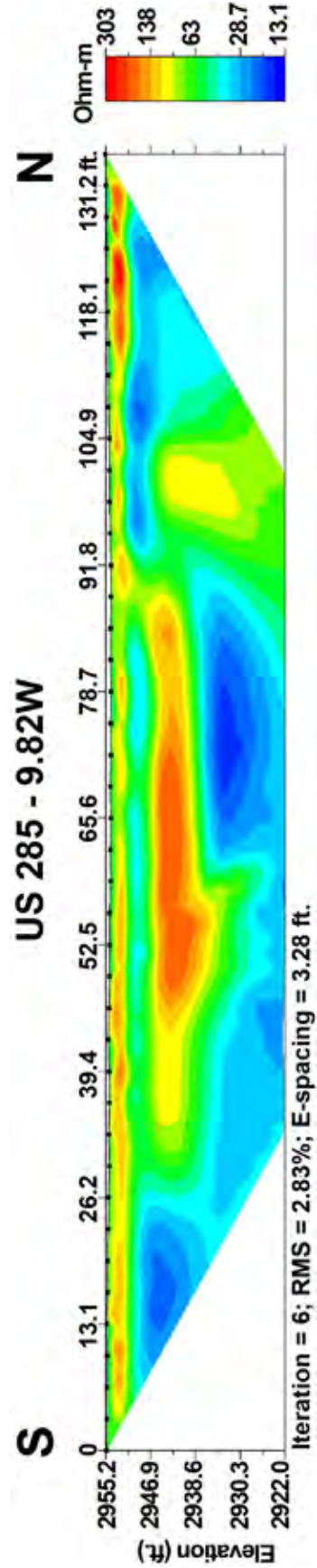


Figure A14. Station 9.82W profile.



Figure A15. Station 12.0E sinkhole A.



Figure A16. Station 12.0E sinkhole B.



Figure A17. Station 12.0E sinkhole C.

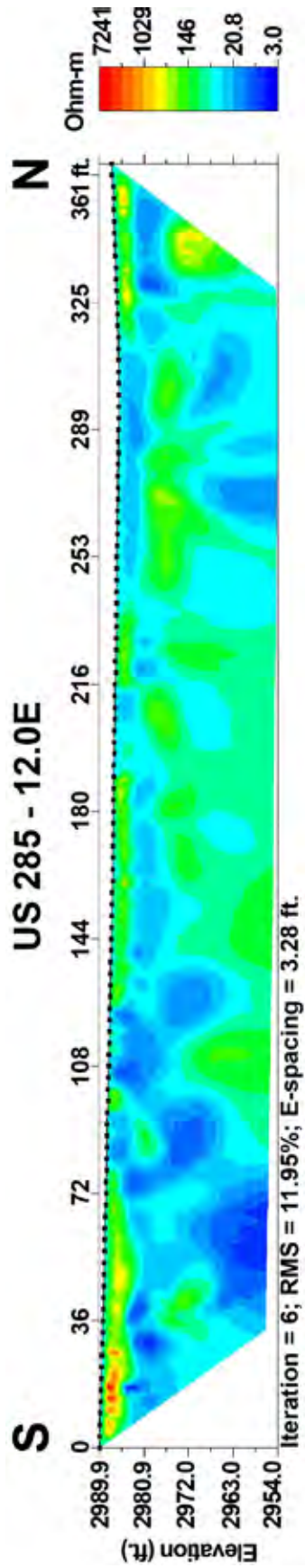


Figure A18. Station 12.0E profile.

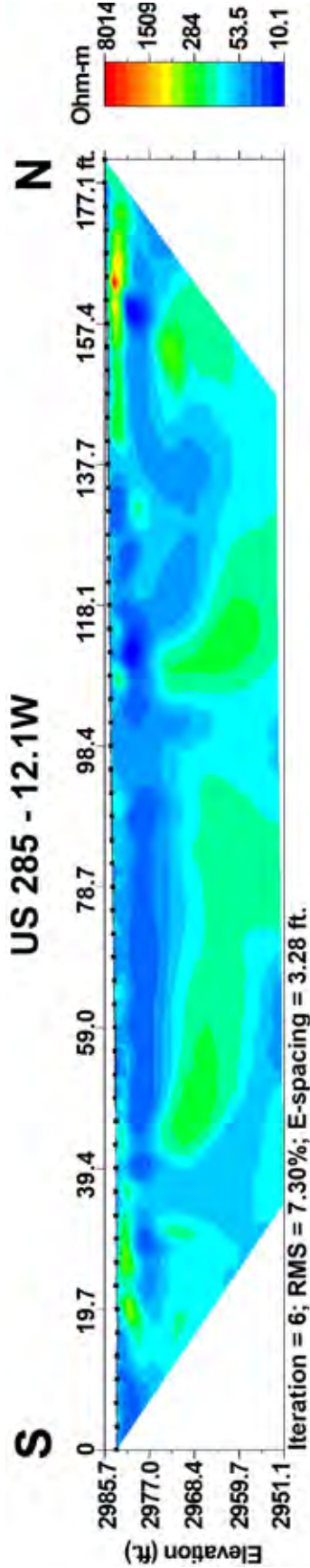


Figure A19. Station 12.1W profile.

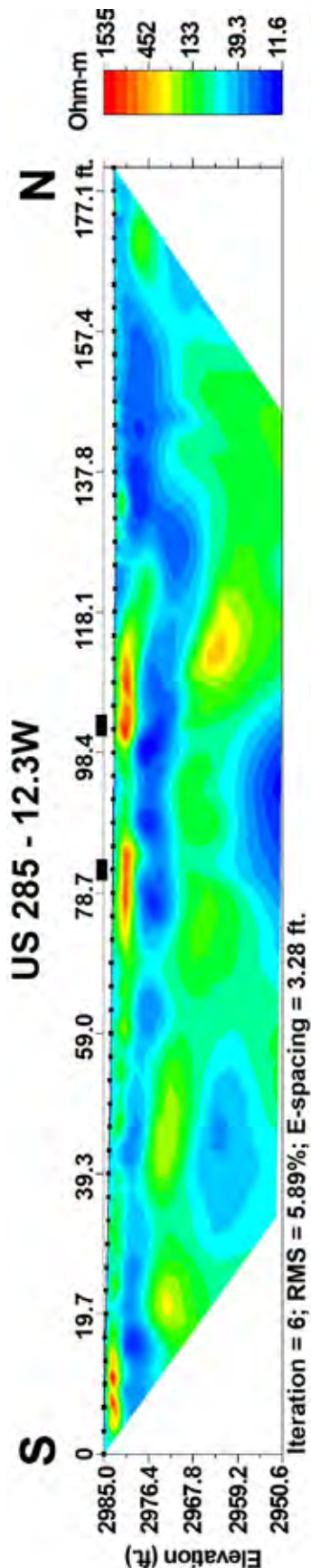


Figure A20. Station 12.3W profile.

of investigation was ~35 ft (~11 m), total survey length 184 ft (56 m), and the RMS error was 9.13% (Figure A21). A distinct pod of high resistivity is present ~10 ft (~3 m) bgl at the south end of the survey line. **Estimated hazard potential 7, based on high resistivity anomaly at south end of profile and proximity to surface karst features across the highway.**

Station 14.07E

Two sinkhole occur at this location. One is small (2 ft long x 1 ft wide x 2 ft deep, or 0.6 m long x 0.3 m wide x 0.6 m deep) near the south end of the ER survey line at 36 ft (11 m) on the profile. The other sinkhole is larger (4 ft long x 7 ft wide x 2 ft deep, or 1.2 m long x 2.1 m wide x 0.6 m deep) and near the north end of the ER survey at 194 ft (59.1 m) on the profile, 20 ft (6 m) west of the ER survey line.

The ER survey was conducted on 27 March 2017. Depth of investigation was ~34 ft (~10.4 m), total survey length 230 ft (70 m), and the RMS error was 8.18% (Figure A22). A laterally continuous near-surface layer of higher resistivity probably reflects air-filled porosity in soil and weathered bedrock. No deeper resistivity anomalies are present. The sinkholes do not manifest on the profile. **Estimated hazard potential 3, because of presence of the rather large sinkhole at north end of line.**

Station 14.1E

This station is so designated because it begins near karst feature 285E-14.1. The ER survey line is directly adjacent to karst feature 285E-14.2a, a sinkhole 4 ft (1.2 m) in diameter, 7 ft (2.1 m) deep, in gypsum bedrock with a small entrance to a possible cave that has slight airflow.

The ER survey was conducted on 27 March 2017. Depth of investigation was ~34 ft (~10.4 m), total survey length 276 ft (84 m), and the RMS error was 10.55% (Figure A23). The ER survey line passes directly adjacent to the sinkhole with the possible cave entrance mentioned above. A high resistivity anomaly is clearly visible ~5 ft (1.5 m) bgl between ~177 and 203 ft on the profile. **Estimated hazard potential 8, because of presence of surface karst and near-surface resistivity anomalies.**

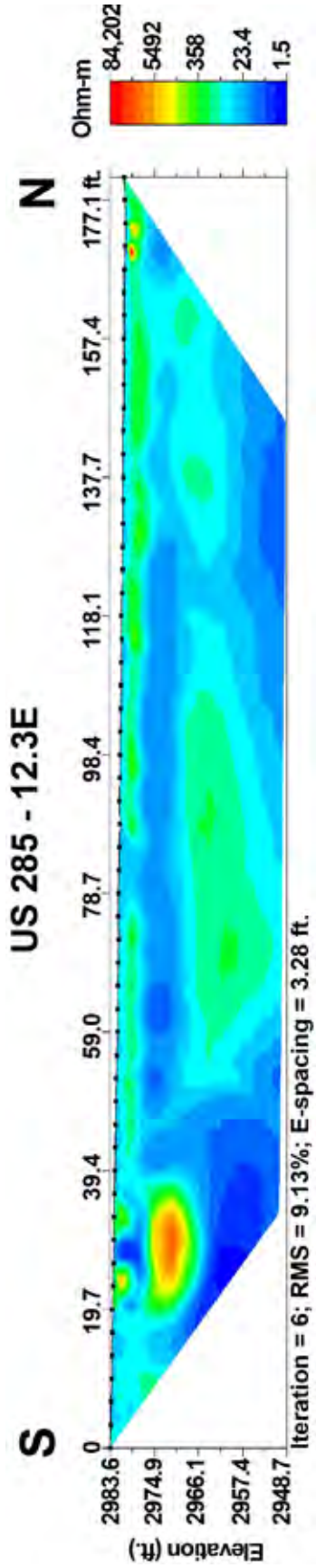


Figure A21. Station 12.3E profile.

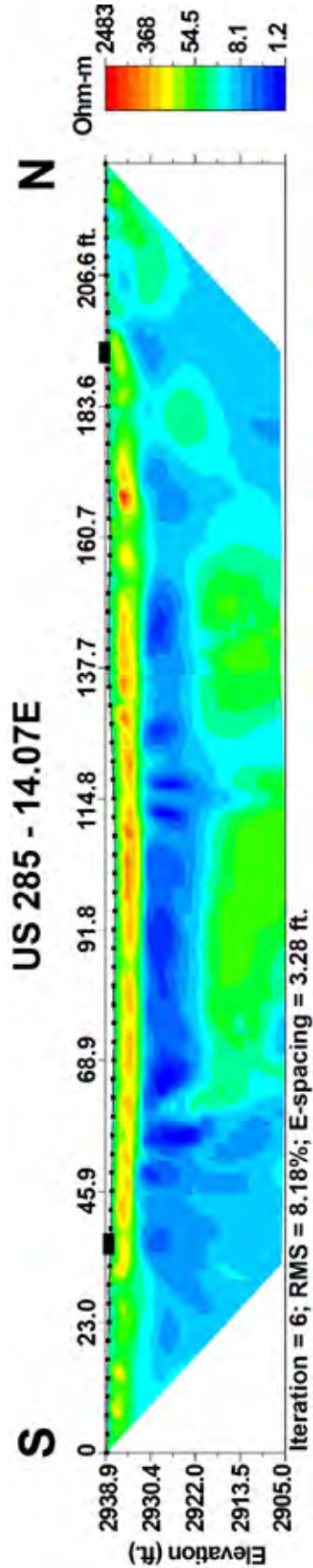


Figure A22. Station 14.07E profile.

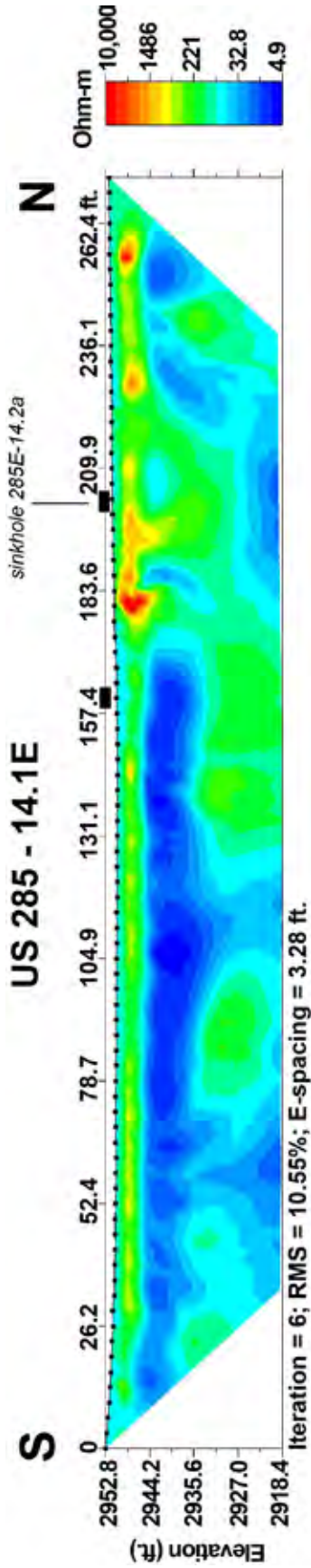
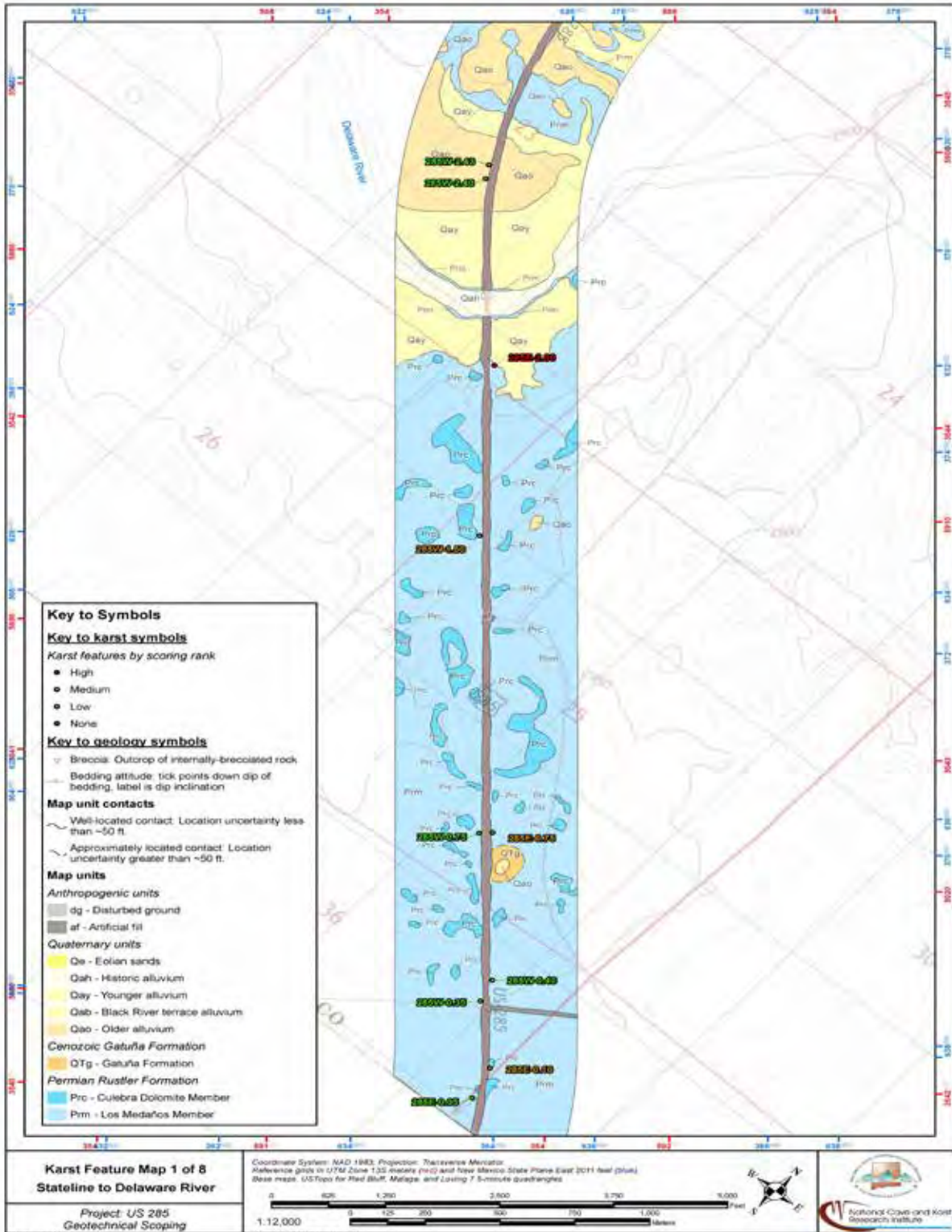
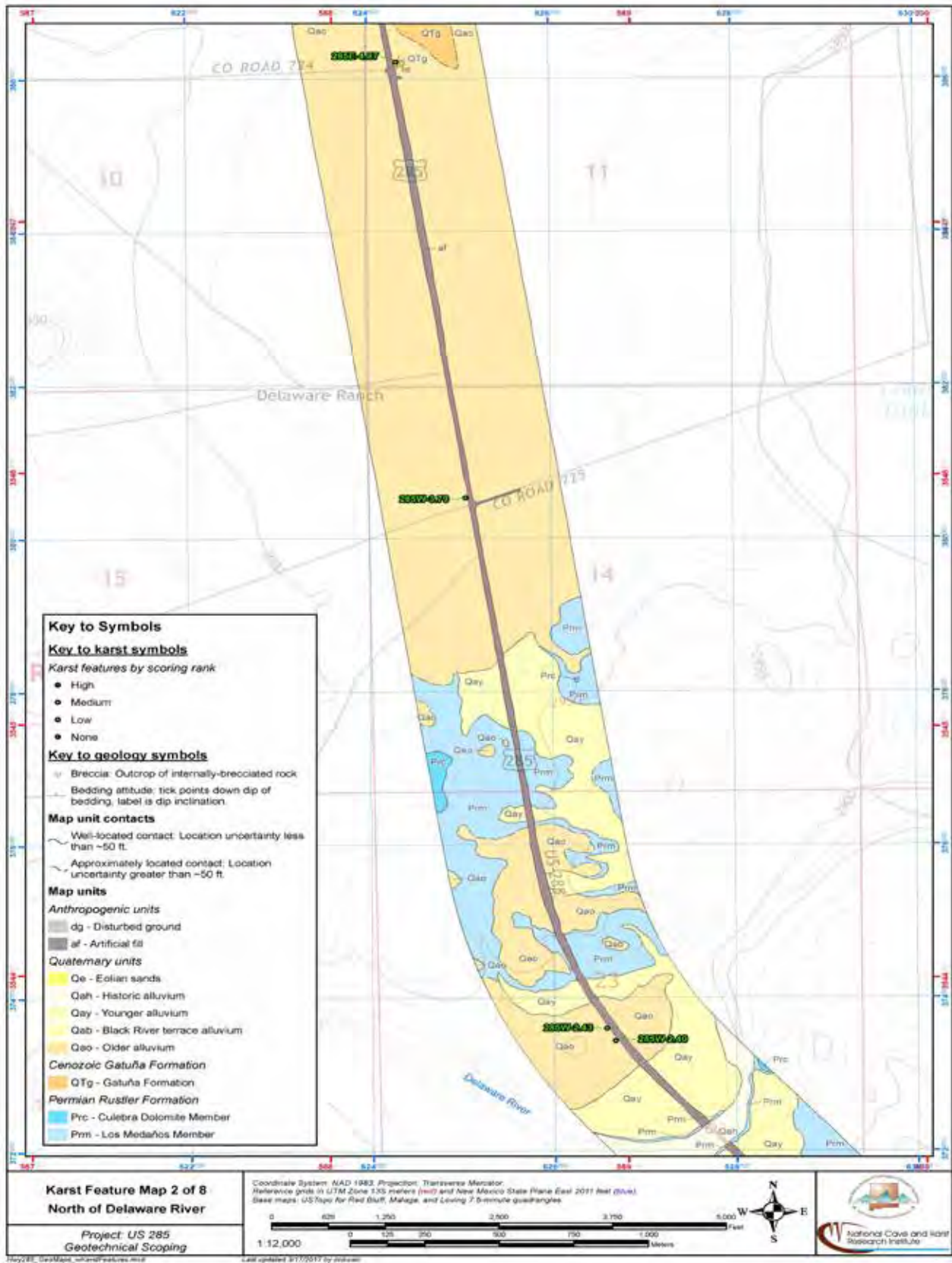
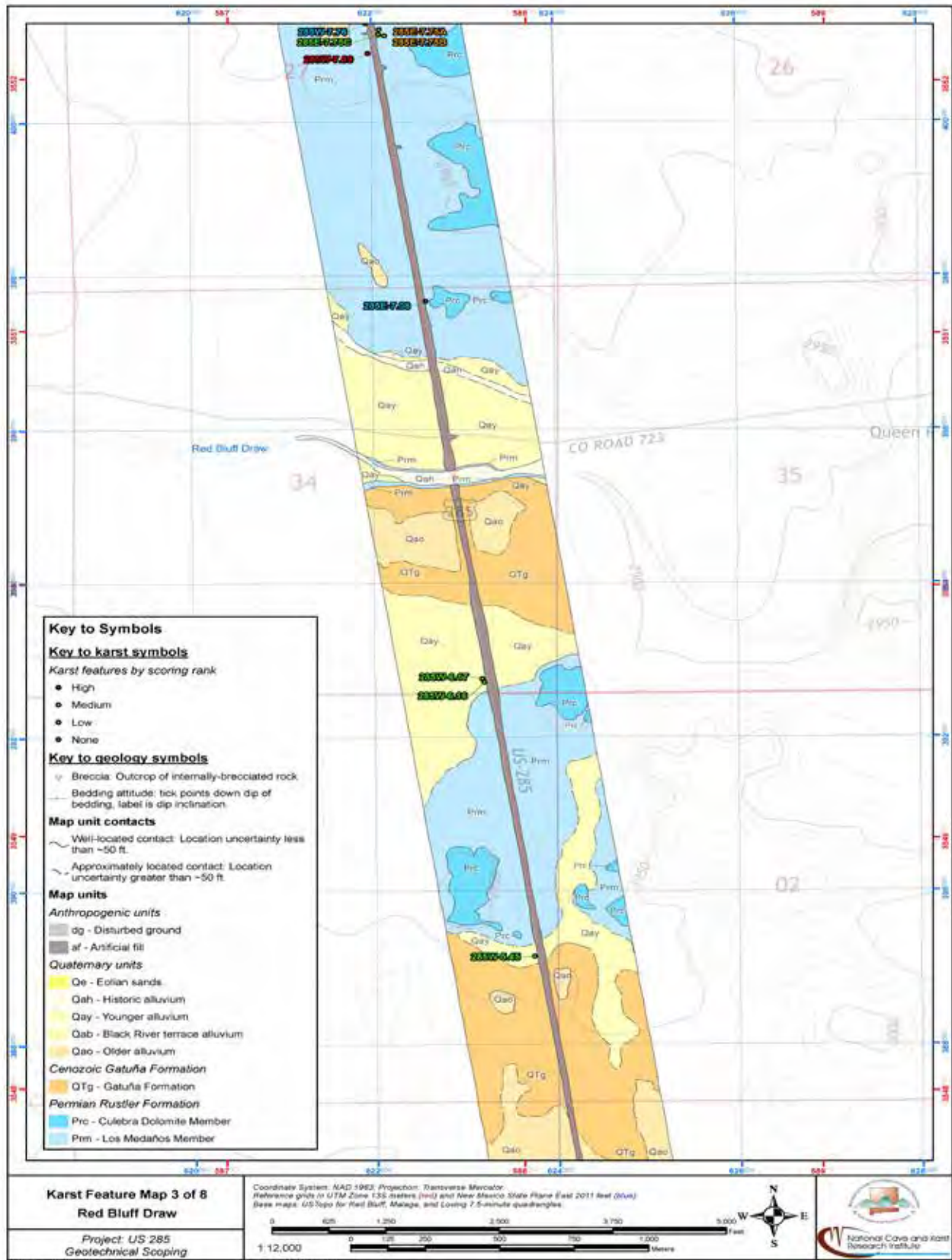


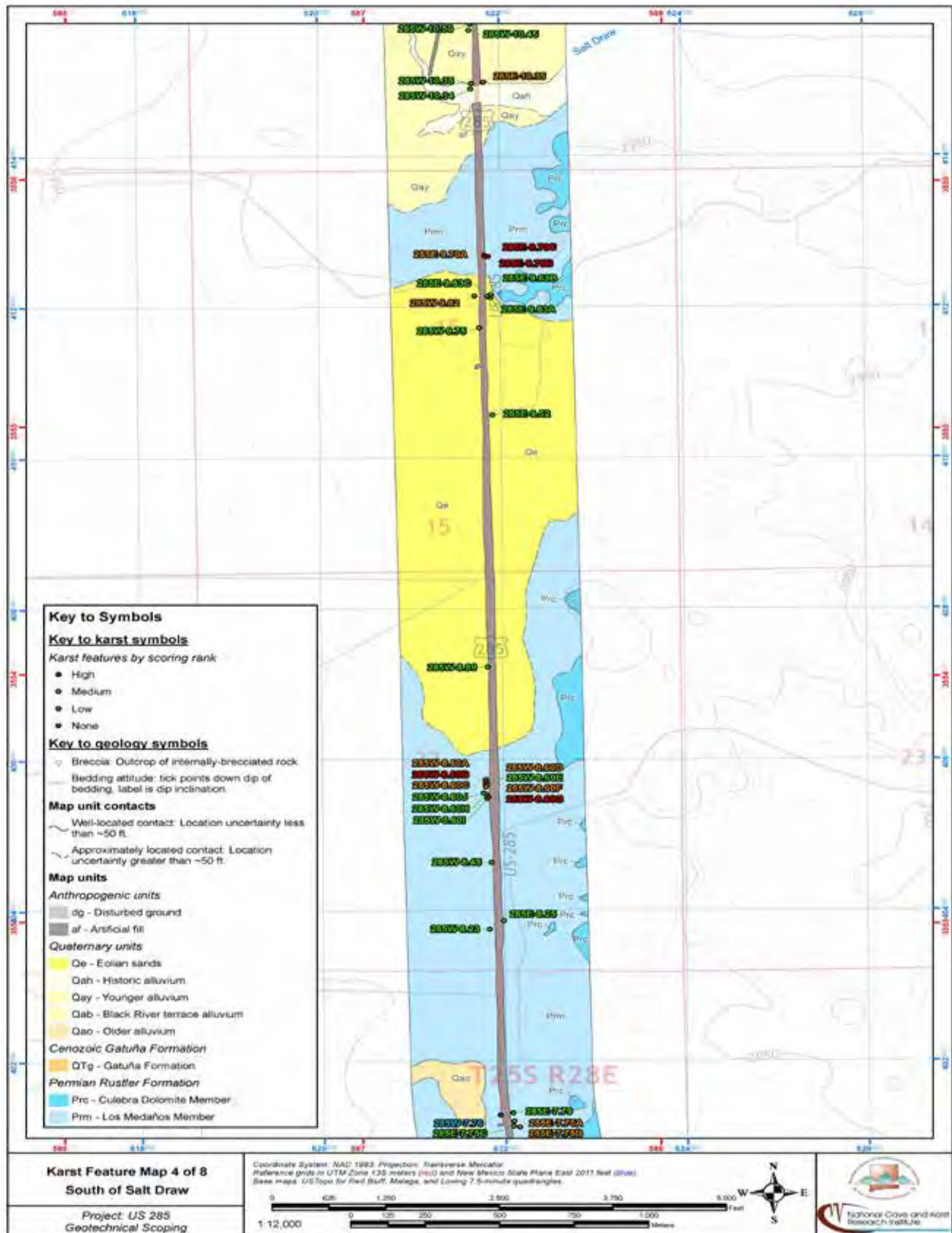
Figure A23. Station 14.1E profile.

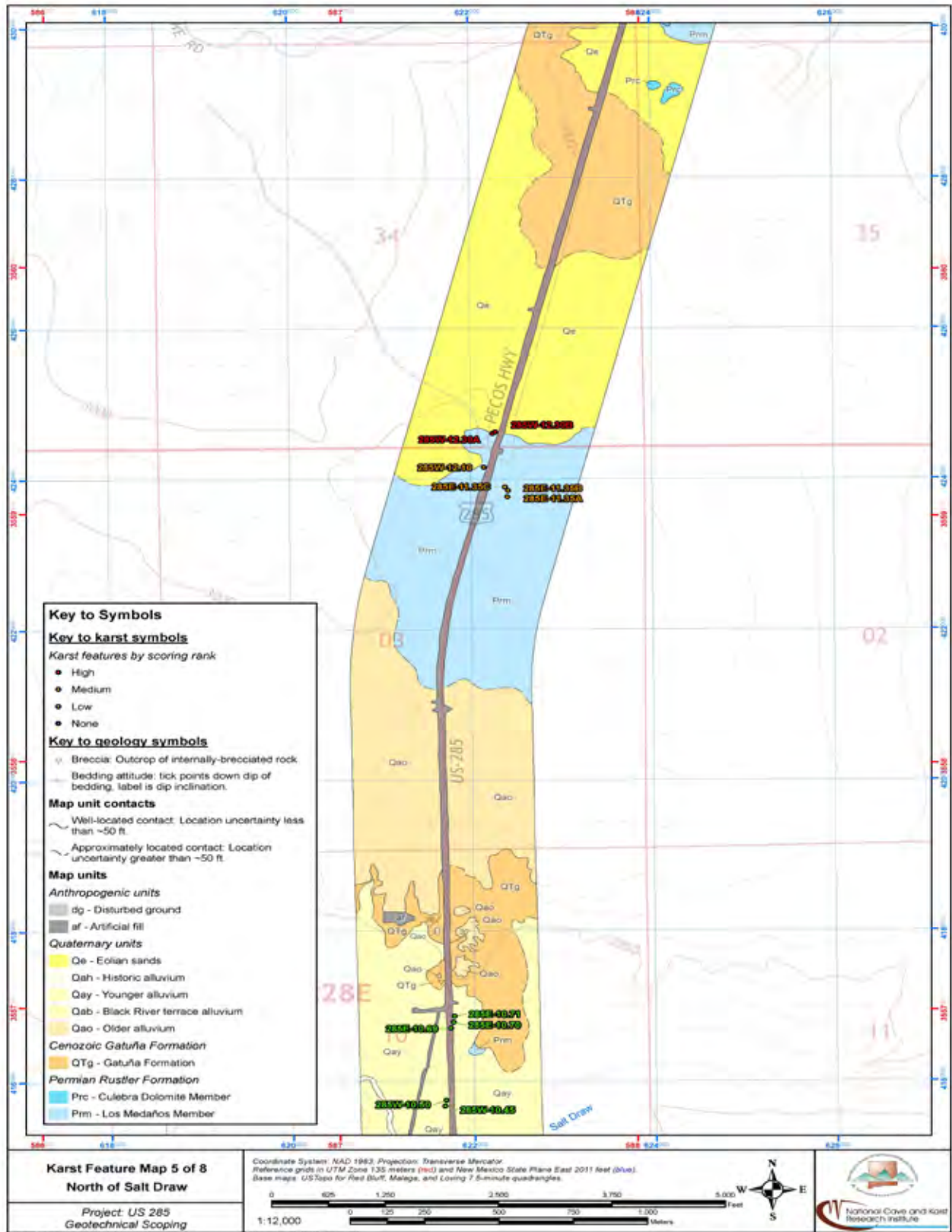
**Appendix B:
Detailed Geologic and Topographic Map
of the Study Area, With Karst Features
(pages 67-74)**

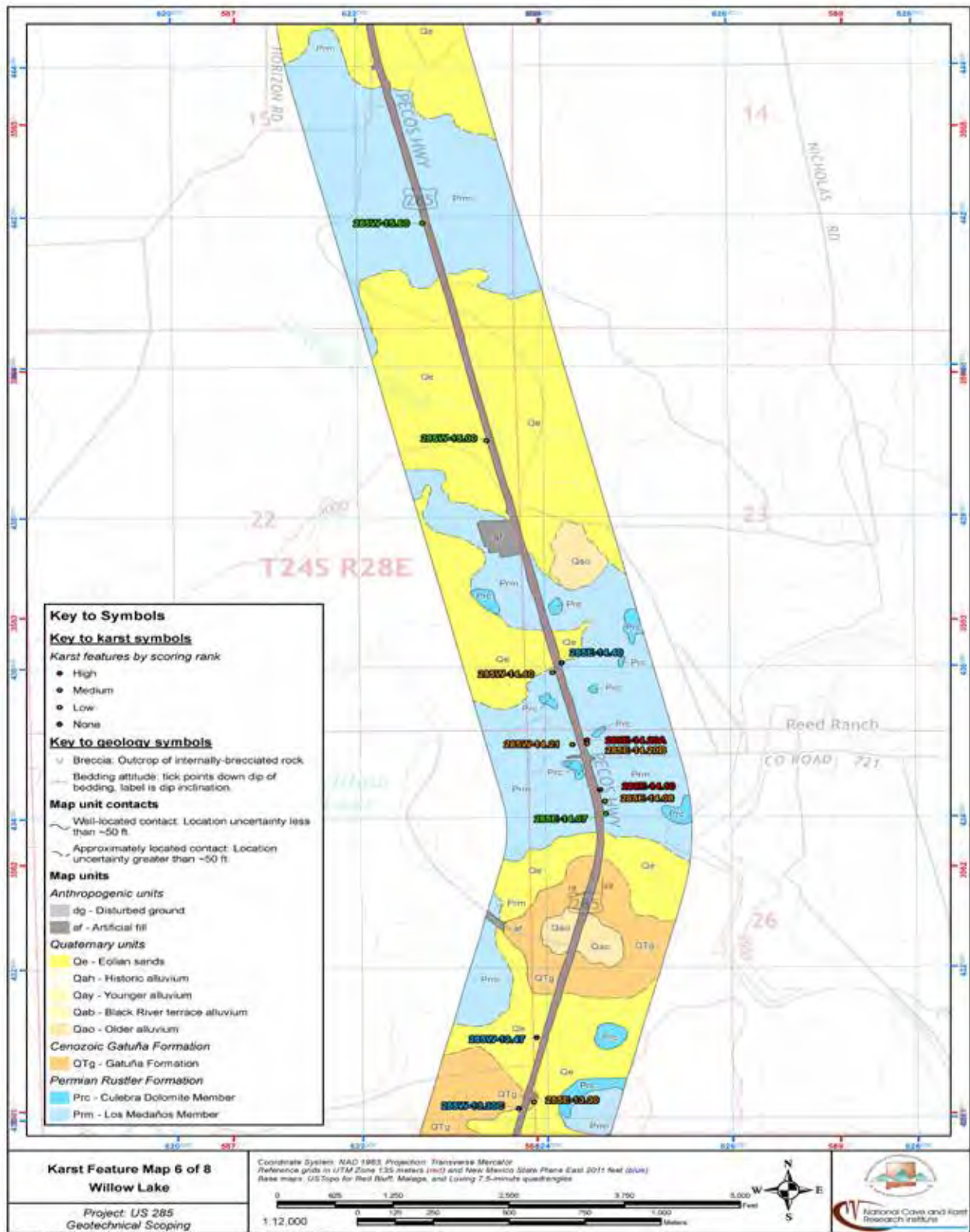


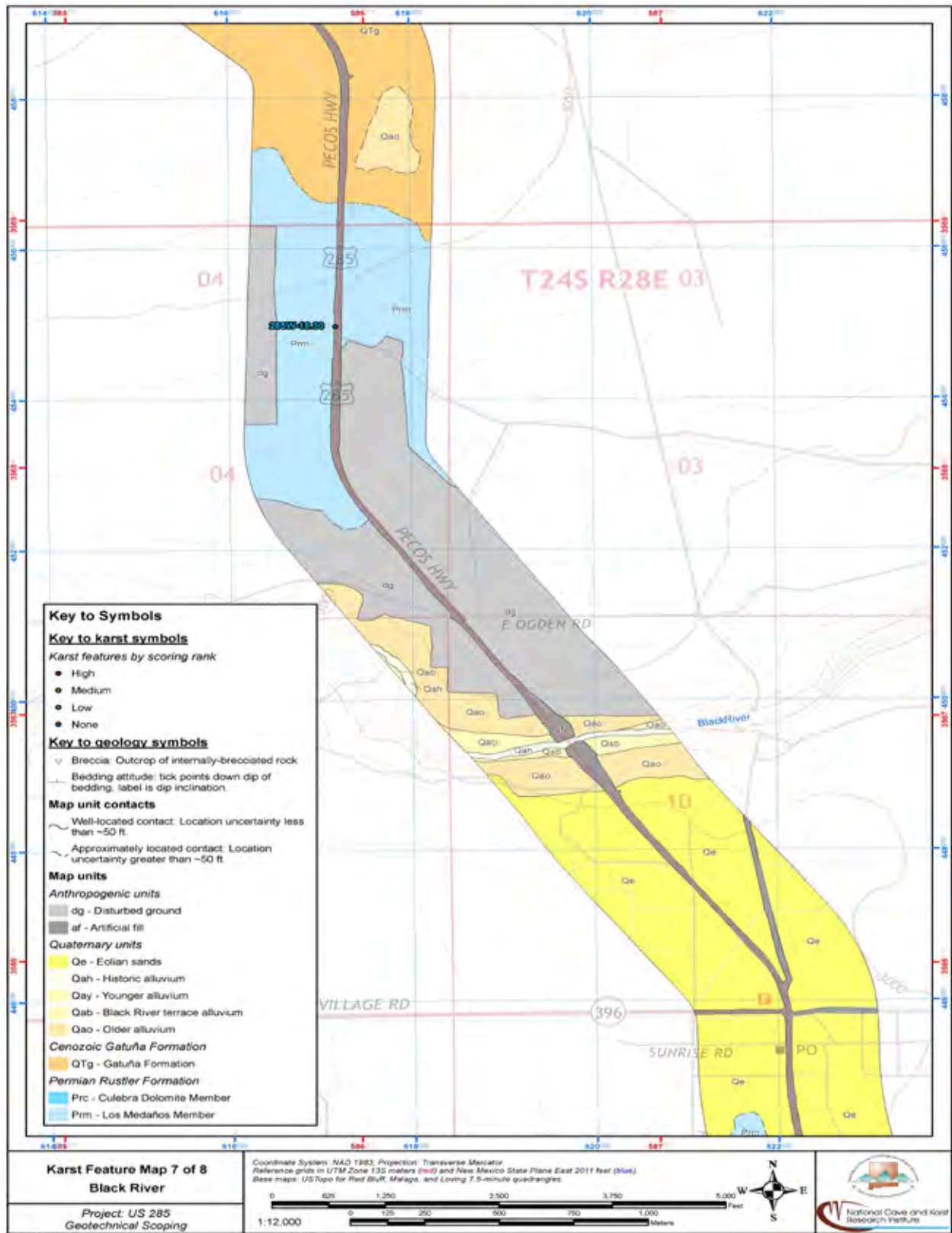


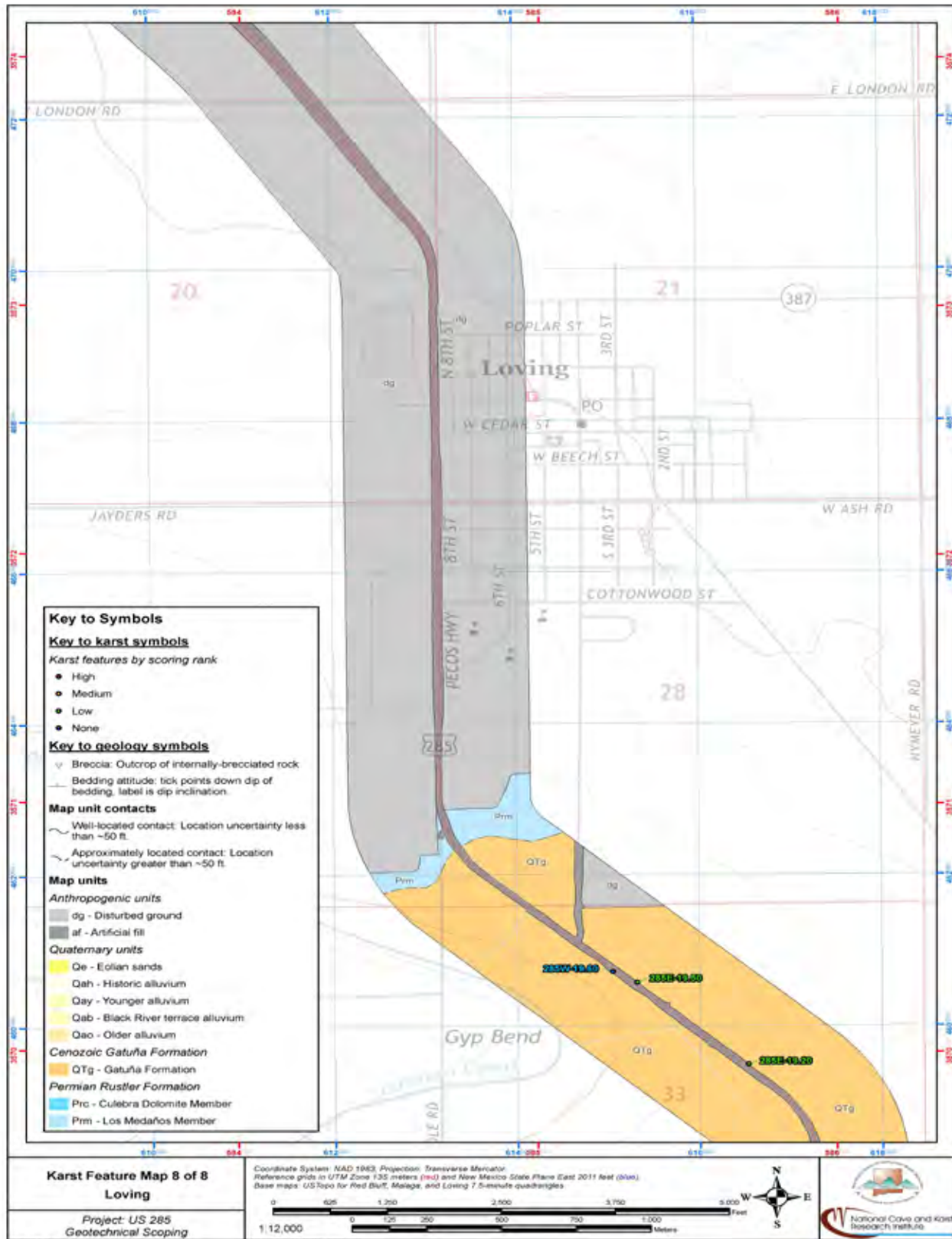




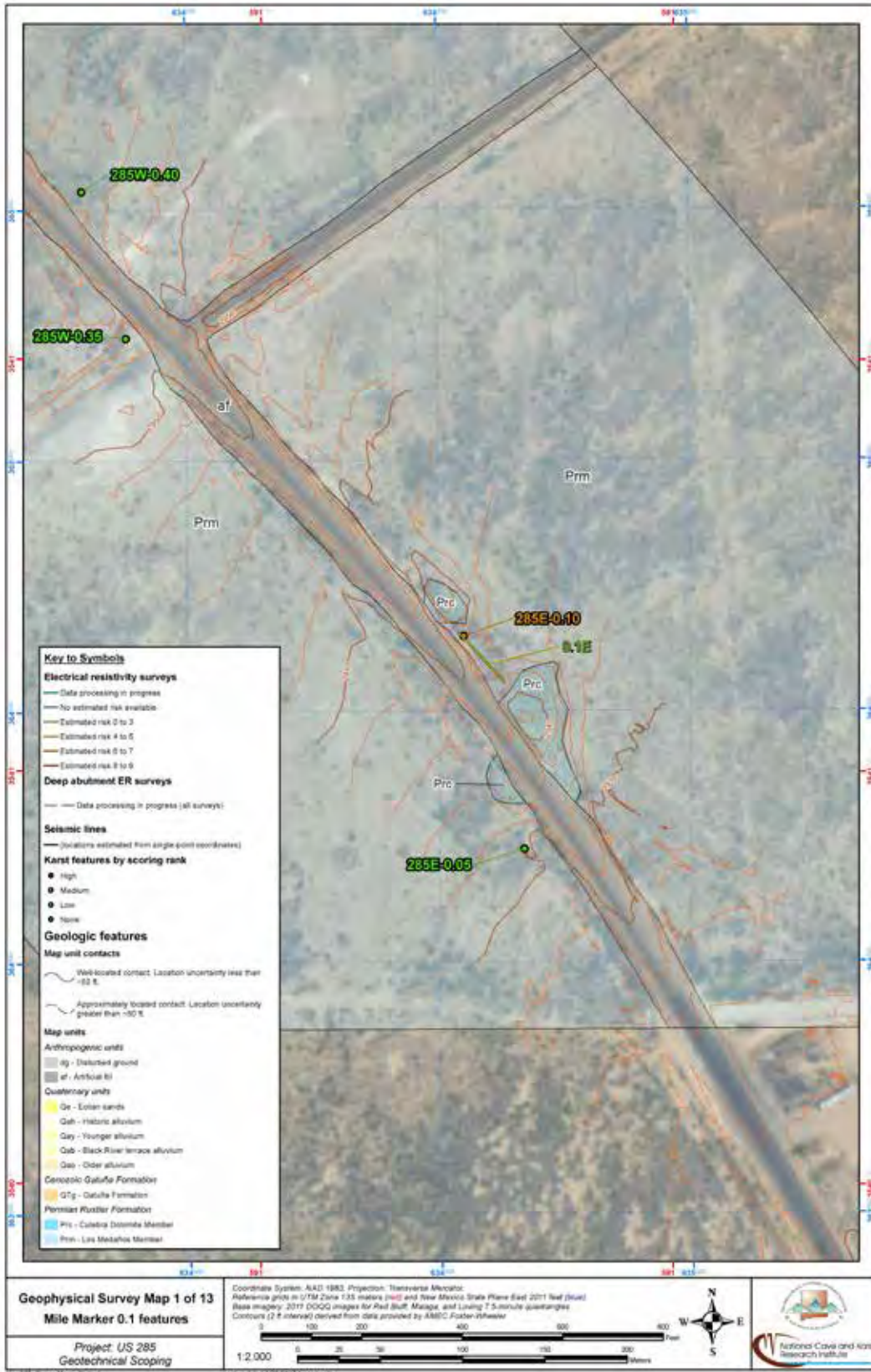


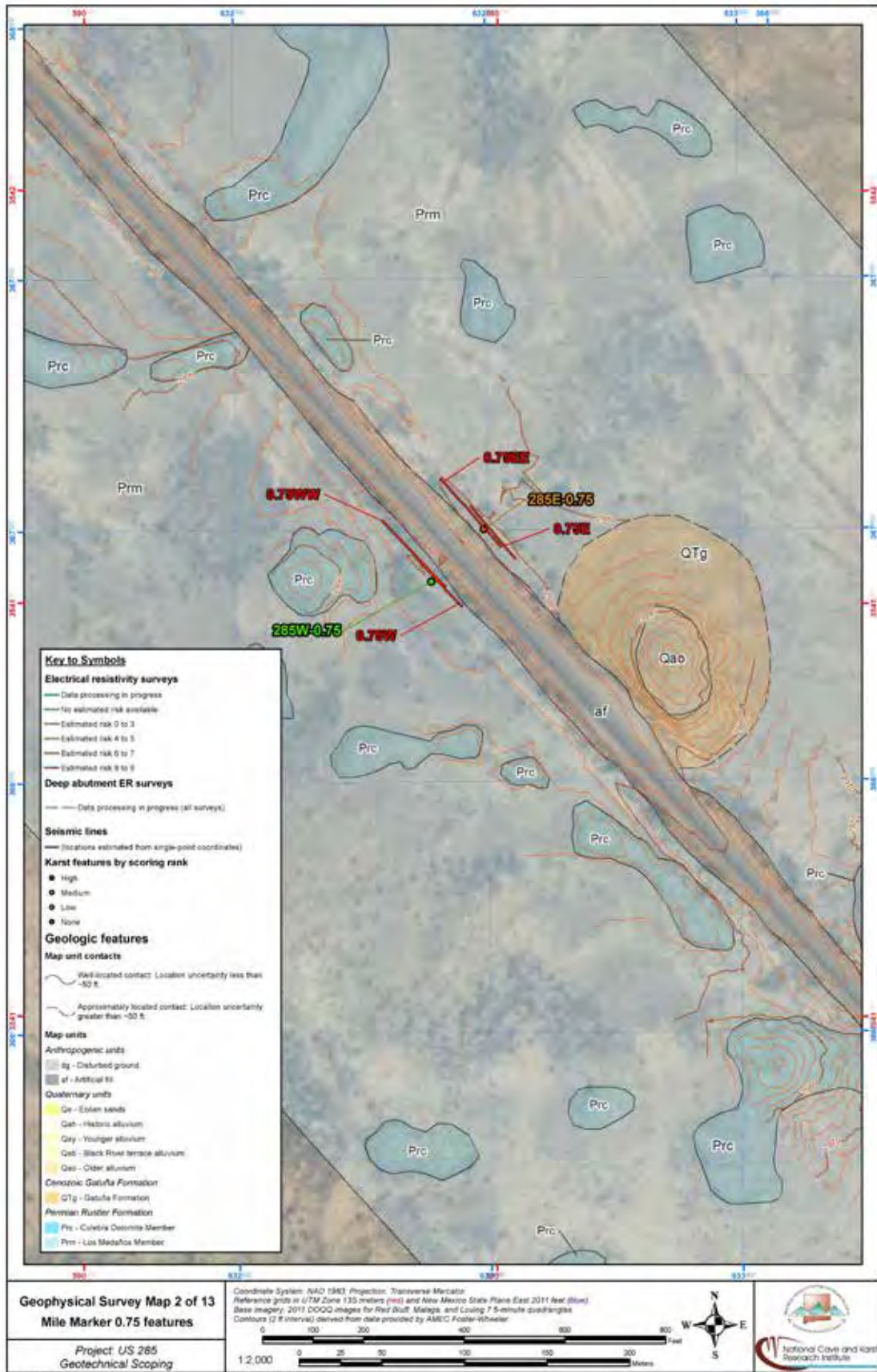


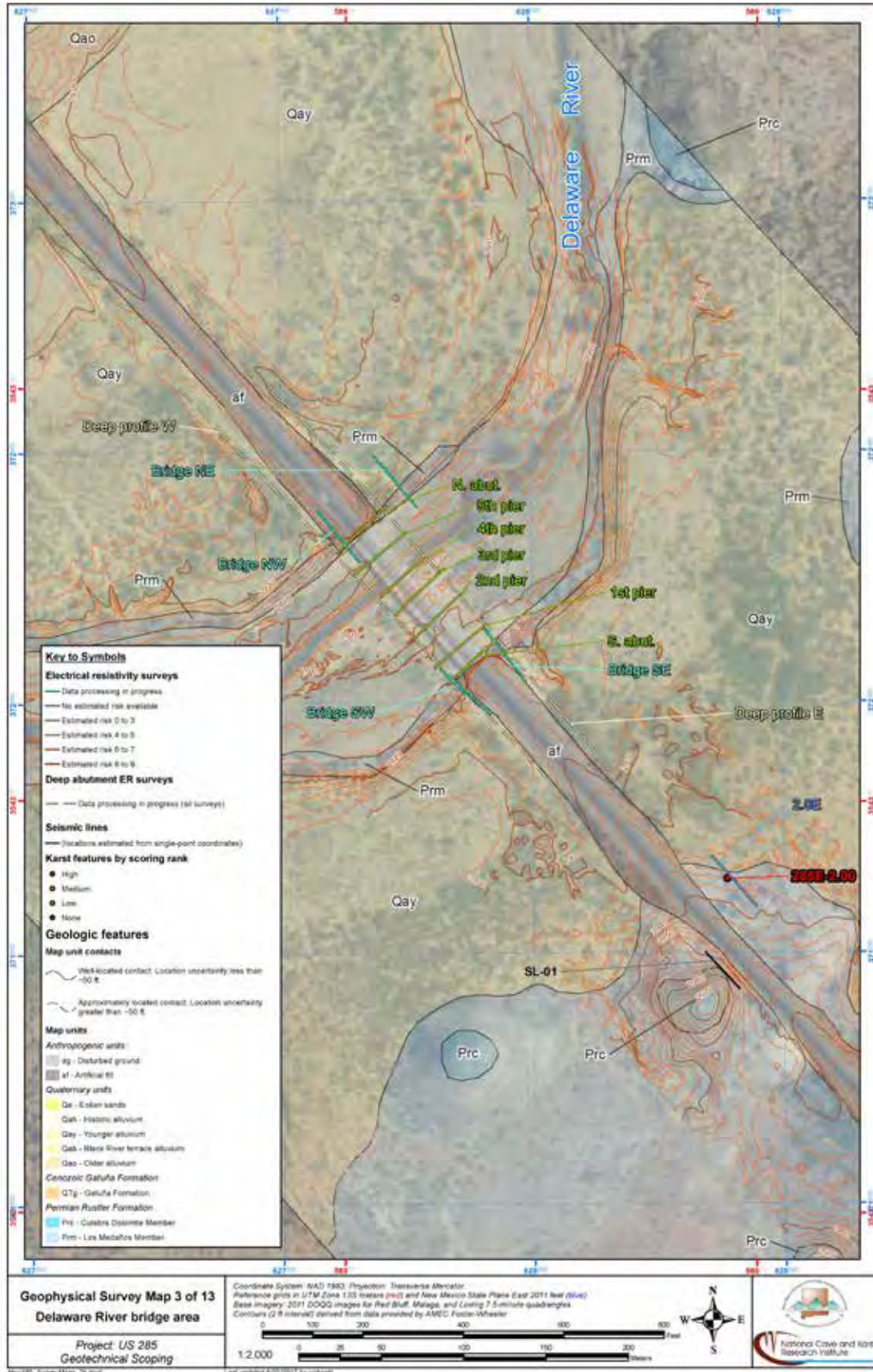


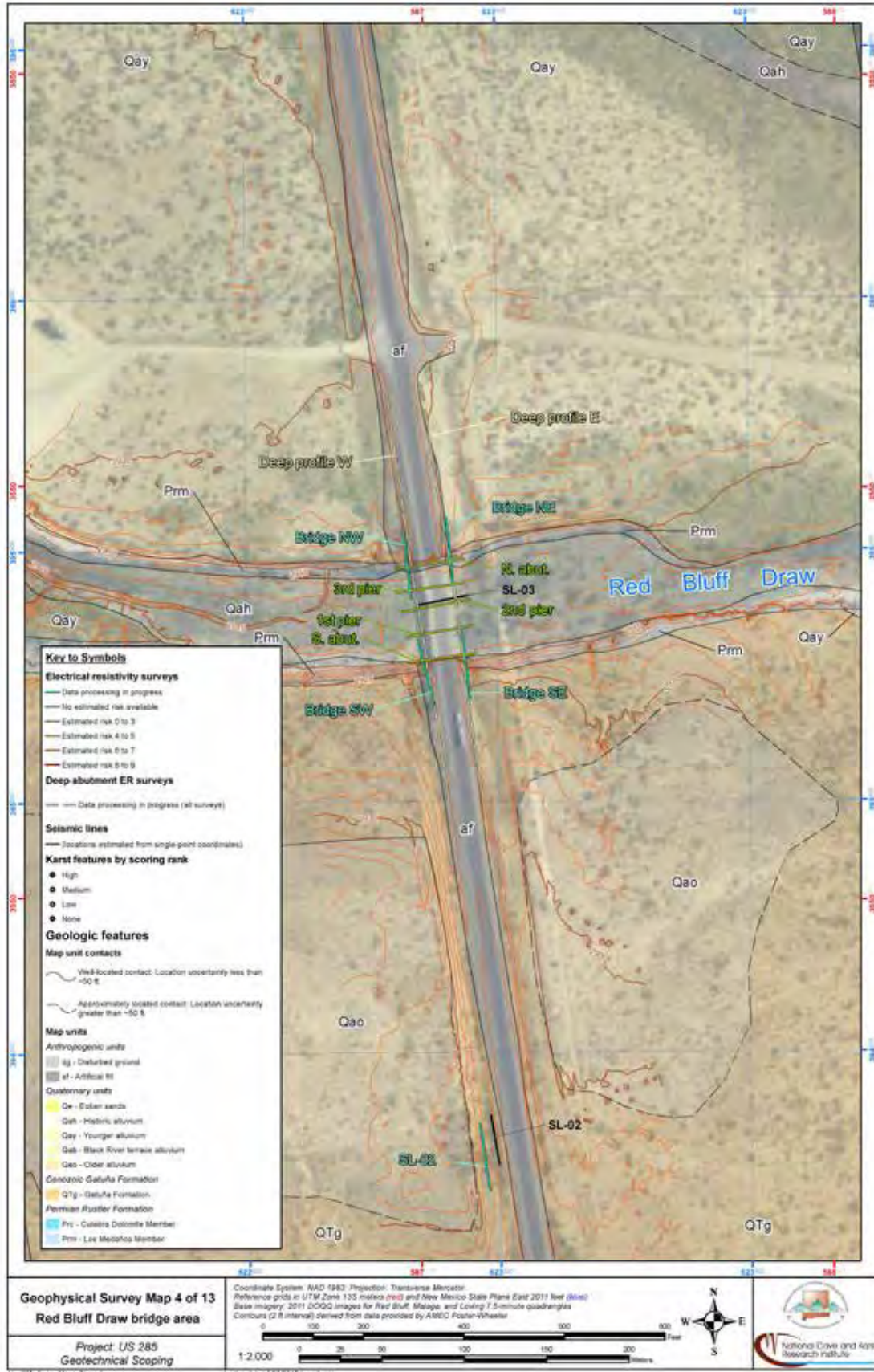


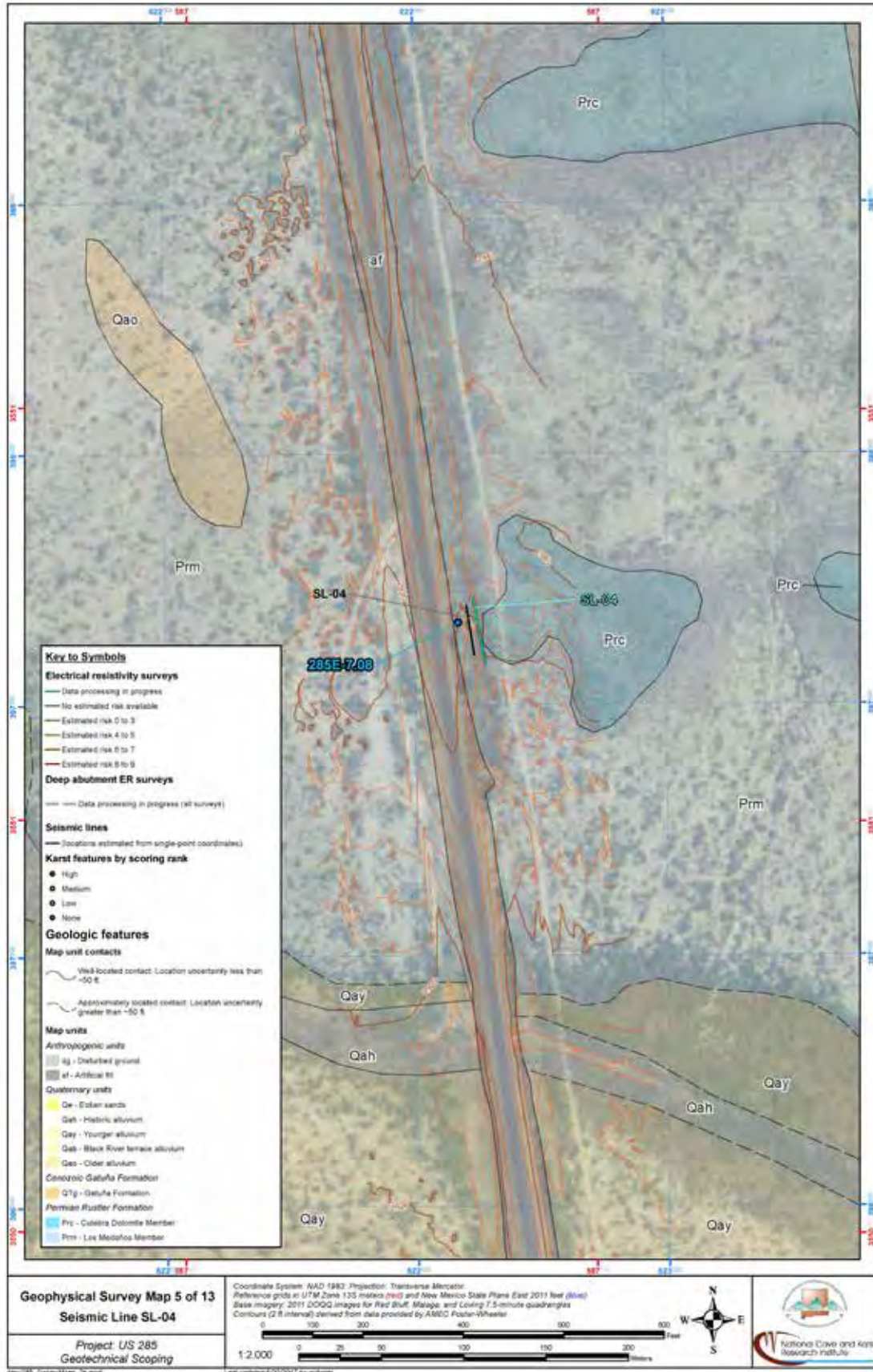
**Appendix C:
Detailed Geologic, Aerial Photo, Karst Feature,
and Electrical Resistivity Map of the Study Area
(pages 76-88)**

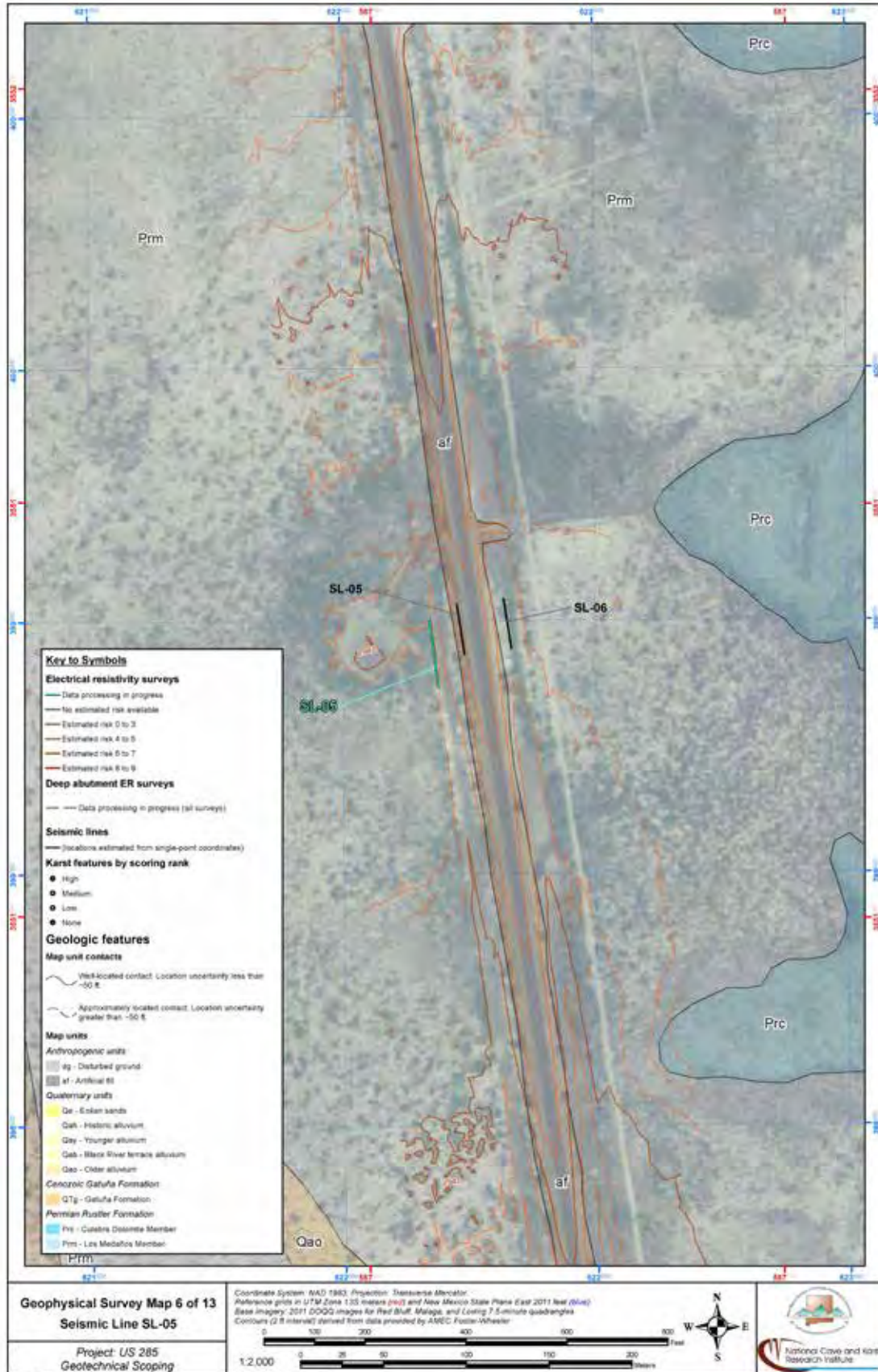


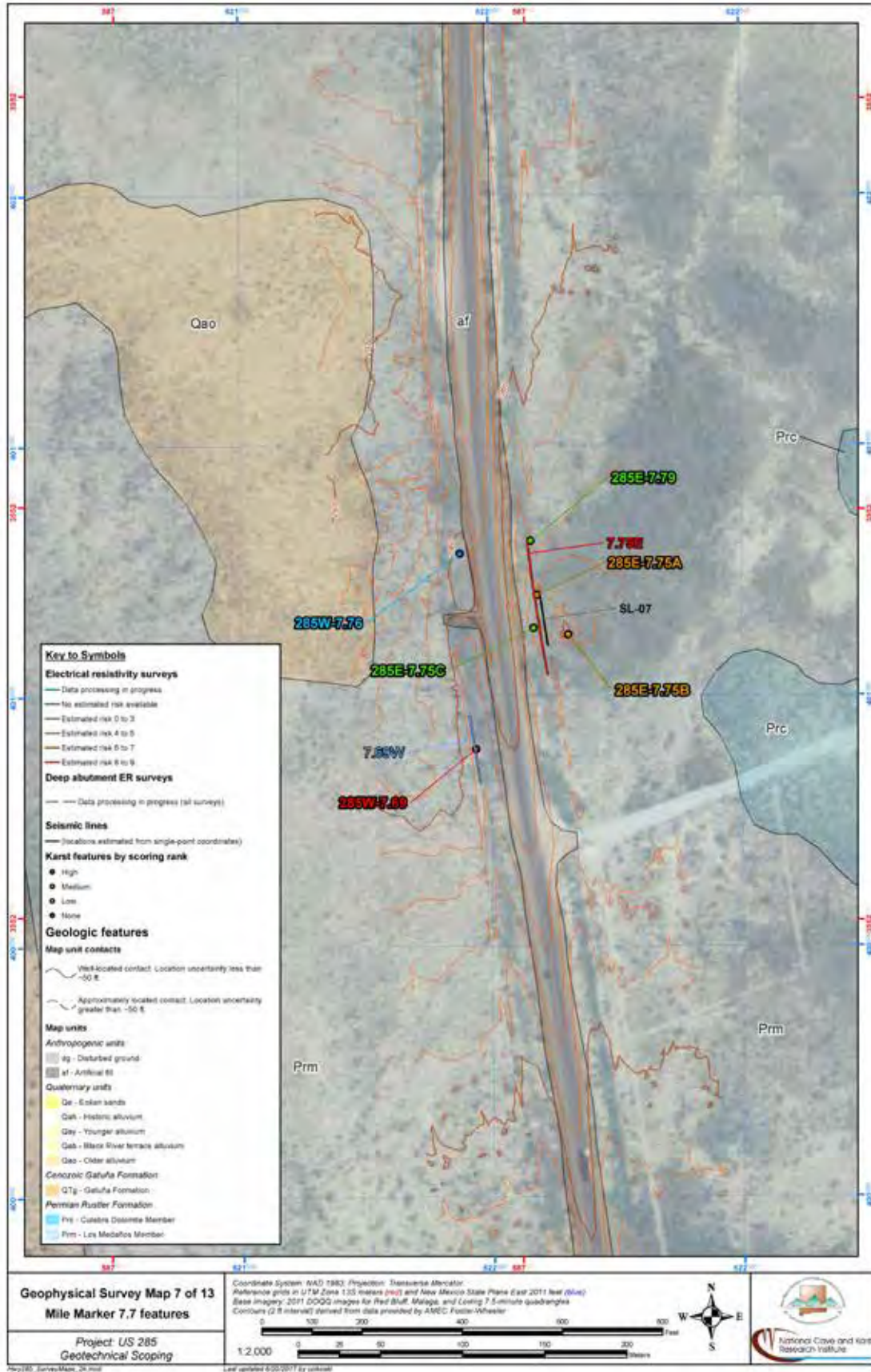


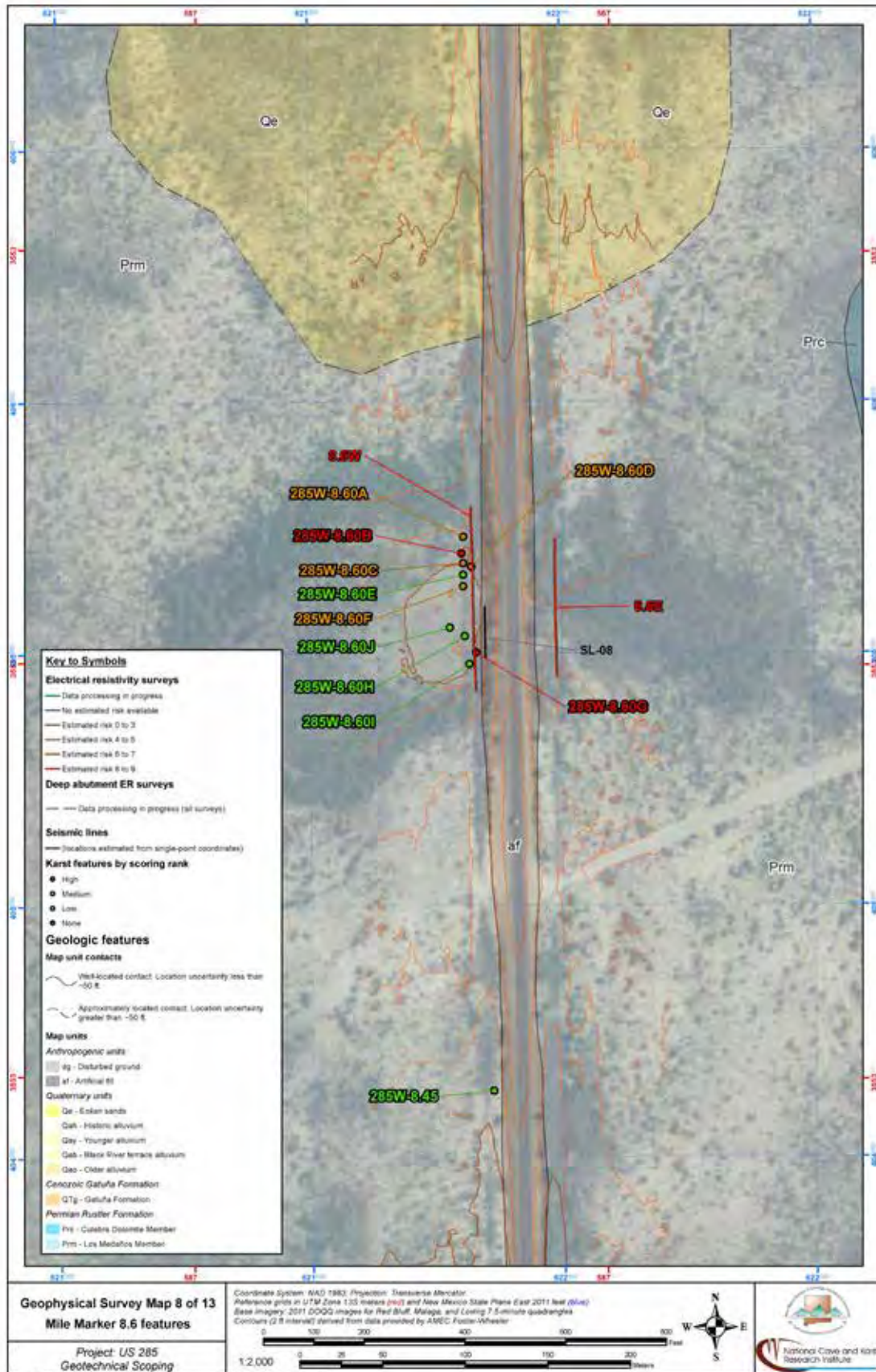


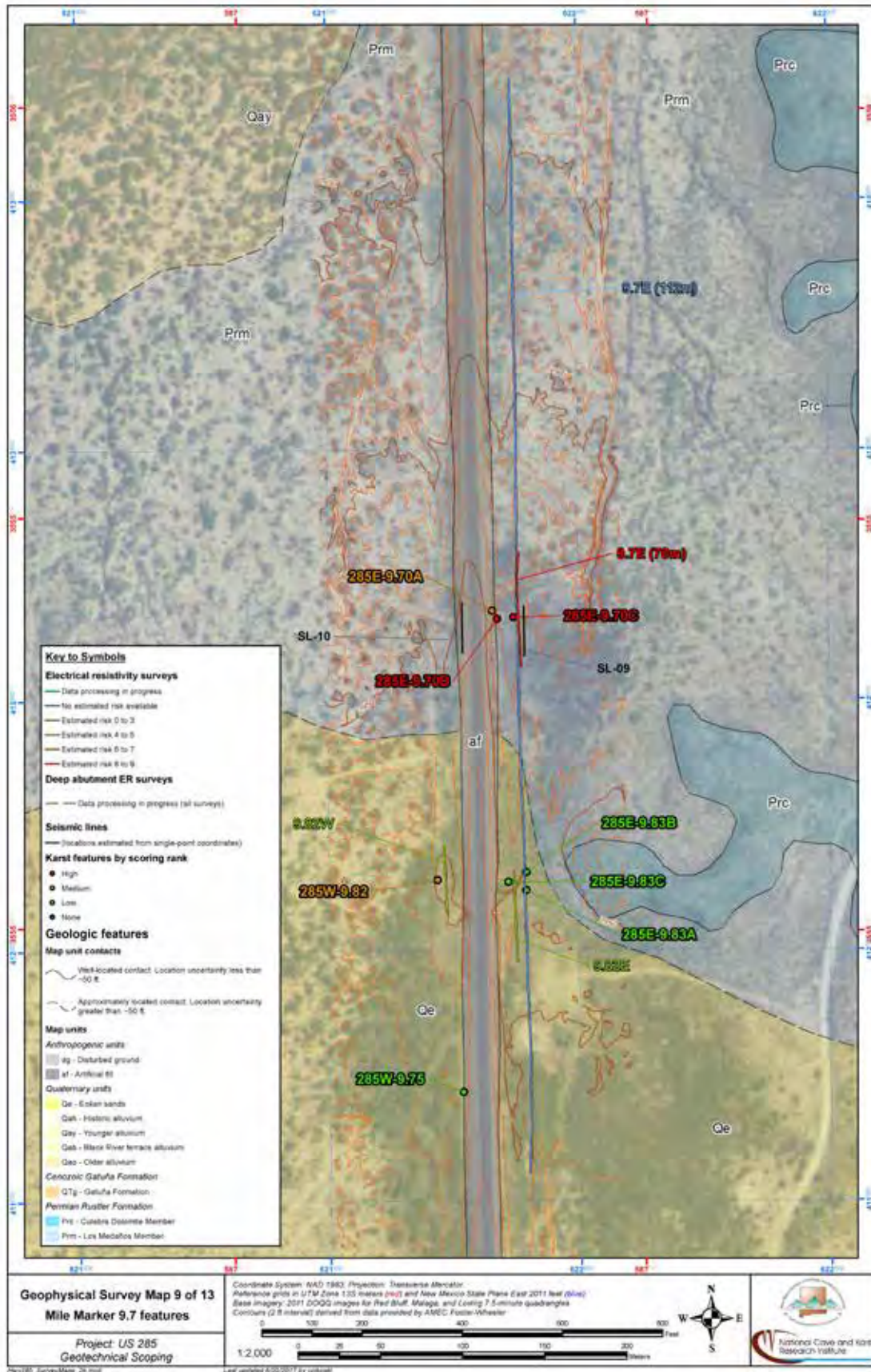




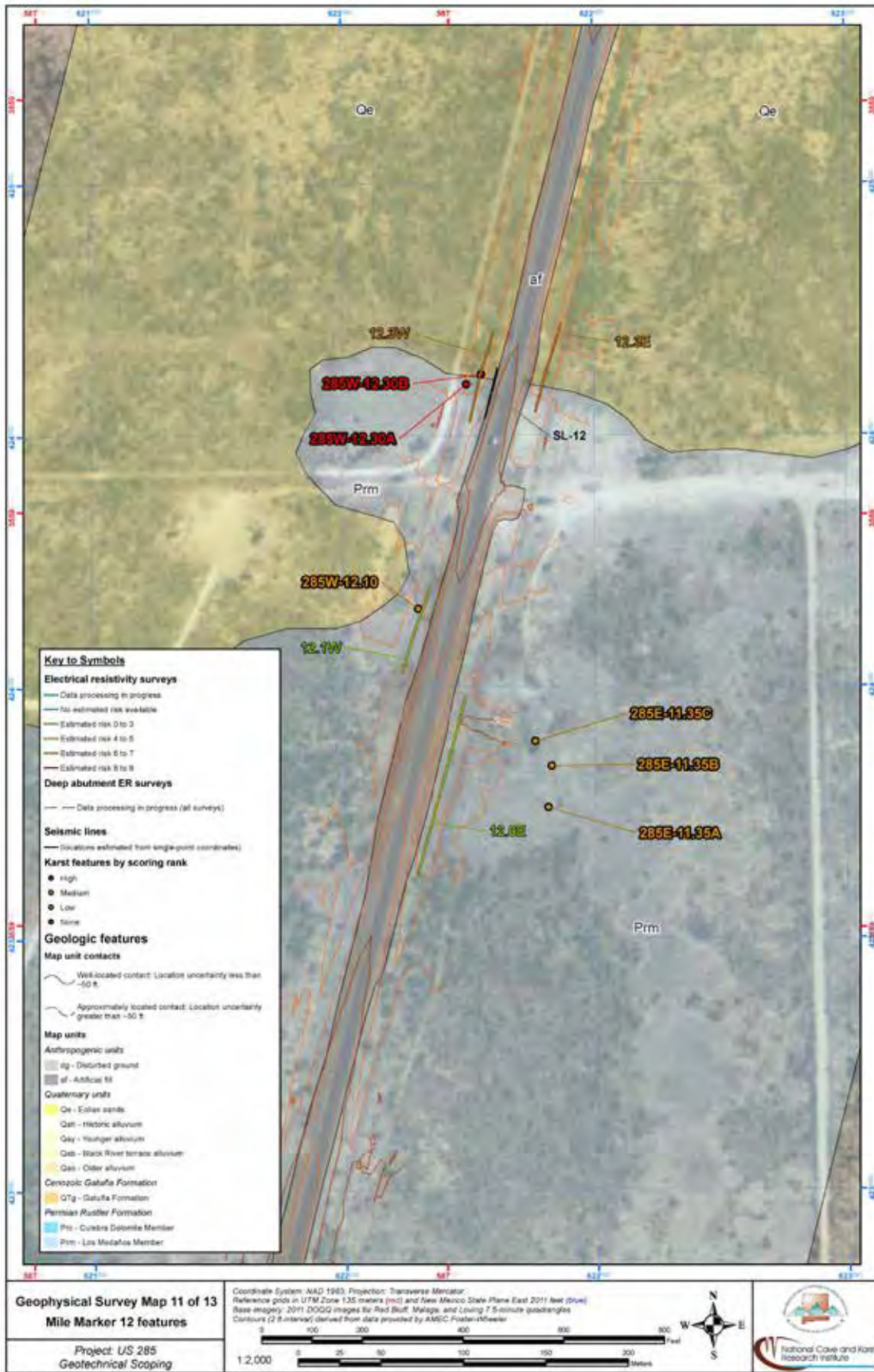


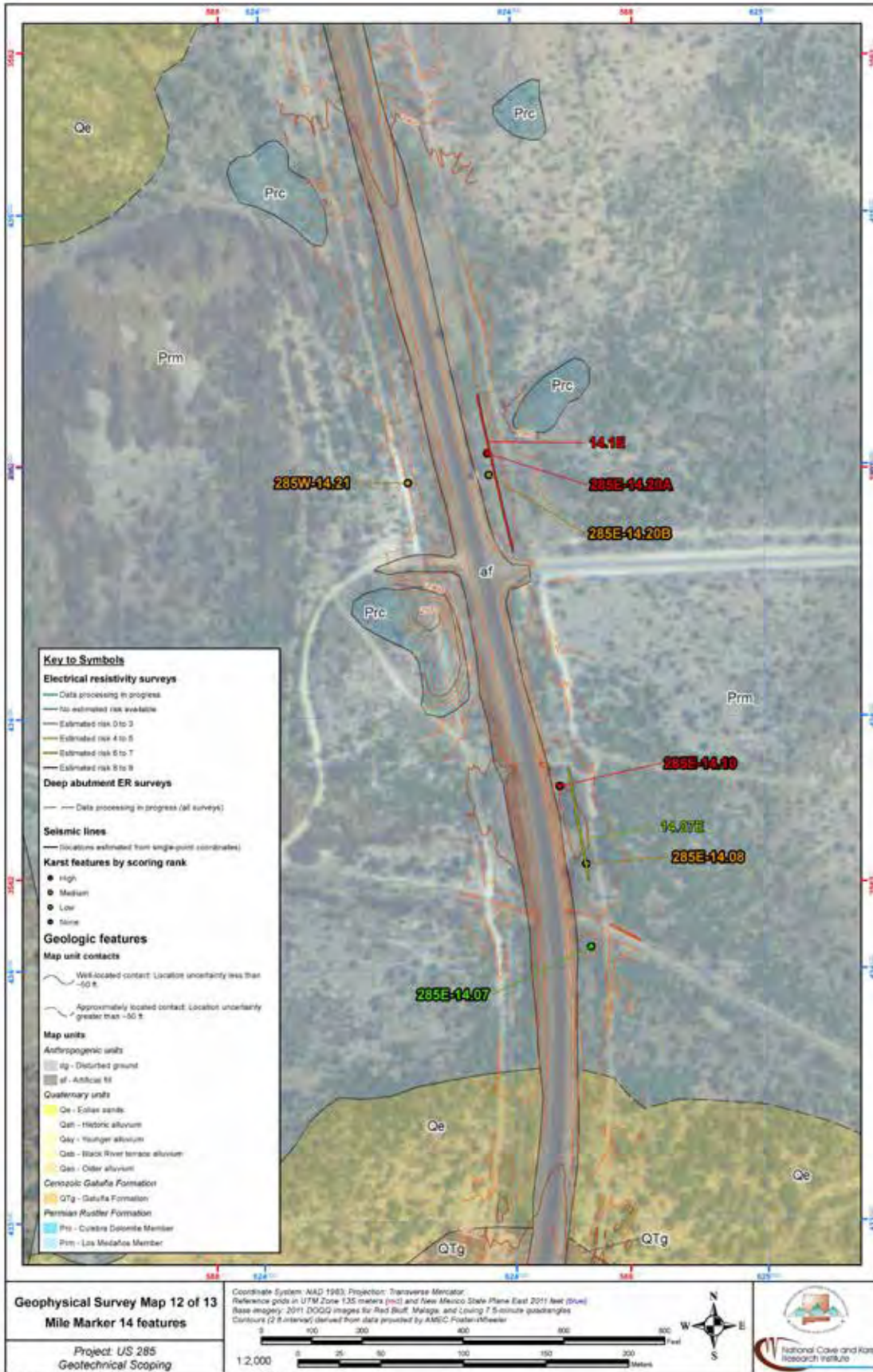


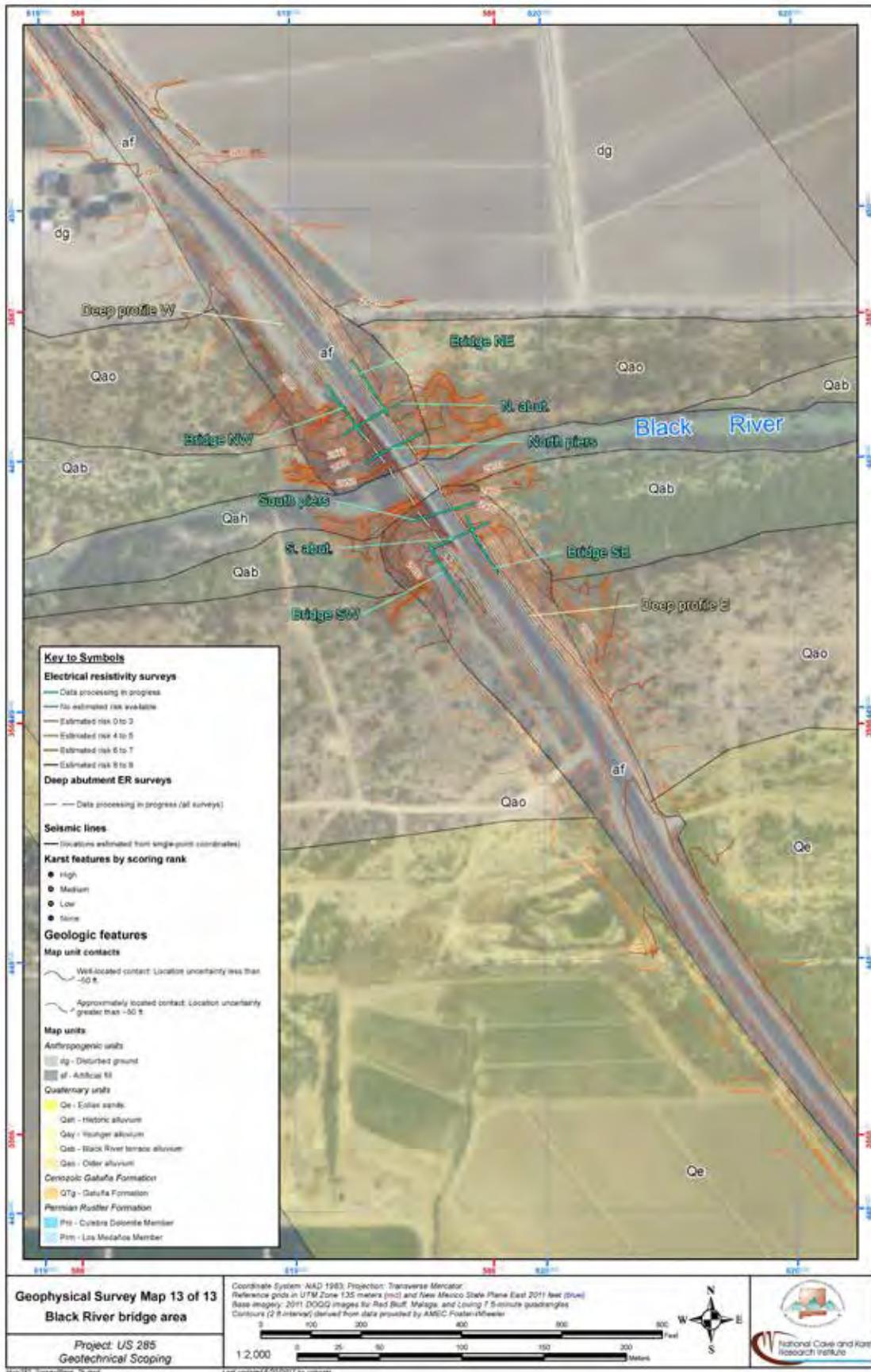












**National Cave
and Karst Research Institute**
400-1 Cascades Avenue
Carlsbad, New Mexico 88220 USA

